TAMPEREEN TEKNILLINEN YLIOPISTO
TAMPERE UNIVERSITY OF TECHNOLOGY

Adam Orłowski

Membrane-associated Proteins do care about Lipids – Perspective Based on Atomistic Molecular Dynamics Simulations

Julkaisu 1244 • Publication 1244

Tampere 2014

Tampereen teknillinen yliopisto. Julkaisu 1244
Tampere University of Technology. Publication 1244

Adam Orłowski

Membrane-associated Proteins do care about Lipids – Perspective Based on Atomistic Molecular Dynamics Simulations

Thesis for the degree of Doctor of Science in Technology to be presented with due permission for public examination and criticism in Sähkötalo Building, Auditorium S3, at Tampere University of Technology, on the 6th of October 2014, at 12 noon.

Tampereen teknillinen yliopisto - Tampere University of Technology
Tampere 2014

Doctoral candidate

Adam Orłowski, M.Sc.
Biological Physics and Soft Matter Group
Department of Physics
Tampere University of Technology

Supervisor

Ilpo Vattulainen, Prof.
Biological Physics and Soft Matter Group
Department of Physics
Tampere University of Technology

Pre-examiners

Manuel Prieto, Prof.
Centro de Quimica-Fisica Molecular
Complexo Interdisciplinar, IST
Universidade de Lisboa

Antti Poso, Prof.
School of Pharmacy
University of Eastern Finland

Opponent

Rainer Böckmann, Prof.
Computational Biology
Department Biologie
Universität Erlangen-Nürnberg

ISBN 978-952-15-3362-4 (printed)
ISBN 978-952-15-3380-8 (PDF)
ISSN 1459-2045

Abstract

TAMPERE UNIVERSITY OF TECHNOLOGY
ADAM ORŁOWSKI: Membrane-associated proteins do care about lipids—perspective based on atomistic molecular dynamics simulations

This thesis consists of three original articles that deal with lipid-protein interactions investigated using atomistic molecular dynamics simulations method, which in some cases were complemented with experimental data. Since very few molecular details of these important interactions are known, the data shown in this thesis can help to understand and develop a broader view on the role of lipids in protein's function.

In the first part of this thesis, the membrane-binding part of the COMT protein was studied using the atomistic molecular dynamics simulations. The results indicate that the role of the transmembrane helix and the linker part of this protein is to enclose the enzymatic part of the protein in the close vicinity of the membrane, and therefore to keep it in the specific membrane-water interface environment. Moreover, the particular kind of protein fold, which includes a specific salt bridge in the linker part of the protein, was found in almost all of the simulations, and this information was evaluated further to reveal that this can be the general folding motif for all similar proteins that possess one transmembrane helix and a short linker part that joins it with the rest of the protein. By continuation of the urge to explain the role of the membrane in enzymatic function of COMT, another idea was also investigated: namely, the suggestion that ligands for that enzyme might have different characteristics in regard to their affinity to how the membrane was evaluated, to check whether the membrane binding part of COMT role is indeed meant to make it more accessible to those ligands which stay close to the membrane. This idea was studied with the atomistic molecular dynamics simulations where two COMT ligands—dopamine and L-dopa—were simulated with the membranes of various compositions, and furthermore the results were validated by experiments. The data from that study was consistent with the suggested idea of preferential binding of some ligands to lipids, but also this finding has been shown to have more possible implications for the neurotransmission process and other highly important physiological processes.

The second part of this work focuses on the role of cholesterol in hydrophobic matching of peptides and the resulting sorting of transmembrane peptides according to their hydrophobic length. Experimental data from collaborating team suggested that under negative mismatch and the presence of cholesterol in membranes, peptides could lat-

erally sort. Nevertheless, molecular mechanisms of that were unclear. Atomistic molecular dynamics simulations performed for this part of the thesis revealed that cholesterol increases the significance of the negative hydrophobic mismatch, and thus it shifts preference of proteins in such conditions to cluster into domains to minimize the mismatch. In the second part of this study, extended atomistic molecular dynamics simulations showed that cholesterol has a preference to stay in the vicinity of the peptide under negative mismatch when compared to a positive mismatch case. Even more strikingly, cholesterol orientates around the negatively mismatched peptide in a special geometrical configuration with its rough side exposed in the direction of peptide.

In summation, studies for this work demonstrated a view on some aspects of the lipid-protein interactions at the molecular level retrieved through the atomistic molecular dynamics simulations. Importantly, many of the aspects presented here were validated with experiments or suggested explanation for the phenomena observed beforehand by experimental methods. Certainly, lipids are important for the function of proteins, and as it is shown in this thesis, joining experimental and computational approach is a very good way to understand this complicated interplay better and to provide atomistic details of these dynamic processes.

Preface

Work for this thesis has been conducted at the Department of Physics of the Tampere University of Technology during the years 2010–2014. It consists of three articles that deal with the lipid-protein interactions studied using the atomistic molecular dynamics simulations.

The first steps toward the research for this thesis started in 2008 when Prof. Marta Pasenkiewicz-Gierula helped the author of this thesis organize a research visit to the University of Helsinki where the author had a pleasure to work with Dr. Alex Bunker and Dr. Tomasz Rog. Therefore, I would like to thank people involved in this fruitful collaboration.

In addition, my great thanks go to my doctoral thesis supervisor Prof. Ilpo Vattulainen, who gave me a chance to work as a summer student in his group and later on to start my doctoral studies in 2010. I want to express my greatest gratitude to Prof. Ilpo Vattulainen who provided me with the best possible environment to develop myself in science, for his help, but also for his trust in me, and equally important, for being a very flexible, tolerant, and kind supervisor.

I want to emphasize the role of Dr. Tomasz Rog in all stages of my scientific career. Many thanks for his patience, time spent to help and support me, and for his contribution to my scientific development. Also, I would like to thank Dr. Tomasz Rog for providing good support in all other matters.

Both Prof. Ilpo Vattulainen and Dr. Tomasz Rog showed me the right path to conduct the research for this thesis in the best possible way, and I could not wish for more than I received from them during this process.

I want to express my appreciation to collaborating teams, which made my research more solid, and my visits in their groups were such a unique experience. I would like to thank the group in Tampere for the magnificent atmosphere, kindness, openness, and help in research and in life. All of you made my time in Tampere pleasant and memorable.

Special thanks go to my family, which always supported me by all possible means.

Tampere, May 2014

Adam Orłowski

Contents

List of Figures

List of Tables

List of Publications

Author's Contribution

1 INTRODUCTION 1

2 OVERVIEW 4

2.1 Lipids as building blocks for membranes 4

2.1.1 Glycerophospholipids (GP, phospholipids) 6

2.1.2 Sphingolipids (SP) 7

2.1.3 Sterol Lipids (ST, sterols) 8

2.2 Cell membrane models 8

2.3 Cell membrane structure and composition 12

2.4 Function of cell membranes 13

2.5 How lipids modulate protein function 15

2.5.1 Membrane-mediated protein regulation 16

2.5.2 Lipid-mediated protein regulation 18

2.5.3 Lipid-protein interactions in the spotlight 21

3 BACKGROUND 23

3.1 COMT protein 23

3.2 Role of membrane in neurotransmission 25

3.3 Hydrophobic mismatch 26
3.4 Cholesterol and its role in hydrophobic mismatch 28
4 METHODS 31
4.1 Molecular dynamics (MD) simulations 32
4.1.1 Starting structures for MD simulations 32
4.1.2 Force field and its derivation 33
4.1.3 Force fields in practice 36
4.1.4 Generating appropriate dynamics and physical conditions 36
4.2 Analysis methods 37
4.2.1 Qualitative and quantitative measures 38
4.2.2 Directed interactions 38
4.2.3 Collective properties 39
4.2.4 Protein analyses 40
5 OVERVIEW OF THE SYSTEMS STUDIED IN THIS WORK 41
5.1 Article 1 41
5.2 Article 2 41
5.3 Article 3 42
5.4 Unpublished results 42
6 CORE RESEARCH FINDINGS 43
6.1 Membrane is a unique environment for protein function 43
6.1.1 Role of the membrane-binding fragment of the COMT protein 44
6.1.2 Importance of binding of dopamine and L-dopa to membrane 46
6.1.3 Conclusions 48

6.2 Cholesterol and hydrophobic mismatch of peptides 49

6.2.1 Cholesterol modulates hydrophobic mismatch and sorting of peptides .. 49

6.2.2 Orientation of cholesterol varies in the vicinity of the mismatched peptide 50

6.2.3 Conclusions 55

CONCLUDING REMARKS 57

REFERENCES 59

List of Figures

FIGURE 1. Lipid vesicles as a foundation of the earliest forms of life on Earth (upper panel - adapted from (Szostak et al. 2001)) and proteins embedded in a lipid bilayer (lower panel - adapted from (Stroud 2011)). 2

FIGURE 2. Schematic picture of an amphipathic lipid. The polar headgroup is depicted in red, and the non-polar hydrocarbon chain in blue. 4

FIGURE 3. Chemical structures of the representative lipids' categories from (Fahy et al. 2005). a) Fatty Acids (FA), b) Glycerolipids (GL), c) Glycerophospholipids (GP), d) Sphingolipids (SP), e) Sterol Lipids (ST), f) Prenol Lipids (PR), g) Saccharolipids (SL), h) Polyketides (PK). Adapted from (Fahy et al. 2005). 6

FIGURE 4. Glycerophospholipid (GP) types built by substitution of the headgroup moiety (X). Adapted from (Aktas et al. 2014). 7

FIGURE 5. Schematic picture of a sterol (left) and chemical structure of cholesterol (right). 8

FIGURE 6. Schematic representation of the Pauci-Molecular (sandwich) membrane model (Danielli & Davson 1935) (up), and the fluid mosaic model (Singer & Nicolson 1972) (down – adapted from: http://www.uic.edu/classes/bios/bios100/lectf03am/fluidmos.jpg accessed 07.05.2014). 10

FIGURE 7. Lipid raft concept. Adapted from (Lingwood & Simons 2010). 11

FIGURE 8. Cell with its organelles depicted (Picture adapted from: Mariana Ruiz Villarreal: http://en.wikipedia.org/wiki/File:Animal_cell_structure_en.svg accessed on 07.05.2014; public domain). 13

FIGURE 9. Diffusion through a membrane of some compounds (green and blue arrows) and impermeability to some molecules (yellow and red). 15

FIGURE 10. Crystal structure of the Na+K+ATPase dimer (blue) with the bound cholesterol (red) (pdb record: 4HYT). Picture made using VMD package (Humphrey et al. 1996). 19

FIGURE 11. Schematic picture of the MB-COMT protein attached to a membrane by its transmembrane domain helix and a linker. 23

FIGURE 12. Synapse (adapted from http://scienceblogs.com/purepedantry/2007/03/06/neuron-to-glia-synapse-on-axon/ accessed 07.05.2014). 25

FIGURE 13. Schematic overview of the possible hydrophobic mismatch conditions: positive mismatch (TM helix longer than the hydrophobic thickness of a membrane) on the left, and negative mismatch (TM helix shorter than the hydrophobic membrane thickness) on the right. 26

FIGURE 14. Possible adaptations of transmembrane proteins and lipids to a hydrophobic mismatch. Adapted from (Killian 1998). 27

FIGURE 15. Gradient of cholesterol content in cell membranes. Adapted from (Lippincott-Schwartz & Phair 2010). 28

FIGURE 16. Time evolution of the secondary structure of the MB-COMT protein's membrane binding fragment given by six independent simulations (a-f). 44

FIGURE 17. Helical structures (green and blue) of the MB-COMT linker part with the salt bridge between the residues ARG27 (yellow) and GLU40 (silver). Membrane lipids are depicted as tan lines and MB-COMT in gold as a "new cartoon" representation. Picture made using VMD (Humphrey et al. 1996). 45

FIGURE 18. Snapshots showing simulated systems (a, c, e, g, i, k) at the beginning, and (b, d, f, h, j, e) at the end of simulations (a, b, e, f, i, j). Dopamine molecules are shown in blue, and (c, d, g, h, k, l) L-dopa molecules in red. Lipid molecules depicted here are (a, b, c, d) PC and (e, f, g, h) PC-PE-PS, and (i, j, k, l) SM-PC-CHOL. Water is not shown for clarity. Snapshots were prepared using the VMD package (Humphrey et al. 1996). 46

FIGURE 19. Density profiles of dopamine (a, c, e) and (b, d, f) L-dopa (black line), lipids' nitrogen (blue line), lipids' phosphate (pink line), and all lipid atoms (red line). Data corresponds to (a, b) PC, (c, d) PC-PE-PS bilayers, and (e, f) SM-PC-CHOL. Position of the lipid bilayer is shown schematically. 47

FIGURE 20. Hydrophobic mismatch between a transmembrane peptide and a lipid bilayer determines bilayer structure, helix orientation, and fold. (A) Snapshots from the MD simulations with LW21 TM peptide (red) embedded in C16:1 and C24:1 PC (headgroups are depicted in dark blue, chains in light blue) in the presence and absence of cholesterol (gray). Positive and negative mismatch are indicated by blue and red color, respectively. (B) Distance profiles of lipid chain order (S_{cd} order

parameter of the *sn*-1 chain) with respect to the helix backbone at 0 nm (t = 500 ns) for C16 : 1 and C24 : 1. Black denotes 0% cholesterol, red 20% cholesterol. The S_{cd} parameter shown here represents the average value of the S_{cd} profile along the hydrocarbon chain. (C) Membrane thickness (P-P distance in units of nanometers) with respect to the helix backbone at 0 nm (t = 500 ns) for C16:1 and C24:1. Black stands for 0% cholesterol, red 20% cholesterol. (D) Bar graph of the average tilt angle of LW21 in the four simulations in units of degrees (see axis). (E) Fold adopted by LW21 over the simulation time in percent (see legend). 50

FIGURE 21. Radial distribution function of the center of mass (COM) of cholesterol molecules around the peptide's COM projected on the membrane plane, averaged over four peptides present in each system: black – PC24 (negative mismatch) and red – PC16 (positive mismatch). 51

FIGURE 22. Panel A shows the reference axes used in the two-dimensional density distribution calculations shown in panels D–G. The origin of the axis is C13 colored in yellow. The vector between C13 (yellow) and C18 (orange) points along the x-axis. The triangle between C18 (orange), C13 (yellow), and C10 (blue) is in the xz-plane and is depicted in red. Panel B shows a schematic view of cholesterol as a projection in the reference xy-plane from the terminal acyl chain toward the head as shown in Panel C by the arrow. Two-dimensional density distributions in (D, F – upper and lower layer) positive mismatch and (E, G – upper and lower layer) negative mismatch for the peptides around a tagged cholesterol molecule. The different faces of cholesterol can be distinguished in panels D–G: the smooth α-face corresponds to the region x<0 and the rough β-face to x>0. 53

FIGURE 23. Schematic picture of cholesterol behavior under negative (upper scheme) and positive (lower scheme) mismatch. In case of negative mismatch, cholesterol tends to orientate its rough face toward the peptide and concentrate closer to it, while the behavior is opposite in positive mismatch. 55

List of Tables

TABLE 1. Sphingolipid families (Stillwell 2013). 7

TABLE 2. The average lipid composition of a mammalian liver cell (Stilwell 2013). 13

TABLE 3. Average number of lipids for varying distances from the peptide center of mass, and the percentage of cholesterol among all lipids at that distance. The fixed total value of Nchol/(NPC+NChol) in each system is 20%. 52

List of Symbols and Abbreviations

CL	cardiolipin
COMT	catechol-o-methyltransferase
ER	endoplasmic reticulum
GPCR	g-protein coupled receptor
Km	Michaelis constant
Ld	liquid disordered
Lo	liquid ordered
LW21	K2W2L8AL8W2K2 peptide
MB-COMT	membrane bound catechol-O-methyltransferase
MD	molecular dynamics
NMR	nuclear magnetic resonance
OPLS-AA	optimized parameters for liquid simulations all-atom
S-COMT	soluble catechol-O-methyltransferase
PA	phosphatidic acid
PC	phosphatidylcholine
PE	phosphatidylethanolamine
PG	phosphatidylglycerol
PI	phosphatidylinositol
PIP2	phosphatidylinositol4,5-bisphosphate
PME	particle mesh ewald
PS	phosphatidylserine

RDF	radial distribution function
REMD	replica-exchange molecular dynamics
Scd	deuterium order parameter
TM	transmembrane
VMD	visual molecular dynamics

List of Publications

1) **Orłowski, A.**, St-Pierre, J.-F., Magarkar, A., Bunker, A., Pasenkiewicz-Gierula, M., Vattulainen, I., & Róg, T. 2011. Properties of the membrane binding component of catechol-O-methyltransferase revealed by atomistic molecular dynamics simulations. *Journal of Physical Chemistry B*. 115:13541-13550.
2) Kaiser, H.-J., **Orłowski, A.**, Róg, T., Nyholm, T.K.M., Chai, W., Feizi, T., Lingwood, D., Vattulainen, I., & Simons, K. 2011. Lateral sorting in model membranes by cholesterol-mediated hydrophobic matching. *Proceedings of the National Academy of Sciences*. 108:16628-16633.
3) **Orłowski, A.**, Grzybek, M., Bunker, A., Pasenkiewicz-Gierula, M., Vattulainen, I., Männistö, P.T., & Róg, T. 2012. Strong preferences of dopamine and L-dopa towards lipid head group: Importance of lipid composition and implication for neurotransmitter metabolism. *Journal of Neurochemistry*. 122:681-690.

In this thesis, the candidate also presents additional results to complement those presented in Article 2. These unpublished data will be later submitted for publication (**Orłowski, A.**, Martinez-Seara, H., Mokkila, S., Róg, T., Vattulainen, I. Cholesterol-protein interactions modulated by hydrophobic matching. Manuscript under preparation (2014)), but since the manuscript at the time of writing this thesis is still incomplete, the candidate prefers not to include the draft of the paper in this thesis. Yet, the key results of that study will be discussed in the end of this thesis.

Author's contribution

The author has played an active role in all stages of the research reported in this thesis. Simulated systems in all publications were prepared and simulated by the author of the thesis (except the REMD simulations of the linker in Article 1). All of the MD simulation data analyses presented in the articles were performed by the author of this thesis, if not stated differently in the thesis text. The author took an active part in the writing of Article 2 and wrote Articles 1 and 3. Additionally, the author played a key role in all stages of work regarding the unpublished work.

1 Introduction

When looking back to the very early beginning of life on Earth, there are many unknowns and doubts that we encounter if we want to describe it accurately. Details of the processes that led to the formation of the early forms of life are still mysterious. However, there is an agreement that the compartmentalization and isolation of the interior of a protocell from exterior environment was the necessary step, taken about 3.5 billion years ago, for the establishment of the first forms of what can be classified as life (Szostak et al. 2001). It is the spontaneous self-assembly of amphiphilic molecules (called lipids) into vesicles which is thought to provide this mechanism of isolation for the protocells that allowed life to occur in its present form (Monnard et al. 2002). The uniqieness of how lipid complexes are established, as well as the driving forces for their division, are in the core of the conceptual protocells, which are thought to be the earliest forms of life (Chen 2006; Szostak et al. 2001) (Figure 1).

Interactions within the protocells between the lipids and many other molecules were becoming more and more complicated, leading to complex systems that are nowadays represented in all living organisms (Chen 2006). In this complicated process, cells controlled a set of many different kinds of biomolecules. Nowadays, cells serve as a unique environment for biological processes. While the number of these molecular species is huge, they can be grouped into four main groups: carbohydrates, lipids, proteins, and nucleic acids. They are required to cooperate with each other in a very specific manner that allows the biological processes to function properly and in such a way that homeostasis of a living cell is maintained. The principles of these interactions are in the main focus of the contemporary natural sciences. We are now equipped with the knowledge of the main ingredients of biological systems, but we still lack detailed information about the interactions between them. There are different approaches to reveal the rules of those phenomena, but due to technical limitations, one can study successfully only a limited scope of the molecular world to unlock its unique detals. Substantial problems, which are discussed further, are related to experimental studies of lipid-protein interactions. Nevertheless, all of these small findings on biomolecular interactions encompass a bigger picture of biological functions and rules that govern them. Their understanding is a crucial step to better grasp the malfunctions of this complicated biochemical machinery, which takes place in many fatal diseases. It is also the case with lipid-protein interactions, which were historically very often ignored and thought to be irrelevant for

protein function. Nonetheless, the role of lipids has recently become more and more acknowledged, and it has been shown to be very important for a proper function of living cells. It is now widely accepted that virtually all biological proceses are somehow related to membranes. Therefore, it is challenging and also fascinating to study lipid-protein interactions (Hilgemann 2003).

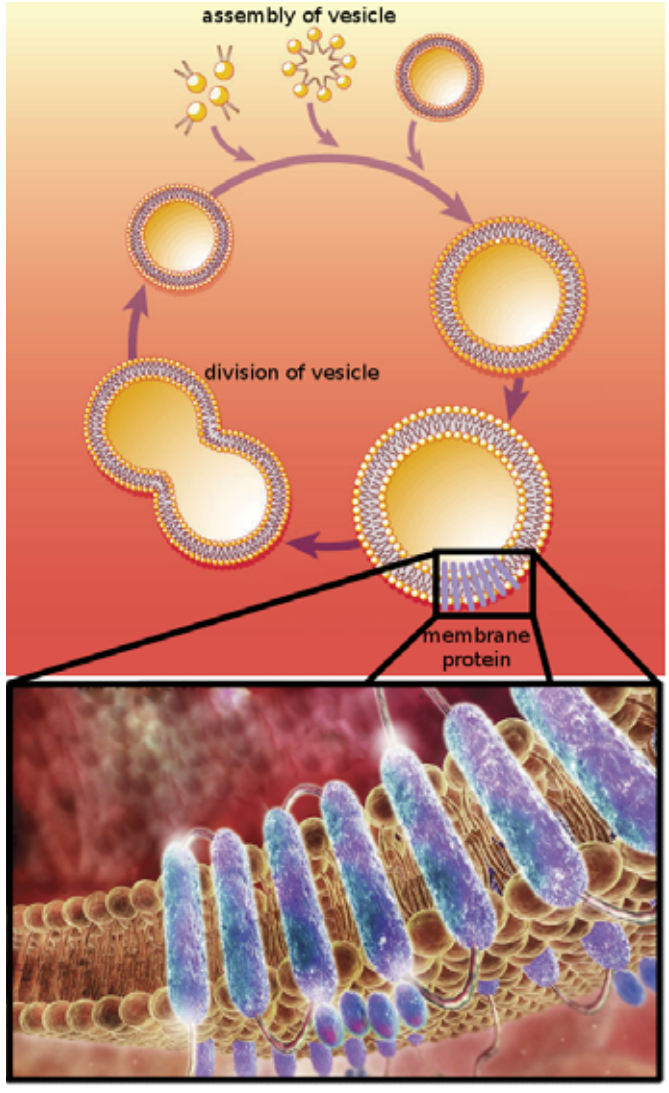

FIGURE 1. Lipid vesicles as a foundation of the earliest forms of life on Earth (upper panel - adapted from (Szostak et al. 2001)) and proteins embedded in a lipid bilayer (lower panel - adapted from (Stroud 2011)).

In the research work described in this thesis, lipid-protein interactions were investigated using the atomistic molecular dynamics simulation method. The simulation results were often complemented by “wet lab” experiments conducted by the collaborating research groups. Both the specific case of a membrane protein (COMT), as well as a non-specific synthetic model transmembrane peptide (LW21) were studied in the context of lipids. The two leading general themes in the thesis are therefore:

1. membrane as a unique environment for protein function; and

2. cholesterol modulating the hydrophobic mismatch of peptides.

The results strongly support the idea that lipids do matter for proteins, and that they influence each other in a manner that cannot be ignored. For instance, it has been shown elsewhere that membrane environment changes dramatically the kinetic characteristic of COMT (Myöhänen et al. 2010). This mysterious phenomenon was investigated in this thesis, leading to novel insight on the issue, and further the results have been found to have even broader implications in other biological processes, such as (quite surprisingly) neurotransmition, or transmembrane protein folding. Another aspect of the presented research is directly related to a very interesting observation of a cholesterol gradient inside cells (high content in plasma membrane, and lower in membranes inside the cell). This gradient has been postulated to play a role in the trafficking of peptides according to their length (Bretscher & Munro 1993). However, the molecular mechanism has remained unknown. Herein, the atomistic molecular dynamics simulations provided an explanation for that. Moreover, novel insight into non-specific cholesterol-peptide interactions was also shown through the observation of preferential geometrical orientation of cholesterol in the vicinity of a negatively mismatched peptide.

In the next chapter, a basic overview of lipids, membranes, proteins, and the interactions between them is given. It is followed by Chapter 3, which contains background information related to the main themes of the thesis. Chapters 4 and 5 describe the methodology and give an overview of the systems used in the studies. Finally, Chapter 6 presents the main results that are accompanied with concluding remarks and a discussion of the presented results.

2 Overview

Proteins and nucleic acids have been subjects of intensive studies during the last century, and many breakthroughs have been achieved in the field. It was possible, due to the rapid development of techniques that allow for the examination of three-dimensional structures of these molecules, to study, for example, their dynamics and chemistry. Nevertheless, lipid membranes have not received similar attention, and for a long time they were thought to be just a solvent for membrane proteins and building blocks for membranes. The next five paragraphs provide basic facts about lipids and membranes together with their historical background, and the chapter is closed with a discussion of membrane proteins.

2.1 Lipids as building blocks for membranes

It is the Greek term “lipos,” meaning fat, from which the word “lipids” is derived. Insolubility in water, which is the main feature of lipids, is related to the presence of long hydrocarbons in their structure. Yet, biologically relevant lipids are amphipathic, meaning that they also contain a hydrophilic head group (Figure 2). This “amphipathic” nature of lipids is the reason why biological membranes form in the first place.

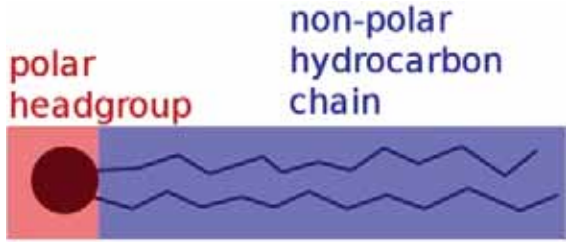

FIGURE 2. Schematic picture of an amphipathic lipid. The polar headgroup is depicted in red, and the non-polar hydrocarbon chain in blue.

It is important to realize that there are thousands of different lipid species, which are asymmetrically distributed over the exoplasmic and cytoplasmic leaflets of membranes (van Meer 1989). It is rather impossible to consider that such diversity would be a coincidence (Dowhan 1997). Moreover, when not only major differences of lipids are considered but also minor ones resulting, for example, in differences in acyl chain saturation level, the number of distinct lipids increases drastically. As an example, human tears contain more than 30,000 molecular species (Nicolaides & Santos 1985; Borchman et al. 2007). Knowledge about the complexity of lipid compositions is gained through novel methods, such as high-throughput lipid profiling in an emerging field of lipidomics (Shevchenko & Simons 2010). Based on the data obtained using lipidomics, a comprehensive classification for lipids has been proposed, and it has been suggested to divide lipids into eight main classes (Figure 3) (Fahy et al. 2005):

- FA. Fatty Acids
- GL. Glycerolipids
- GP. Glycerophospholipids
- SP. Sphingolipids
- ST. Sterol Lipids
- PR. Prenol Lipids
- SL. Saccharolipids
- PK. Polyketides

Of these eight classes, the most interesting ones from the perspective of biological membranes are glycerophospholipids, sphingolipids, and sterols. Further complexity of lipids in all of these classes (discussed below) arises from modifications of the hydrophilic headgroups and the hydrophobic hydrocarbon tails (Coskun & Simons 2011).

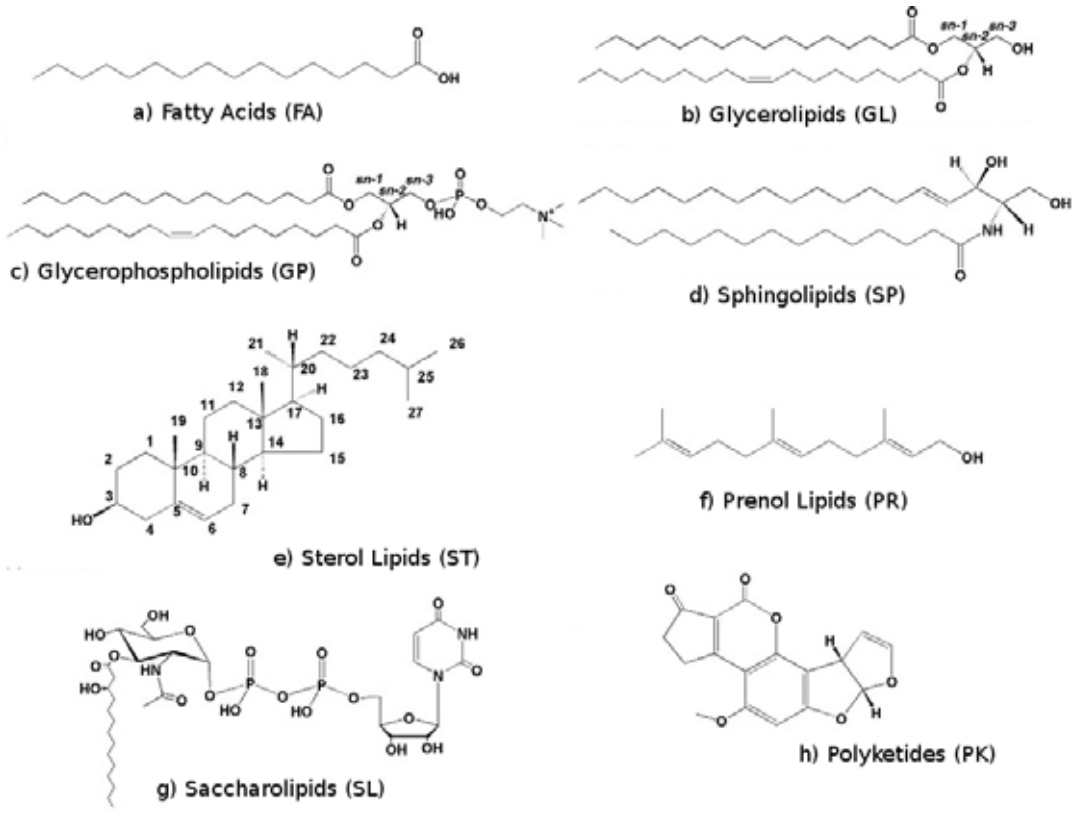

FIGURE 3. Chemical structures of the representative lipids' categories from (Fahy et al. 2005). a) Fatty Acids (FA), b) Glycerolipids (GL), c) Glycerophospholipids (GP), d) Sphingolipids (SP), e) Sterol Lipids (ST), f) Prenol Lipids (PR), g) Saccharolipids (SL), h) Polyketides (PK). Adapted from (Fahy et al. 2005).

2.1.1 Glycerophospholipids (GP, phospholipids)

By modification of the headgroup of glycerophospholipids, different chemical moieties can be added into the sn-3 position of the glycerol backbone ("X" in Figure 4). By doing so, many phospholipids (from which some are anionic) can be constructed, such as: phosphatidylcholine (PC), phosphatidylethanolamine (PE), phosphatidylserine (PS), phosphatidylglycerol (PG), phosphatidylinositol (PI), and phosphatidic acid (PA). A very unusual lipid, which is also interesting from the physiological perspective, is a phospholipid called cardiolipin (CL), which consists of two PAs joined together by a glycerol group. This lipid is found almost exclusively in the mitochondrial inner membrane, where by cooperation with membrane proteins it fulfills its physiological role—this is discussed in more detail later.

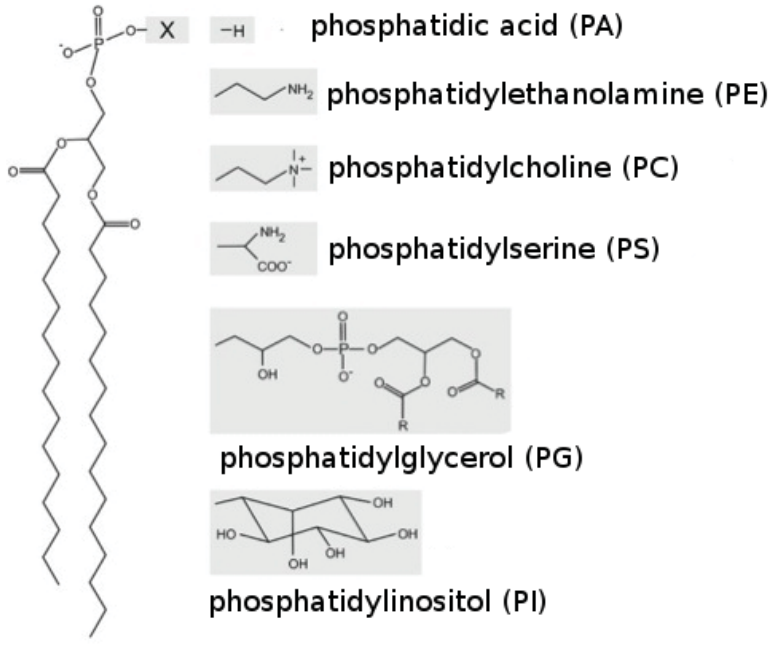

FIGURE 4. Glycerophospholipid (GP) types built by substitution of the headgroup moiety (X). Adapted from (Aktas et al. 2014).

2.1.2 Sphingolipids (SP)

Sphingolipids are based on a sphingosine lipid backbone, which is amide-linked to a variable fatty acid to form a ceramide (Figure 3 d). Theoretically, it is possible to create thousands of possible lipids through different permutations (Yetukuri 2008), and more than 60 different sphingolipids have been found so far in humans (Stillwell 2013). Different sphingolipids are grouped according to their polar head group substituents (see Table 1).

TABLE 1. Sphingolipid families (Stillwell 2013).

Name	Headgroup
Ceramide	-H
Sphingomyelin	Phosphocholine, phosphoethanolamine
Cerebroside	Glucose or galactose
Globoside	Di, tri, or tetra saccharide
Ganglioside	Complex oligosaccharide (with at least one sialic acid)

2.1.3 Sterol Lipids (ST, sterols)

Sterols are composed of three parts: polar head, rigid sterol ring, and tail (Figure 5 – left). The polar head anchors the lipid into a membrane-water interface, while the rigid sterol ring is responsible for many of the lipid functions and resides in the hydrophobic core of a bilayer. One of the most common and widely studied sterols is cholesterol, whose function and properties are discussed in detail below. Cholesterol's structure, similarly to all sterols, consists of three elements that are important for its membrane-related functions: the rigid steroid rings, the small hydrophilic 3β-hydroxyl group, and a short hydrocarbon chain (Figure 5 – right) (Róg et al. 2009). Importantly, modifications of the structural elements of this sterol change the properties that it exerts on a lipid membrane (De Kruyff et al. 1973). The steroid ring of cholesterol includes four rings—three with six carbons and one with five. The rings establish a flat and rigid structure. Two methyl groups give rise to cholesterol's asymmetry—there is a flat side (α-face) and a rough one with two methyl substituents (β-face) (Róg et al. 2009).

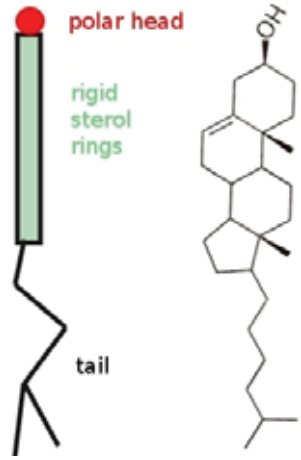

FIGURE 5. Schematic picture of a sterol (left) and chemical structure of cholesterol (right).

2.2 Cell membrane models

The first theoretical picture of cell membranes, resulting from studies on plasma membranes was attributed to Wilhelm Pfeffer, who concluded that the cell barrier is a thin and semi-permeable layer (Stillwell 2013). He compared it to an artificial copper ferrocyanide membrane. This hypothesis was improved 20 years later by Charles Ernest Overton, who showed the lipid nature of plasma membranes. Overton also determined the principles of membrane permeability and related them to the solubility of solutes in oil. Later on, he extended his theory and showed the relationship between anesthetic efficacy, membrane permeability, and their solubility in oil—which is now referred to as

the Meyer-Overton Theory (Overton 1901). Overton also observed the active transport of some solutes through biological membranes and described it as “uphill” transport. The next big step in the research on biological membranes was achieved in 1925, when Gorter and Grender showed for the first time that plasma membranes of erythrocytes are arranged in bilayer configuration by lipids (Gorter & Grender 1925). Yet, despite all these findings, nobody proposed a general model for lipid membranes, until in 1935 when Danielli and Davson proposed their Pauci-Molecular membrane model (Danielli & Davson 1935) in which proteins are attached to the membrane surface to form a protein-lipids-protein “sandwich” (Figure 6 – upper panel). It was an important step in the development of models for biological membranes, since it concentrated on lipids forming the core of membranes and also included proteins as one of the ingredients of the model. Although, it did not predict proteins’ incorporation into a lipid bilayer, and it was also limited to a static picture of membranes with a very limited variability of lipids and their distribution. Nevertheless, it was the first major step toward a realistic model for the biological membranes. The Pauci-Molecular model was extended to all plasma membranes of all cells and organelles by electron microscopy observations, and was then named the “unit membrane” model by J. David Robertson (Robertson 1959; Robertson 1960). Despite the progress, there was not yet agreement on the model for biological membranes that would have included all the known features and characteristics of it (Stoeckenius & Engelman 1969), until the “fluid mosaic” model was proposed by Singer and Nicolson (Figure 6 – lower panel). In this model, the membrane was defined as “an oriented, two-dimensional viscous solution of amphipathic proteins (or lipoproteins) and lipids in instantaneous thermodynamics equilibrium” (Singer & Nicolson 1972). In this model, proteins can be both peripherally and integrally asymmetrically associated with a membrane in a “mosaic-like” pattern. Also, for the first time, the dynamics and the fluidity of membranes was underlined, and until this day, it is the feature that has remained as the main obstacle in understanding the properties of lipid-protein complexes.

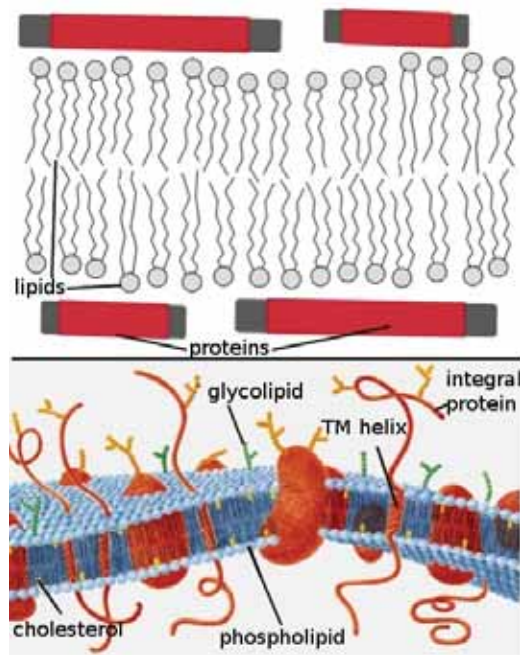

FIGURE 6. Schematic representation of the Pauci-Molecular (sandwich) membrane model (Danielli & Davson 1935) (up), and the fluid mosaic model (Singer & Nicolson 1972) (down – adapted from: http://www.uic.edu/classes/bios/bios100/lectf03am/fluidmos.jpg accessed 07.05.2014).

The fluid mosaic model changed the paradigm in biomembrane research, but yet it could not explain some of the phenomena observed in membranes, and even more importantly, it did not include some of its significant features such as the lipid composition diversity or domain formation. Regarding the latter, self-organization of lipids in membranes was not introduced in the fluid mosaic model despite the fact that in the early 1970s many reports indicated that the lipid "domains" of a distinct physical characteristic existed in model membranes (Philips et al. 1970; Shimshick & McConnell 1973; Grant et al. 1974; Lentz et al. 1976; Schmidt et al. 1977). Such regions were referred to as "clusters of lipids" (Lee et al. 1974) or "quasicrystalline" in case of regions surrounded by crystalline lipid molecules, which had been observed in membranes (Wunderlich et al. 1975). With the use of the X-ray diffraction method, another model of membrane heterogeneity was referred to as the "lipids in a more ordered state" (Wunderlich et al. 1978), which was accompanied with other reports of lipid phase separation (Estep et al. 1979; Demel et al. 1977). At the same time, these observations were related to the physiological context by some researchers (Schmidt et al. 1977; Gebhardt 1977) with the emphasis on lipid-protein interactions as a core of membrane-mediated processes (Marcelja 1976; Mouritsen & Bloom 1984). The biological context of lipid domains was also present in the "lipid plate" model by Jain & White (Jain & White 1977), where the separation of two distinct phases (Ld – lipid disordered, and Lo – lipid ordered) in biological mem-

branes was proposed to exist, thereafter shown to be mainly due to the presence or absence of cholesterol in a membrane (Ipsen et al. 1978). Israelachvili revisited the fluid mosaic model by introducing a concept in which lipids and proteins could adjust to each other (Israelachvili 1977), which served as a basis for the “mattress model” by Mouritsen & Bloom (Mouritsen & Bloom 1984), who provided the basic principles for understanding the adaptations of proteins and lipids in hydrophobic mismatch and the resulting potential of proteins in lipid sorting. In the early 1980s, lipid domains were formalized and described by Karnovsky et al. (Karnovsky et al. 1982) but without their physiological context. These two—lipid domains and their physiological role—were bridged together in the model used for explaining the mechanism of lipids and proteins sorting from the trans Golgi network to the plasma membrane (Simons & van Meer 1988), which later evolved into a new concept of “lipid rafts” that was formalized and described by Kai Simons and Elina Ikonen in 1997 (Simons & Ikonen 1997). This model proposes that some of the lipids present in membranes (sphingolipids and sterols) associate with proteins, resulting in segregation potential (Lingwood & Simons 2010) (Figure 7).

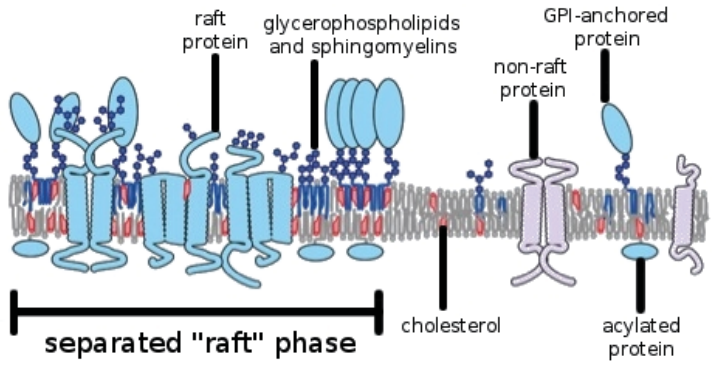

FIGURE 7. Lipid raft concept. Adapted from (Lingwood & Simons 2010).

A more precise description of lipid rafts follows: “self-associative properties unique to sphingolipid and cholesterol in vitro could facilitate selective lateral segregation in the membrane plane and serve as a basis for lipid sorting in vivo” (Simons & Ikonen 1997). Thus, it emphasizes the role of lipids in lateral organization and compartmentalization, which make membranes a non-random entity where functionality can be modulated by lipid composition. Therefore, lipid rafts are known to be a platform for proteins involved in cell signaling events (Lingwood & Simons 2010; Simons & Toomre 2000; Smart et al. 1999; Foster et al. 2003; Bini et al. 2003). This concept has dramatically changed the perception of biological membranes and membrane protein function. In principle, it provides a picture where lipids and membranes play an active functional role in cell physiology. Just to name a few examples: apoptosis, cell adhesion and migration, synaptic transmission, organization of the cytoskeleton, and protein sorting during both exocytosis and endocytosis have been reported to be lipid raft-dependent (Brown & London 1998; Simons & Toomre 2000; Harris & Siu 2002; Tsui-Pierchala et al. 2002). Lipid rafts have been suggested to be necessary for the

budding of the HIV virus with the plasma membrane (Ono & Freed 2005), and they have been reported to be the entry point for toxins to infected cells (Kovbasnjuk et al. 2001). Nevertheless, there has been also a lot of concern regarding the character, definition and even the existence of lipid rafts (Munro 2003). More specifically, methods used formerly for the detection of lipid rafts—resistance to solubilization by the detergent Triton X-100, and sensitivity to cholesterol depletion—have been criticized, and they leave space for other interpretations too (Heerklotz 2002; Pizzo et al. 2002; Edidin 2003). Moreover, rafts are very difficult to visualize in living cells, and when they are studied by indirect methods, their main features are not so easy to characterize (Anderson & Jacobson 2002; Kenworthy 2002). Despite the problems in defining lipid rafts, this concept definitely changed the paradigm and the research of the biological membrane for a long time.

2.3 Cell membrane structure and composition

All the membrane models presented above were developed to provide descriptions for complicated membrane structures that are present in all living cells. Membrane in a cell creating a barrier for itself is called a plasma (cell) membrane, but there are also other lipid membranes, internally inside a cell, that separate compartments and thereby provide distinct environments for many biochemical processes that need to be separated from each other (Figure 8). Cell trafficking is based on transport between interconnected membranes of the nuclear envelope, the rough and smooth endoplasmatic reticulum, the Golgi apparatus, lysosomes, vacuoles, and other types of small vesicles together with the plasma membrane. In total, the human body is composed of ~63 trillion cells, and there are enough membranes in a human body to cover the Earth millions of times. Nevertheless, the plasma membrane is the most dynamic and well known from all of the biological membranes (Stillwell 2013).

Table 2 provides the average lipid composition of a mammalian liver cell (Stilwell 2013). However, it has to be noted that the distribution of lipids differs between the cell organelles as well as even between the two lipid bilayer leaflets. For instance, PS is found exclusively in the inner leaflet of a membrane. Studies on the composition of membranes and the distribution of lipids in a cell are still in progress, and detailed compositions of lipids, as well as their distribution in cell compartments, needs to be revealed and associated with the function (Llorente et al. 2013).

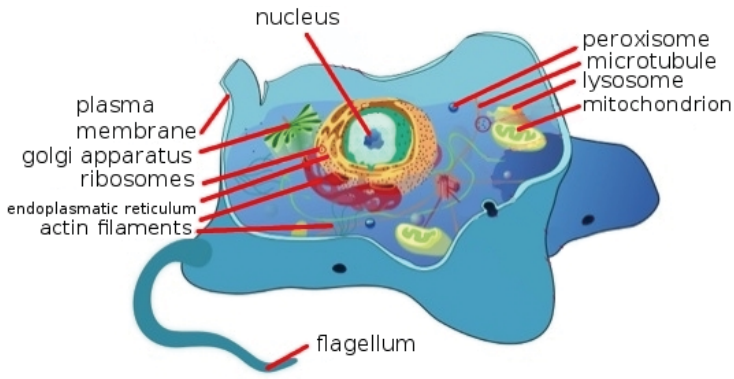

FIGURE 8. Cell with its organelles depicted (Picture adapted from: Mariana Ruiz Villarreal: http://en.wikipedia.org/wiki/File:Animal_cell_structure_en.svg accessed on 07.05.2014; public domain).

TABLE 2. The average lipid composition of a mammalian liver cell (Stilwell 2013).

Lipid	Mol (%)
PC	45–55
PE	15–25
PI	10–15
PS	5–10
PA	1–2
CL	2–5
SM	5–10
Cholesterol	10–20

2.4 Function of cell membranes

Historically, membranes were thought to be just barriers isolating cells from the outside world, or to separate cell compartments from each other. This border, however, cannot be passive and impermeable. Cells must be able to uptake some molecules from the outside and also remove unnecessary ingredients (Figure 9). Importantly, water is crucial for membrane structure and stability. The hydrophobic effect resulting from the separation of water from hydrocarbon chains is the main stabilizing force for membrane structure, though lipid headgroup-water interactions are also important. Thus, the shape of resulting lipid aggregates depends on the interplay between many forces, such as the van der Waals forces between fatty-acid chains and the forces between the electric dipoles of the lipid headgroups. Water molecules present in spaces between lipids headgroups can form

intramolecular and intermolecular hydrogen bonds between them. Dehydration of the headgroup region in a phospholipid bilayer causes the N^+ end from the choline group to move closer to the hydrocarbon layer (Bechinger & Seelig 1991). It was shown that the liquid-ordered (raft) and gel phases of membranes demonstrate a strong difference in hydration (M'Baye et al. 2008).

Very special energy-dependent active transport through the membrane is necessary to achieve ion gradients, in which sodium ions are excluded from the cell and potassium ions are taken to the inside, therefore establishing the so-called membrane potential. The calcium gradient maintained by cells has a significant role in many physiological processes (Berridge et al. 2000). In a more general view, ions can take part in membrane activities such as fusion, phase transitions, or transport across membranes (Bockmann et al. 2003). Ions can affect physical properties of membranes, including their electrostatics and fluidity: for instance, NaCl and $CaCl_2$ can modulate the order of lipid chains, decrease area per lipid of a membrane, and therefore also increase membrane thickness (Bockmann et al. 2003; Cevc 1990; Mukhopadhyay et al. 2004; Pandit et al. 2003; Miettinen et al. 2009). The mechanism is related to the binding of ions to the carbonyl groups of lipids, which in turn has implications for the lipid headgroup conformation, lipid-lipid interactions, and order of water (Mukhopadhyay et al. 2004; Sachs et al. 2004). More specifically, binding of Na^+ ions to the carbonyl oxygen can lead to the establishment of lipid complexes with reduced mobility, accompanied by bilayer thickening by $\sim$2 Å, which in turn increases the order parameter of the fatty acyl chains, alters the electrostatic potential, and rigidifies it (Bockmann et al. 2003). Importantly, these effects are more pronounced and occur mainly in the high salt-concentration regime for divalent ions like Ca^{2+} (Pabst et al. 2007). The role of ions in membrane-mediated protein activation is also recognized; for example, it has been shown by live-cell fluorescence resonance energy transfer and NMR experiments that increased Ca^{2+} concentration can induce dissociation of $CD3_{CD}$ from the membrane in T-cells, and as a consequence, CD3 tyrosine phosphorylation could take place (Li et al. 2014; Shi et al. 2012). Although it is rather weakly understood what binding of ions to membranes can cause for lipid-protein interactions, it is accepted that ionic protein–lipid interactions are critical for the structure and function of membrane receptors, ion channels, integrins, and many other proteins (Xu et al. 2008; Paddock et al. 2011; Hansen et al. 2011; Whorton & MacKinnon 2011; Kim et al. 2011; van den Bogaart et al. 2011; Heo et al. 2011). Very interestingly, it has been recently shown that lipids' conformation can be influenced by membrane composition, such as cholesterol content, and this can further modulate membrane function in physiologically relevant ways. For instance, lipid-protein interactions can be modulated in such a manner (Lingwood et al. 2011).

Nowadays it is generally accepted that biological membranes are involved in all cellular activities other than isolation, including inter-cellular communication, cell-cell recognition, and cellular signaling or energy transduction events (Stillwell 2013).

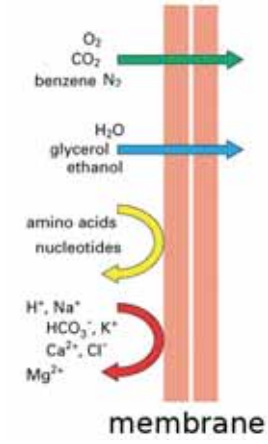

FIGURE 9. Diffusion through a membrane of some compounds (green and blue arrows) and impermeability to some molecules (yellow and red).

2.5 How lipids modulate protein function

Although lipids are very abundant and show a rather huge diversity, they do not have any biochemical catalytic activity, which proteins do have. Therefore, any consideration of membranes as physiological active units needs to take into consideration proteins that are associated with membranes. There are different ways that proteins can be attached to a membrane, and thus membrane proteins are classified into four groups: peripheral, amphitropic, integral, and lipid-linked. Intuitively, these four groups are given in the order from the weakest (periphal) to the strongest (lipid-linked) association of a protein with a lipid bilayer. Within these groups, there are subdivisions characterizing structurally and functionally the lipid-protein complex, as it is listed below (Stillwell 2013):

I. Peripheral

A. Bound to protein

B. Bound to lipid

II. Amphitropic

III. Integral

A. Endo and ecto

B. Trans-membrane

Type I: single trans-membrane α-helix

Type II: multiple trans-membrane spans by α-helices

Type III: membrane domains of several different polypeptides assembling to form a channel through the membrane – β-barrels

IV. Lipid-linked

A. Myristolylated

B. Palmitoylated

C. Prenylated

D. GPI-linked

Nearly half of all known proteins have some association with a membrane (Stillwell 2013) and around 20–30% of all genes in the genome encode proteins which are integral membrane proteins (Krogh et al. 2001). By merging two facts—diversity of lipids in membranes is much higher than needed to form simple bilayers (Bretscher 1973), and the number of proteins embedded in them—it becomes obvious that Nature has not wasted its resources and energy to evolve to that state without any particular and practical reason. Lipids are therefore not only forming the platforms for membrane proteins and borders for compartments in cells, but they also serve as functional units in complex biochemical pathways, where the interplay between lipids and proteins is crucial for a proper functioning of a cell—what is recently recognized more than ever before (Hilgemann 2003).

The lipid composition of a membrane can have an impact on proteins in two distinct ways. It can be tuned by the bulk physical properties of the membranes (Sackmann 1984) like hydrophobic thickness, rigidity, fluidity, membrane curvature, lateral pressure, or electrostatic potential, and/or through specific lipid-protein interactions, which could stoichiometrically and allosterically modify protein structure and function (Coskun & Simons 2011; Contreras et al. 2012). The next two paragraphs discuss these two types of protein modulation by membranes and lipids.

2.5.1 Membrane-mediated protein regulation

The life of a membrane protein starts with its synthesis, followed by membrane insertion and assembly to a proper topology at the endoplasmic reticulum (ER). Membrane is involved in many of these steps and the final result of this process is shaped by the membrane properties such as surface charge (Dowhan & Bogdanov 2009) or hydrophobicity (Geest & Lolkema 2000).

Transmembrane proteins must in many cases passively partition into the bilayer hydrophobic core, and moreover it has been shown that lipid-protein charge interactions determine the protein topol-

ogy (Van Klompenburg et al. 1997; Bogdanov et al. 2008). More specifically, zwitterionic lipids, such as PE, can act as a chaperone in protein folding in a very similar way to the protein molecular chaperones (Bogdanov & Dowhan 1998). Noticeably, collective charge properties of lipids play a key role here rather than the strict structural requirements of proteins and lipids, and such "lipochaperone" could remove the energy barrier or prevent the formation of an energy barrier in the folding of membrane proteins (Bogdanov & Dowhan 1999).

Once the membrane protein is properly folded, assembled, and inserted into the ER, it has to be very often transferred to its final destination (membrane), where it is supposed to function, for instance to the Golgi complex, endosomes, lysosomes, and very often to the plasma membrane. Hydrophobic mismatch (the difference between the transmembrane protein length and the lipid bilayer's hydrophobic core thickness) and cholesterol gradient in cell compartments (from low concentration in the Golgi complex to a very high concentration in the plasma membrane) play an important role in this process, allowing proteins to be sorted according to their transmembrane segments' length (Lundbaek et al. 2003; van Meer et al. 2008). Very importantly, by controlling the hydrophobic mismatch, protein function can be regulated, as it has been shown for KcsA, MscL, and Ca^{2+}-ATPase (Lee 2011). It can serve as a passive silencing mechanism of proteins' function on their way to their final destination. In this type of protein regulation it has been suggested that changing the hydrophobic mismatch can cause new protein conformations that are not present under non-mismatched conditions. For instance, in the case of Ca^{2+}-ATPase, Ca^{2+}-binding sites are located between the TM helices of the protein, and such changes in the packing of the helices caused by the mismatch could possibly lead to changes in the Ca^{2+}-binding site (Lee 2011). In such a way, Gramicidin A channel may undergo a conformational change to a non-channel structure under extreme negative hydrophobic mismatch (Mobashery et al. 1997; Kelkar & Chattopadhyay 2007; Basu et al. 2014).

When a protein is nicely settled in a proper membrane, its function can be regulated by dynamic, structural, and thermodynamic membrane properties (Nielsen et al. 1998; Phillips et al. 2009; Bagatolli 2013). In principle, hydrophobic interactions between membrane lipids and membrane proteins couple the protein conformation to the physical properties of the membrane (Epand & Epand 1994). Thus, for instance the aforementioned Ca^{2+}-ATPase conformational state can be affected by the phase of the membrane, resulting in low activities in the gel phase environment (Lee 2003; Starling et al. 1995a; Starling et al. 1995b). Another membrane feature that modulates proteins is related to the curvature stress of a membrane that can modulate, for instance, the gramicidin A monomer-dimer reaction (Lundbaek & Andersen 1994; Lunbaek et al. 1997) or rhodpsin function (Brown 1994).

The lateral pressure across a membrane is its physical property that is expansive in the headgroup region, tensile in the interfacial regions, and again expansive in the acyl-chain region. The pressure changes exert a stress on integral membrane proteins, and therefore it was proposed as an amplifier of small changes in membrane composition, having a mechanistic link to protein function (Can-

tor 1997). Interestingly, lateral pressure changes caused by the action of anesthetics on membranes were linked to the receptors' desensitization (Cantor 1998), but also other specific lipids, like sterols, or solutes and drugs penetrating the membrane can have a similar effect on many other proteins (Mouritsen & Jørgensen 1998; Bagatolli et al. 2010). Molecular dynamics simulations indicated that the lateral pressure is also relevant for lipid rafts (Niemelä et al. 2007), as well as for protein activation (Ollila et al. 2011). Tension within a cell membrane that serves as a mechanism for mechanosensitive channels like MscL (Hamill & Martinac 2001) was also found to induce opening of some ion channels (Patel et al. 2001). Membrane elasticity as a general mechanism for protein regulation was also suggested to be significant (McIntosh & Simon 2006). Membrane curvature stress that results from the average molecular shape of different lipid molecules is coupled to membrane proteins' function and is also linked to formation of lipid domains and laterally differentiated regions of membranes (Mouritsen 2013).

It has to be also noted that many of these physical properties of membranes that can shape protein function are interrelated, and changes in one of them would inevitably perturb another. As an example, the aforementioned lateral pressure changes have been speculated to be a physical mechanism for protein regulation by hydrophobic mismatch through shifting of the balance of the pressure between the headgroup and the acyl-chain regions (Cantor 1999).

The membrane-mediated protein regulation, described above, was for a long time thought to be the only mechanism of influence of lipids on proteins, but this turned out to be false because of the possibility of a specific lipid-mediated protein regulation, which is described in the next section.

2.5.2 Lipid-mediated protein regulation

The second way of how membranes can modulate proteins is through single lipid species. In such a case, it is important to answer the question of whether some lipids prefer to stay in the close vicinity of a membrane protein, or is it so that the lipids simply do not care about the protein in their neighborhood? Or, even further, do membrane proteins have specific binding sites for lipids? These questions are still partly unresolved, but it seems that both options are possible—there are weakly associated annular lipids, but also ones that are destined for specific binding sites of membrane proteins. Some of the lipids indeed constitute the so-called first shell of lipids around an integral protein, and they are referred to as annular lipids (Lee 2011). These lipids can follow protein laterally and move significantly slower than other lipids in the bulk (Niemelä et al. 2010). However, many reports have shown that single lipid species are tightly affecting some membrane protein functions as well (Fry & Green 1980; Gimpl et al. 1997; Gomez & Robinson 1999; Tang et al. 2006; Bao & Duong 2013). This brings up a second issue questioned earlier: are there lipids that can constitute to membrane protein function by specific lipid-protein interaction? Studies with structural methods have shown that some lipids are indeed integrated very tightly with membrane proteins, and even after detergent treatment they stay attached to the protein, resulting in crystal structures of proteins resolved with lipids in their structure (Cherezov et al. 2007; Raunser & Walz 2009;

Hunte & Richers 2008; Payandeh et al. 2011). To date, X-ray diffraction, electron crystallography, and NMR have revealed over 100 specific lipid binding sites in membrane proteins, including lipids such as PC, PIP2, PI, PE, PG, and CL, or cholesterol (Yeagle 2014). These lipids can find their way to the binding sites of the proteins by simple diffusion in the membrane, and direct interaction can influence membrane proteins' conformation, and thus also their function. Importantly, this mechanism would also explain the observation of so many lipid species in biological membranes.

It can be either headgroup that binds by polar interactions to the protein or acyl chain contacts with the protein groove which are stabilized by the van der Waals effect, though joint effects of both are also possible (Marsh 1990; Lee 2003; Palsdottir & Hunte 2004; Ernst et al. 2010; Smith 2012; Dowhan & Bogdanov 2012). For instance, cholesterol was found to be tightly bound to Na^+K^+ATPase (Laursen et al. 2013) (Figure 10), and this explained the earlier observation of cholesterol modulating Na^+K^+ATPase activity—increasing cholesterol content in the membrane (up to the native membrane cholesterol level) enhanced the enzyme activity, while other sterols of similar structure did not express such influence (Yeagle et al. 1988).

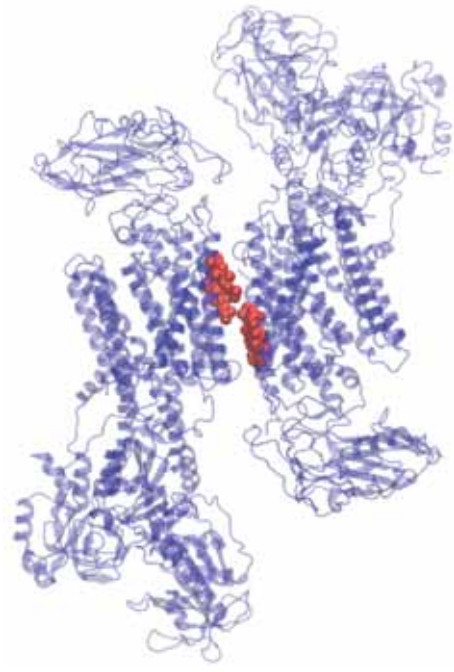

FIGURE 10. Crystal structure of the Na+K+ATPase dimer (blue) with the bound cholesterol (red) (pdb record: 4HYT). Picture made using VMD package (Humphrey et al. 1996).

Many other important proteins were found to include the cholesterol binding site in their structure, just to name a few of them: rhodopsin (Albert et al. 1996; Ruprecht et al. 2004; Albert & Boesze-Battaglia 2005), serotonin receptor (Wacker et al. 2013), micro-opioid receptor (Manglik et al.

2012), human A2A adenosine receptor (Liu et al. 2012), turkey β1 adrenergic receptor (Warne et al. 2011), and human β2 adrenergic receptor (Cherezov et al. 2007), which are all GPCRs and non-GPCR proteins such as amyloid precursor protein (Barrett et al. 2012), caveolin-1 (Epand et al. 2005), benzodiazepine receptor (Li & Papadopoulos 1998), the HIV-1 transmembrane protein gp41 (Vincent et al. 2002), and the mammalian seminal plasma protein PDC-109 (Scolari et al. 2010). In GPCRs, it was confirmed that specific sterol binding is important for the structure and stability of this class of receptors (Hanson et al. 2008), although the molecular specifics of the role of that binding remain elusive. A specific amino acid motif for cholesterol binding is present in some of the proteins (Jafurulla et al. 2011). This amino acid sequence present in the transmembrane part of many proteins is termed the cholesterol recognition/interaction amino acid consensus (CRAC) motif (Li & Papadopoulos 1998), which is defined as the presence of the pattern -L/V-(X)1-5-Y-(X)1-5-R/K-, where (X) 1-5 refers to the 1-5 residues of any amino acid. Interestingly, such lipid binding motifs have also been found for other lipids such as the signature sequence (VXXTLXXIY) within the TMD for sphingolipids (Contreras et al. 2012). In the case of cholesterol, two ways of the receptors' function modulation have to be considered: direct means by specific lipid-protein interactions and changes in physical properties of membranes caused by the presence of cholesterol. However, the joint effect of the two mechanisms is suggested as well (Paila & Chattopadhyay 2009).

Cardiolipin (CL), which is a very abundant lipid in mitochondria, was found to be very important for physiological processes taking place in this organelle (Schlame & Ren 2009). An anaerobic respiratory complex of Escherichia coli-NarGHI has shown enhanced activity in the presence of this anionic phospholipid both in vivo and in vitro (Arias-Cartin et al. 2011). CL associates with the NarGHI complex and can restore functionality of a nearly inactive detergent-solubilized enzyme complex. Similarly, CL is also a key player in the proton uptake of cytochrome bc1 where it is proposed to ensure structural integrity of the proton-conducting protein environment and to directly take part in the proton uptake (Lange et al. 2001; Pöyry et al. 2013). CL was also shown to be essential for trimer formation of Formate Dehydrogenase-N (Jormakka et al. 2002). Another striking example of the lipid-protein functional complex was revealed by the X-ray crystal structure of the Kir2.2 channel in complex with a derivative of phosphatidylinositol 4,5-bisphosphate lipid (PIP2). This physiologically minor but very dynamic phospholipid was found to control the resting membrane potential through the specific induction of the large conformational change of the channel, similar to neurotransmitter activation of ion channels at synapses (Hansen et al. 2011). More precisely, an allosteric mechanism of gating by PIP2 was proposed to be possible through the docking of the PIP2 headgroup between the cytoplasmic and the transmembrane domain of the channel, which could result in the opening of the inner helix gate. Additionally, the binding site of the specific amino acid sequence motif was recognized for the PIP2 binding site of Kir2.2, and similarly it was found in many other ion channels. In case of ion channels that are integral membrane proteins, specific binding of lipids to the intersubunit protein grooves can modulate their function by providing a "lubricant-like" mechanism, enhancing the stability of the protein and/or facilitating movements of the

subunits (Povedae al. 2014; Lee 2004). PIP2 can also diminish the repulsion between two positively charged arginine residues by introducing a negatively charged lipid headgroup between them, as it was shown for the KcsA channel (Triano et al. 2010).

Even though many examples of lipid specificity and their role in membrane protein function are known, the molecular mechanism of such regulation is still very shallowly understood. It seems that it is just a glimpse of a complicated framework of many specific lipid-protein interactions that we understand so far.

2.5.3 Lipid-protein interactions in the spotlight

The role of lipids in cellular processes and their interplay with proteins is a field which grows exponentially, leading to a much broader understanding of important biological and physiological processes, many of which are related to fatal diseases. After more than 40 years after the suggestion of the fluid mosaic model (Singer & Nicolson 1972), it is now apparent that lipid bilayers are complicated systems which are not just environments for proteins, but they also play an active role in their function. All in all, the main problem in understanding the function of biological membranes and membrane proteins is their complexity and dynamics, which are very often linked to membrane physical features that are frequently neglected (Bagatolli & Mouritsen 2013).

The apolar hydrophobic core of a membrane is separated from two aqueous compartments by an aqueous-hydrophobic interface. Therefore, proteins that are embedded in membranes exist in a unique environment, and when integral membrane proteins are extracted from cell membranes they are in most cases not soluble. This means that very special isolation protocols are required to study membrane proteins experimentally. On the other hand, organic solvents can easily solubilize lipids. These two opposite preferences (solubility of lipids and membrane proteins) are therefore difficult to join together and study at the same time, though any attempt should be encouraged given that ~50% of current drug targets are membrane proteins (Lindahl & Sansom 2008). There is a lot of effort in development of new methods and systems to overcome problems related to membrane protein research, but so far the results have not been satisfactory (Bill et al. 2011). Additionally, it is even more difficult to work with membrane proteins on the level of their interactions with a single lipid species. Very often, procedures for purification of membrane proteins for structural studies include steps of removal of native lipids, and thus native lipids are often out of the picture.

It seems that current state-of-the-art studies of lipid-protein interactions are not impressive, and very often this topic is neglected by researchers (Coskun & Simons 2011). Due to technical limitations of the methodology, and the complexity of lipid-protein interactions, novel and interdisciplinary methods might be the way to understand them better.

In the next chapter, the background for the research conducted for this thesis will be presented in such a manner that current state-of-the-art studies in the field are discussed, also covering the most emerging questions that have been tackled in the studies.

3 Background

3.1 COMT protein

In Article 1, an important neurochemistry-related protein, catechol-O-methyltransferase (COMT), was studied as an example of proteins whose function can be modulated by a lipid membrane. COMT is a special case of proteins which exist in two isoforms: S-COMT as a water soluble form and MB-COMT in its membrane-bound form comprised of the catalytic part (that is similar to S-COMT) bridged to a 24-residue long linker, which in turn couples this complex to a lipid membrane through a transmembrane helix with 26 residues, see Figure 11 (Ulmanen & Lundström 1991; Reenilä & Männistö 2001). The 3D crystal structure of S-COMT has been resolved (Vidgren et al. 1994), while the structure of the 50-residue long part of MB-COMT remains unknown.

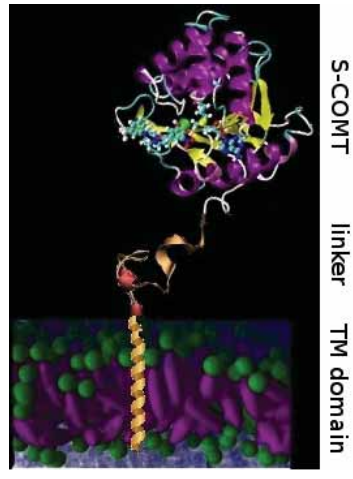

FIGURE 11. Schematic picture of the MB-COMT protein attached to a membrane by its transmembrane domain helix and a linker.

In general, the protein's main function is inactivation (through O-methylation using s-adenosyl-l-methionine) of catecholamine neurotransmitters such as dopamine, epinephrine, norepinephrine, caffeine, and catechol steroids (Guldberg & Marsden 1975). MB-COMT has a lower Km (Michaelis constant) value for dopamine and a higher affinity for catechol substrates than S-COMT (Myöhänen et al. 2010; Bai et al. 2007). The membrane bound form of COMT is abundant in the brain, where it is an important factor in modulating cortical dopamine signaling (Matsumoto et al. 2003; Käenmäki et al. 2010; Meyer-Lindenberg et al. 2005; Papaleo et al. 2008). S-COMT, on the other hand, is present mainly in peripheral tissues and is responsible for metabolism of catechol compounds (Grossman et al. 1985; Männistö & Kaakkola 1999; Soares-da-Silva et al. 2003; Nunes et al. 2009). Due to its function, this protein is related to many human behaviors and diseases, such as cognition, psychiatric disorders, chronic pain, and breast cancer (Weinberger 2005; Harrison & Weinberger 2005; Tan et al. 2009; Parl et al. 2009) Therefore, not surprisingly, one of its ligands—L-dopa—is an important drug used in the treatment of Parkinson's disease, very often together with the COMT inhibitor tolcapone. It implies that inhibitors of COMT are widely studied to increase efficiency of such treatment with L-dopa (Männistö & Kaakkola 1999). However, the most beneficial drug in such treatments would be an inhibitor that would be specific to MB-COMT but not S-COMT, since inhibiting both isoforms of COMT results in liver toxicity as it has been observed for tolcapone, probably caused by intoxication activity in liver (Chen et al. 2011). To date, there is no such specific inhibitor, and in general very little is known about the MB-COMT specificity compared to S-COMT at a molecular level. This is striking considering that these two isoforms share exactly the same catalytic part and differ only in the 50 residue-long membrane binding part. To date, only one study concerning this issue has been reported (Bai et al. 2007), and the role of the membrane environment has been totally neglected. What makes this protein particularly interesting in the context of biological membranes is its activity. It would be rather unexpected that two isoforms of COMT (S- and MB-COMT) have different enzymatic kinetics towards the same ligands (despite the fact that their catalytic part is identical with regard to their sequence and structure (Reenilä & Männistö 2001)) without any role of the lipid membrane where they are anchored. Thus, it is obvious that the lipid membrane must have a severe impact on the biochemical processes related to COMT. Nevertheless, it is not understood why and how this happens. One possible mechanism would be that the membrane binding part of MB-COMT has some impact on the protein function itself, as was proposed by Bai et al. (Bai et al. 2007). However, it is also tempting to tackle this issue from the opposite perspective considering the ligands' points of view and propose that MB-COMT is more efficient and more active toward the substrates that are more accessible and likely to be found in the vicinity of the membrane. This would also imply a more general mechanism for many other proteins of a similar characteristic to COMT, existing in both soluble and membrane-bound forms.

3.2 Role of membrane in neurotransmission

Following the consideration of the peculiar COMT enzymatic activity presented above, it is worth looking from a broader perspective at the neurotransmission process and the role of biological membranes in it. In principle, there are two types of synapses (Figure 12) that constitute a functional junction between two neurons or between a neuron and a specialized cell: an electrical synapse and a chemical synapse (Binder et al. 2008).

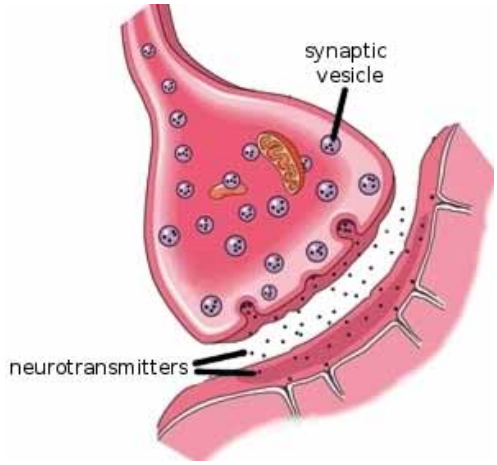

FIGURE 12. Synapse (adapted from http://scienceblogs.com/purepedantry/2007/03/06/neuron-to-glia-synapse-on-axon/ accessed 07.05.2014).

The action of a chemical synapse is initiated by depolarization of the pre-synaptic neuronal membrane, which is followed by the final release of neurotransmitters from the pre-synaptic vesicle to the synaptic cleft. Neurotransmitters diffuse through the synapse and bind to the proper receptor at the post-synaptic membrane, and thus the desired action on the postsynaptic cell can be triggered. This is the very simplified and widely accepted picture of neurotransmission, which can be found in many textbooks (Binder et al. 2008). Despite the fact that many studies have been performed on synaptic vesicle fusion with the presynaptic membrane, exocytosis, and signal transduction, there are very few studies which deal with the interactions of neurotransmitter molecules with other components of a cell, for instance with lipids in membranes (Jodko-Piorecka & Litwinienko 2013). It may come as a surprise since such behavior of neurotransmitter molecules might be of high relevance to processes which are dependent on proper diffusion of neurotransmitters through the synaptic cleft, and such interactions could limit their accessibility for the receptors and other relevant enzymes—including COMT, which neutralizes them. In addition, a significant clue for the importance of that issue comes from the fact that the structures of some neurotransmitters are similar to those of aromatic amino acids that have been shown to preferentially associate with the membrane-water interface (MacCallum et al. 2008). In general, many amphipatic molecules like anes-

thetics, drugs, antibiotics, and fluorescent probes can bind to membranes (Schreier et al. 2000). Moreover, the binding of anesthetics to membranes has been suggested to cause changes in the membrane lateral pressure, which in turn causes conformational changes in proteins (Cantor 1997; Cantor 1998). This becomes even more exciting assuming that the hypothesis of the importance of interactions of neurotransmitters and a lipid membrane in the synaptic membrane is valid in the synaptic non-specific transmission of nerve signals (Cantor 2003). Regardless of all these significant observations and the hypothesis evoked, there are very few reports dealing with the interactions of neurotransmitters and membranes. When Article 2 was written, there was only one experimental and one computer simulation study investigating interactions of a lipid bilayer with neurotransmitters: glutamate, acetylcholine, γ-aminobutyric acid, and glycine (Wang et al. 2011). Ever since, only a few others have appeared (Jodko-Piorecka & Litwinienko 2013; Peters et al. 2013).

3.3 Hydrophobic mismatch

Integral membrane proteins consist of a hydrophobic segment that allows them to integrate in a stable manner with a membrane. In optimal conditions, the difference between the length of this hydrophobic part of a protein and the thickness of a lipid bilayer is negligible (Hessa et al. 2007). However, all eukaryotic membranes contain a variety of different lipids with different acyl chain lengths or saturation levels (Ejsing et al. 2009), and also integral membrane proteins with various transmembrane domain lengths are found in biological membranes (Sharpe et al. 2010; Killian 1998). It implies that in a real situation, there is often a mismatch between the protein hydrophobic length and the hydrophobic thickness of a lipid bilayer (Strandberg et al. 2012). This phenomenon is referred to as the hydrophobic mismatch. The negative hydrophobic mismatch is defined as a situation where the protein is shorter than the hydrophobic thickness of the membrane core, and positive mismatch describes the opposite situation (Figure 13).

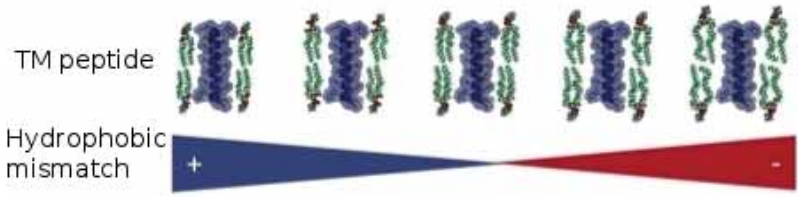

FIGURE 13. Schematic overview of the possible hydrophobic mismatch conditions: positive mismatch (TM helix longer than the hydrophobic thickness of a membrane) on the left, and negative mismatch (TM helix shorter than the hydrophobic membrane thickness) on the right.

Membranes and membrane proteins have to live with the hydrophobic mismatch, thus there are many possible scenarios of how they adjust to each other, see Figure 14.

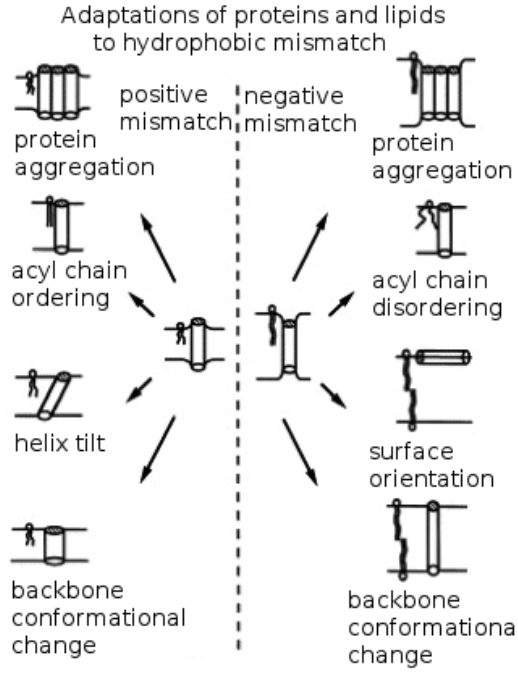

FIGURE 14. Possible adaptations of transmembrane proteins and lipids to a hydrophobic mismatch. Adapted from (Killian 1998).

In this spirit, the “mattress model” predicts that embedding a helical transmembrane protein into a fluid bilayer causes adaptations of lipids to the mismatch (Mouritsen & Bloom 1984) in order to minimize the exposure of hydrophobic surface area to water. Due to biological membranes’ and proteins’ complexity, it is however not trivial to estimate which adaptation mechanisms will dominate (Strandberg et al. 2012).

The adaptations of lipids and proteins under hydrophobic mismatch can have an impact on membrane structure and function, as well as have more crude effects on the mismatched protein activity, stability, and conformation. It might even lead to a formation of microdomains and resulting molecular sorting of proteins and lipids (Killian 1998; Strandberg et al. 2012). Physical mechanisms governing those effects have been proposed to be of physiological significance, for instance in lateral sorting of proteins according to their hydrophobic length in a secretory pathway (Schmidt & Weiss 2010; Sperotto et al. 1989). Nevertheless, it is not known how significant hydrophobic mismatch is in the organization of proteins in biological membranes. Some insight on molecular mechanisms governing has been recently obtained from molecular dynamics simulation results (Schmidt & Weiss 2008; Schäfer et al. 2011). Still, the complexity of biological membranes calls for further studies on the details of hydrophobic mismatch mechanisms, one of which is discussed in the next paragraph.

3.4 Cholesterol and its role in hydrophobic mismatch

Localization of proteins in different cell compartments according to their hydrophobic length is correlated with the cholesterol content of a membrane where they are destined (Bretscher & Munro 1993; Munro 1995). Nevertheless, the detailed picture of what is the role and the mechanism of cholesterol involvement in the sorting of proteins has not yet been revealed. Thus, it is tempting to take a closer look at this important ingredient of biological membranes (for the structure of cholesterol, see Figure 5) and to investigate its role in hydrophobic mismatch.

Cholesterol is present in eukaryotic cells with varying content, increasing from the internal cell compartments such as ER (1 mol %), through the Golgi complex, into the highest level in plasma membrane (20-25 mol %) (Figure 15) (van Meer 2008; Ikonen 2008). Cholesterol can change membrane properties in a quite sophisticated manner, which can be one of the possible mechanisms of its action on membrane proteins, but also the direct cholesterol-protein interactions can modulate proteins' function as it was discussed earlier for GPCRs (Rosenbaum et al. 2009; Lagerström & Schiöth 2008) and other proteins (Gimpl et al. 2002; Pang et al. 1999). It is also worth considering the possibility that these two mechanisms of cholesterol's impact on protein function can be correlated and that they cooperate with each other in a manner that still needs to be elucidated, as it is discussed later for the correlation of the hydrophobic mismatch and the non-specific affinity of cholesterol to model transmembrane peptides.

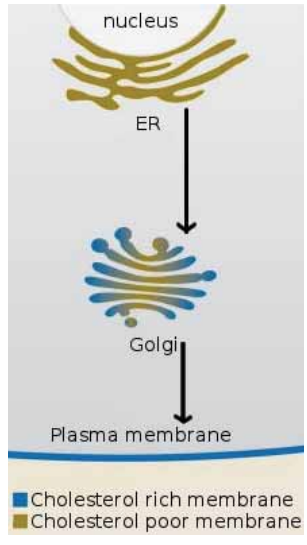

FIGURE 15. Gradient of cholesterol content in cell membranes. Adapted from (Lippincott-Schwartz & Phair 2010).

The most widely known is the role of cholesterol in regulation of membrane permeability (Bittman et al. 1984), fluidity (Yeagle 1985), and other mechanical properties (El-Sayed et al. 1986). Cholesterol can also thicken and rigidify membranes and as a result change the environment where membrane proteins reside. All these effects are possible due to the semi-rigid tetracyclic ring structure of cholesterol which drives cholesterol to stay in close vicinity to saturated hydrocarbon chains of other lipids (such as sphingomyelins) (Simons & Vaz 2004) and to increase membrane order (Ikonen 2008). Therefore, changing the order and condensing the membrane where cholesterol resides (Urbina et al. 1995) can result in the gel/liquid-crystalline phase transition of the membrane with increasing levels of cholesterol (Maulik & Shipley 1996). This effect is, however, positive (promotes ordering and rigidity) in the fluid state (physiologically relevant), with the opposite holding true in gel-phase membranes. This feature (ordering and condensation effect) of cholesterol can be associated with its role in formation of ordered lateral structures (Róg et al. 2009; Chong et al. 2009), referred to as the liquid-ordered phase (Lo) in contrast to the liquid-disorder phase (Ld). Several models have been proposed to explain this phenomenon, such as the “condensed complex” model (Radhakrishnan & McConnell 2005), the “superlattice model” (Chong 1994), and the “umbrella model” (Huang & Feigenson 1999). This is also the fundamental feature of cholesterol for the establishment of distinct functional lipid rafts in a fluid-fluid co-existence (Simons & Ikonen 1997)—described in more detail earlier, as one of the membrane models. Despite all of that, a molecular explanation for the uniqueness of cholesterol and its role in promoting formation of the Lo phase needs to be clarified. One possible explanation is related to the fact that cholesterol has one side that is flat (α-face) and another that is rough (β-face – characterized by the presence of two methyl substituents) (Róg et al. 2009). The two methyl groups of cholesterol on the rough side were suggested to play a key role here, since other sterols, which do not possess these groups, do not promote membrane lateral self-organization (Martinez-Seara et al. 2010). One might also speculate that two distinct sides of cholesterol might also play some role in other processes where cholesterol is involved, such as in adaptations of lipids and proteins to hydrophobic mismatch.

The relation of cholesterol with sorting of peptides in the cell secretory pathway according to their hydrophobic length has very solid foundations. Namely, membrane proteins in Golgi have shorter transmembrane segments (~15 Å) than those found in the plasma membrane (~20 Å) (Bretscher & Munro 1993), but in case of replacement of the TM parts of Golgi proteins with longer ones, they are transferred to the plasma membrane (Cole et al. 1998; Munro 1991) and vice-versa (Sivasubramanian & Nayak 1987). This suggests that the sorting mechanism is due to a physical character of membrane-protein interactions. But what mechanism could that be? Another clue comes from the fact that the cholesterol content of membranes in a cell increases gradually along the secretory pathway to the plasma membrane (van Meer 1989), strikingly correlated with the proteins’ TM lengths. Joining these two facts—membrane-related physical mechanism of sorting of peptides in the secretory pathway and the gradient of cholesterol in a cell—it is suggestive that cholesterol should play a crucial role in that process. Membrane properties (discussed earlier in this paragraph) that are modulated by cholesterol were indeed predicted as one of the crucial pa-

rameters for selective association of matching lipids with TM proteins (Lundbaek et al. 2003), and these macroscopic sorting processes according to the hydrophobic length have been also predicted earlier by theory and simulation (Schmidt & Weiss 2010; Sperotto et al. 1989). Moreover, it has been shown that when the cholesterol level is elevated in the endoplasmatic reticulum, protein translocation is inhibited (Nilsson et al. 2001). Despite indication for selective lipid-protein interactions and hydrophobic matching (Killian & Nyholm 2006; Marsh & Horváth 1998), actual sorting of TM proteins and accompanying lipid co-sorting has not been reconstituted in vitro and additionally its molecular mechanism is unclear.

4 Methods

Due to the aforementioned practical issues related to experimental methods, it is difficult to clarify atomistic-scale events associated with dynamic lipid-protein interactions by using only the experiments. One of the successful approaches to complement experimental findings is to model membrane-protein systems' dynamics in an atomistic manner through molecular dynamics (MD) simulations. MD simulations can provide one with detailed structural information of lipid-protein complexes and also yield insight into the dynamic properties of proteins and lipids in membranes. MD simulations are very often positioned in science as methodology, which stands between theoretical studies and experimental methods, and can very often be a link between these two.

In purely classical atomistic MD simulations, quantum effects are not taken into consideration. It implies that the Born-Oppenheimer approximation must be applied, and consequently only nuclear coordinates, separated from electronic motions, are considered. Nevertheless, in studies of phenomena associated with lipid-protein interactions, such an issue is not problematic because these interactions are well projected within the classical regime. Moreover, quantum approaches would not be feasible for sizes of the studied systems. On the other hand, it is an optimal choice to stay within the atomistic level of approximation and to avoid using coarser descriptions in order to preserve sufficient details of the subtle lipid-protein, protein-protein, and lipid-lipid interactions. Another limitation which comes together with the application of MD simulation to studies of biological systems is the number of features that one can include in simulations. For such a complex system as a biological membrane, it is indeed a challenge. However, in scientific practice there is always a necessity to approximate the systems and phenomena of interest to an appropriate level. Therefore, with all the precautions applied, MD simulations can be used to investigate lipid-protein interactions without any doubts. Especially when this methodology is combined with experimental work, it can bring brand new insight into the scientific questions posed.

4.1 Molecular dynamics (MD) simulations

Alder and Wainwright performed the first molecular dynamics simulation in 1957, when they used the hard-sphere model to describe atoms (Alder & Wainwright 1957). After 19 years of development of the technique, the first 500-atom protein simulation was performed in 1976, resulting in a 9.2 picoseconds long trajectory (McCammon et al. 1977). Later on, rapid progress in computational capabilities, together with improvements of algorithms, has allowed increasing timescales and system sizes. In 1998, the 1 microsecond barrier of simulation time was broken (Duan & Kollman 1998), and nowadays simulations of systems consisting of 1 million atoms over microsecond timescales are becoming common (Sanbonmatsu & Tung 2007). The molecular dynamics simulation technique is becoming a widely used method, and it is especially useful in studies of membrane proteins (Lindahl & Sansom 2008), very often supporting experimental findings and overcoming limitations of experiments, allowing one to describe molecular events at the atomistic level. Regarding the possibilities that it brings, particular attention has been paid to develop special-purpose machines for molecular dynamics simulations by the D. E. Shaw laboratory (Dror et al. 2012). This approach allows for the revealing of the atomistic details of membrane processes in a spectacular way, which can be compared to an in-silico molecular microscope (Dror et al. 2012). Through multi-microsecond timescales (Dror et al. 2012) it was shown, for instance, how the β2AR receptor is activated by a drug molecule (Dror et al. 2011). Exploration of protein folding pathways through MD simulations is now also possible (Lindorff-Larsen et al. 2011). A very practical aspect of drug design was also achieved by MD simulations on this special-purpose machine, elucidating the spontaneous way of drugs binding to a protein (Shan et al. 2011). Therefore, molecular dynamics simulation is undoubtedly one of the methods, which will be used to study lipid-protein interactions in the future as well, providing us with a better picture of related complex and important processes.

4.1.1 Starting structures for MD simulations

The starting structure for a system that one aims to simulate should contain all the information about the positions of atoms in the simulated system. This data is crucial, for example, in simulations of proteins due to the complexity of protein structure. Therefore, a reliable source is needed for this information. One of such sources is the protein structure database (pdb database), where the experimentally (X-ray, NMR) resolved atomistic-level structures of proteins are stored and can be downloaded as a pdb file (Berman et al. 2000). When the experimentally solved structure of the protein is not available, it is sometimes possible to prepare its structural model based on similarities between the amino acid sequences of different proteins (Kaczanowski & Zielenkiewicz 2010). This method is called homology modeling (Martí-Renom et al. 2000). In cases where no structure and no homology models are available, it is still possible to determine the structure of small peptides or protein fragments using MD simulation based on the idea that the amino acid sequence determines the structure. There is a special kind of MD simulation for that purpose called replica exchange molecular dynamics (REMD) (Sugita & Okamoto 1999). In the research for this thesis,

membrane protein structures were single transmembrane helices, which could be built from scratch using the VMD software (Humphrey et al. 1996) that can generate the structure of a transmembrane α-helix with a given sequence. Subsequently, these helices were inserted into a lipid bilayer. Additionally, in the case of the MB-COMT protein linker between the transmembrane helix and the catalytic domain of the protein (Article 1), REMD was applied to investigate the most probable structure of this 26-residue long fragment (this part of the research was not conducted by the author of this thesis). Meanwhile, for other types of molecules such as lipids and water, the requirements about the knowledge of molecular structure are less severe than with proteins.

Once the structural information on all the ingredients of the simulated system is obtained, it is possible to merge them to build the whole system. All in all, this step of the simulation preparation will result in a file where starting positions of atoms of the simulated system are included. Starting from this static picture, the system starts to evolve in time through forces acting on the atoms. The recipe for the calculation of these forces is given in the "force field". Description of the ingredients of a force field is provided below.

4.1.2 Force field and its derivation

All the inter- and intra-molecular forces are described in the set of parameters called the "force field." It consists of potential energy functions for bonds, angles, dihedrals, and non-boded interactions, Eq. (1) below, from which forces are derived to calculate the motion of all atoms in the system using Newton's equations of motion, Eq. (8). Usually these terms are described in a simple manner where some energetic penalties are applied to deviations of bond lengths or angle from their equilibrium values. Using the OPLS-AA force field, the potential energy is described as:

$$V(r^n) = V_{bonds} + V_{angles} + V_{dihedrals} + V_{non-bonded} \quad (1)$$

$V(r^n)$ - total energy of n atoms found in positions r;

V_{bonds}, V_{angles}, $V_{dihedrals}$ - energy of bonded interactions: bonds, angles, and dihedrals, respectively; and

$V_{non-bonded}$ - energy of non-bonded interactions.

Bonded interactions can be defined in a force field using different kinds of potential functions. Most commonly used are the functions presented below in Eq. (2–4), which are harmonic potentials for covalent bonds and angles, Eq. (2) and (3), and Ryckaert-Bellemans descriptions for proper dihedral interactions, Eq. (4).

$$V_{bond} = \frac{1}{2} k_{ij}(r_{ij} - r_0)^2 \quad (2)$$

$$V_{angle} = k_\theta(\theta_{ijk} - \theta_0)^2 \quad (3)$$

$$V_{dihedral} = \sum C_n \, (\cos(\phi))^n \quad (4)$$

k_{ij}, k_θ - force constants;

r_{ij} - distance between atoms i and j, r_0 – corresponding equilibrium distance;

θ_{ijk} - angle between atoms i, j and k θ_0 – corresponding equilibrium angle;

ϕ - dihedral angle; and

C_n - dihedral constants.

Very often (including the simulations reported in this thesis), constraint algorithms are employed for bonds in molecules to make it possible to increase the time-step of a simulation by getting rid of high-frequency bond vibrations. The most efficient ones in terms of computational time, and one of the most reliable algorithms, as well, is LINCS (Hess et al. 1997), which was used to constrain all bonds in simulations whose results are presented in this thesis.

Another important potential function for the bonded interaction defines the improper dihedral, which should keep the planar groups stable, Eq. (5):

$$V_{improper}(\xi_{ijkl}) = \frac{1}{2} k_\xi (\xi_{ijkl} - \xi_0)^2 \quad (5)$$

$V_{improper}$ - improper dihedral potential energy;

ξ_{ijkl} - dihedral angle between ijk and jkl planes;

ξ_0 - equilibrium dihedral angle between ijk and jkl planes; and

k_ξ - force constant.

The non-bonded interactions define short- and long-range interactions between atoms. There are two functions used to define it: Lennard-Jones, Eq. (6), interaction to define short-range van der Waals interactions, and the Coulumb interaction for long-range electrostatic interactions, Eq. (7), given as follows:

$$V_{LJ}(r_{ij}) = 4\varepsilon_{ij}\left(\left(\frac{\sigma_{ij}}{r_{ij}}\right)^{12} - \left(\frac{\sigma_{ij}}{r_{ij}}\right)^{6}\right) \quad (6)$$

$$V_c(r_{ij}) = \frac{q_i q_j}{4\pi\varepsilon_0 r_{ij}} \quad (7)$$

V_{LJ} - Lennard-Jones interaction energy, V_c - Coulomb interaction energy;

r_{ij} - interatomic distance between atoms I and j;

ε_{ij} - potential depth;

σ_{ij} - potential zero point; and

ε_0 - dielectric constant, q_i, q_j - atom charges for atoms i and j.

A bit more detailed view on long-range electrostatic interactions, Eq. (7), is necessary due to the slow decay rate of the electrostatic interaction—that is proportional to 1/r. Because of its nature, it is not trivial to compute such a term efficiently in molecular dynamics simulations. Therefore, some special treatment of the electrostatic potential calculation needs to be applied. A simple cut-off at a given distance from the atom has been shown lead to artifacts (Patra et al. 2003). The reaction field method provides some improvement by a correction applied to the electrostatic potential beyond the cut-off distance (Onsager 1936). However, to include the electrostatic interactions in full, the Ewald or Particle Mesh Ewald (PME) methods are the best available option for the time being (Essmann et al. 1995), and therefore PME was used in all the simulations in this thesis. In this method, the long-range electrostatic interaction energy is calculated as an infinite sum over all charges (each represented as a Gaussian charge density) from an infinite 3D lattice formed by periodic images of the simulation box. This sum is, as a matter of fact, calculated as a convergent sum in reciprocal space, which is transformed back to real space. A cut-off is used here to define the range where the real space summation is used, and the point beyond which this calculation is performed in the reciprocal space.

Defining the parameters in Eq. (2–7) for an atomistic force field is a crucial step for the validity of the simulations where they are used, but obtaining them requires a lot of time and resources. Therefore, deriving them is very often a complex and iterative process, which is a separate research topic on its own. It is especially challenging in the case of force fields for lipids, where it must reproduce molecular properties of single lipid molecules but also collective features of a whole membrane. This is not trivial. For example, all-atom force fields for lipids have often underestimated the surface area per lipid (Maciejewski et al. 2014). In principle, properties of molecules, or very often just small parts of them, are calculated from ab-initio calculations and revised against experimental data to find a match between simulations and experiments. Force constants for bonded interactions can be calculated from ab-initio calculations, or they can be taken from spectroscopy results. Partial charge distributions can also be based on ab-initio calculations, but empirical partial charges are sometimes used, too. Lennard-Jones and dihedral parameters are fitted to match experimental data available.

4.1.3 Force fields in practice

The most problematic issue in membrane simulations is to reproduce proper lipid bilayer features. This was not the case for the early versions of CHARMM (Feller & MacKerell 2000), General Amber (Jójárt & Martinek 2007), or Lipid11 (Skjevik et al. 2012) force fields, yet, new improved versions (which were not available when the research for this thesis started) of these force fields (CHARMM 36 (Klauda et al. 2010), Lipid14 (Dickson et al. 2014), and Slipids (Jämbeck & Lyubartsev 2012)) show significant improvement in this regard. There are also other important force fields for membranes that are based on coarse-grained models, like MARTINI (Marrink et al. 2007), which reproduces very well a set of membrane properties, but as it was discussed earlier, in the research for this thesis atomistic details (which are not possible to investigate with MARTINI) mattered. Thus, coarse-grain models were not applied in this work.

In the simulations discussed in this thesis, the parameterization used for lipids is compatible with the Optimized Parameters for Liquid Simulations all-atom (OPLS-AA) force field (Jorgensen et al. 1996) with recalculated torsional parameters, partial atomic charges, and van der Waals (vdW) parameters for the polar and hydrocarbon parts of lipid molecules (Maciejewski et al. 2014). The OPLS-AA force field in its native form includes a large set of parameters for proteins (Kaminski et al. 2001) and drug molecules (Jorgensen 2004), and therefore it could be successfully used for all the simulated systems.

4.1.4 Generating appropriate dynamics and physical conditions

Forces that act on atoms in the simulation are calculated from the potential functions described above, Eq. (1–7), based on the force field parameters, and then they are used to solve Newton's equation of motion for atoms as given by the Eq. (8).

$$m\frac{d^2x^i}{dt^2} = F^i(x(t)) \quad (8)$$

m - atom mass;

x^i - position of atom i;

F^i - force acting on atom i; and

t - time.

Because of the discrete nature of the numerical calculations, some algorithm needs to be used for solving the Newton's equations in MD simulations. One of the commonly used techniques is the "leap frog" algorithm, described by the Eq. (9–10):

$$v\left(t+\frac{\Delta t}{2}\right)=v\left(t-\frac{\Delta t}{2}\right)+\frac{F(t)}{m}\Delta t \quad (9)$$

$$r\left(t+\frac{\Delta t}{2}\right)=r(t)+v\left(t+\frac{\Delta t}{2}\right)\Delta t \quad (10)$$

v – speed of atom, r – position of atom, t – time, Δt – time step, F – force acting on atom.

Another issue that needs to be taken care of in a simulation, in order to make it more realistic, is the finite size of the simulation box. To this end, special conditions at the edges of the simulation box have to be applied. The most practical way of solving this is to assume that the system is surrounded by its own mirror images in all directions by applying the so-called periodic boundary conditions.

In general, MD simulations can be assumed to obey the ergodic postulate which states that time averages of the system correspond to a microcanonical ensemble average. In other words, given enough time to evolve, the ensemble will reproduce the statistical averages (Tupper 2005). The most frequently used ensembles in MD simulations are: canonical (NVT), where the number of particles, volume, and temperature are kept; and isothermal-isobaric (NPT), where the number of particles, pressure, and temperature are controlled. In all the simulations presented in this thesis, the NPT ensemble was used. There are different methods that can be applied in molecular dynamics simulations to fulfill the chosen ensemble conditions, but in principle all of them introduce some correction to the equations of motion to keep the temperature and pressure constant. In practice, these are rather sophisticated algorithms. In this thesis, either Nosé-Hoover (Nosé 1984; Hoover 1985) or velocity-rescaling (Bussi et al. 2007) schemes were applied for controlling the temperature, and Parrinello-Rahman for pressure (Parrinello & Rahman 1981; Nosé & Klein 1983).

When all the necessary ingredients of a MD simulation have been set (starting structures force field, dynamics, and other special algorithms to keep the physical conditions during the simulation (e.g. barostat, thermostat, and periodic boundary conditions)), the simulation can be conducted. For all the simulations in this thesis, the GROMACS simulation package was used as an engine for the MD simulations (Berendsen et al. 1995; Pronk et al. 2013).

4.2 Analysis methods

The output of an atomistic MD simulation consists of the evolution of atom positions in time. One can use this data to elucidate all kinds of information on the properties and the dynamics of the

studied system, and this can often be compared to an in-silico microscope, where a small patch of the physical world is observed repeatedly and can be analyzed with both qualitative and quantitative methods. In that respect, performing simulations is very often seen as preparation of assays for experiments, and analysis of trajectories is then an equivalent of the actual experiment.

4.2.1 Qualitative and quantitative measures

When the simulation is finished, very often the first step is to visually inspect the trajectory using software, such as VMD (Humphrey et al. 1996). This is good practice for several reasons: first of all, to recognize simulation artifacts, and second, to recognize the first key results. Nevertheless, one has to always be able to show quantitatively that the observation is valid, and it is even more appreciated when results coming from simulations can be linked to experimental data. In the articles in this thesis, many of the simulation results were compared to experiments, providing a strong argument for their validity. Below, the most representative examples of the quantitative methods used in the thesis' articles are described. The analysis methods are divided into three groups: direct interactions, collective properties, and protein analyses.

4.2.2 Directed interactions

Molecular interactions can be grouped into different sets, depending on the background of the person that makes such division. Thus, definitions and descriptions of some of them are presented below. Here, we focus on those interactions that are directed in space.

In biological matter, which is relevant for this thesis, the most abundant and significant molecular interactions in this context are: hydrogen bonds and salt bridges.

Hydrogen bond is a directed, attractive, electrostatic interaction between the hydrogen atom covalently bound to an electronegative atom (donor) and another slightly electronegative atom (acceptor) (Muller 1994) in a proper geometrical configuration (Arunan 2011). This interaction plays a crucial role in biological systems, and serves as a base for structures of many macromolecules such as proteins, DNA/RNA, or biological membranes. Although one hydrogen bond is not very strong, ~10-40 kJ/mol, the collective strength of many of them can be decisive for biomolecule's stability. For the molecules used in the simulations for this thesis, OH and NH groups were regarded as hydrogen bond donors, and O or N atoms as acceptors.

Slightly different are the non-covalent, electrostatic interactions mediated or directed by ions or charge centers: a salt bridge or, more generally, a charge pair. Both are basically weak interactions between two oppositely charged groups. Nevertheless, similarly to hydrogen bonds, they are also important for stability of biological macromolecules. Particularly in Article 1, charged pairs defined as an electrostatic interaction between the positively charged methyl groups in the choline moiety of PC and the negatively charged oxygen atoms of neighboring groups of the same or other molecule were calculated using a criterion of 0.4 nm for the distance between two atoms. Similarly, the

distance between the nitrogen atom in the residue side chain (N^{η}) and the ε oxygen atom in the other residue of the side chain (O^{ε}) was used to define the existence of a salt bridge between these amino acids in a peptide chain.

In this thesis' articles, both hydrogen bonds and salt bridges have been analyzed in the simulated systems. Since hydrogen bonds can vary significantly in strength (depending on types of atoms, and their spatial configuration), there is no clear definition or criterion that would serve as a universal condition for all hydrogen bonds (Arunan 2011). Thus, in analysis of MD trajectories one has to clearly define the conditions that serve as a recognition pattern for a hydrogen bond. Herein, for the hydrogen bond, the distance criterion was set to 0.35 nm between the donor and acceptor atoms, and the second criterion as an angle of 35 degrees for the geometrical configuration of hydrogen-donor-acceptor atoms. These conditions applied in the analysis of hydrogen bonds allow to recognize the most important hydrogen bonds, but it has to be remembered that some of them (especially weak hydrogen bonds) are omitted. Nevertheless, this definition was sufficiently accurate to describe the observed phenomena and make accurate conclusions.

Additionally to these two well-described interaction types, non-specific contact interfaces at a given distance between lipids' and proteins' residues were also analyzed to reveal any possible contact regions of the protein with lipids, as it is described in more detail in the articles.

Radial distribution function (RDF) is a quantity which shows collectively the implications of all possible interactions between the chosen moieties as the ratio of the number densities of one of them at a given distance. In general, it gives an idea of the density of the radial distribution of certain atoms, groups of atoms, or molecules from any defined object (atom, group of atoms, or a molecule). RDF and its derivatives were used in this thesis to study lipid-protein and lipid-lipid interactions.

4.2.3 Collective properties

Biological membranes consist of lipids, which collectively contribute to membrane properties through intermolecular interactions between them. For instance, lipids in a membrane cover some area in the membrane plane which can be divided by the number of lipids in that monolayer, and this number is defined as the average area per lipid. Thickness of a membrane is also a result of lipids' collective interactions and is dependent on membrane composition and structure. Another important membrane property is the average order parameter of lipid acyl chains (reviewed in Vermeer et al. 2007), which also is affected by membrane composition, intra- and intermolecular interactions, and the system's state variables. Very importantly, the given order parameter known as the deuterium order parameter (S_{cd}), together with the aforementioned average area per lipid, can be directly measured experimentally and compared with simulation data (Petrache et al. 2000). The lateral pressure profile of a membrane, describing the distribution of local pressure inside a lipid bilayer, can be calculated from the trajectory of MD simulations. It is a rather complex calcula-

tion, but it was successfully applied by Ollila et al. (Ollila et al. 2007) to analyze trajectories of MD simulations (Niemelä et al. 2007; Ollila et al. 2011). There are also other spatial or geometrical properties of membranes that were calculated in the present research work, and they are described more broadly in the articles.

4.2.4 Protein analyses

A separate branch of specific properties that can be analyzed from MD simulation trajectories are related to proteins. The amino acid sequence of a protein reflects in a specific spatial conformation at different levels, starting from the secondary structure up to the quaternary structure. An atomistic molecular dynamics simulation trajectory includes all the information required to retrieve the protein structural properties at all structural levels. Therefore, one can evaluate the secondary structure of the protein during the simulation. Unspecific changes of the protein backbone structure can be characterized by the root mean square displacement (RMSD) of atoms (usually C-alpha of the protein backbone), showing the deviation of atoms' positions from the starting point. Based on the RMSD scheme, single residue fluctuations can also be calculated in terms of the root mean square fluctuation (RMSF). These basic properties were calculated for the membrane proteins simulated in this thesis, together with some more specific measurements described in the articles.

5 Overview of the systems studied in this work

The core of the systems simulated in this thesis consisted of lipid bilayers of various composition together with proteins/peptides, or neurotransmitters which were either embedded in a membrane (for instance, transmembrane helices in Articles 1 and 2) or positioned above it (linker in Article 1 or neurotransmitters in Article 3). All the simulated systems were hydrated with water, and in some of the systems ions were included as well.

5.1 Article 1

In this article, 12 different atomistic molecular dynamics simulations of a lipid bilayer with the 50-residue fragment that differentiates MB-COMT from S-COMT were simulated for either 360 ns (full 50 residue fragment including transmembrane helix) or 100 ns (only the last 24-amino acid residue fragment following the transmembrane helix, positioned above the membrane). In all of the systems, the lipid bilayer was composed of 124 dilinoleylphosphatidylcholine (2-18:2c9 PC) (DLPC) molecules symmetrically distributed in the two leaflets. All of the systems were hydrated with ~8000 water molecules, and 20 K^+ and 20 Cl^- ions were added to mimic a physiological 140 mM KCl salt concentration. The OPLS-AA force field was used, and temperature and pressure were kept constant at 300 K and 1 bar, respectively.

5.2 Article 2

Composition and conditions of four 500-ns long simulations in this article were dictated by the experimental data. Simulated systems were therefore composed of the LW21 (K2W2L8AL8W2K2) transmembrane peptide embedded in single-component bilayers comprised of either di-16:1 or di-24:1 PC lipids, and two other systems were mixtures of these PC systems with 20 mol% cholester-

ol. The systems were hydrated with ~3 500 water molecules, the OPLS-AA force field was used, and temperature and pressure were kept constant at 310 K and 1 bar, respectively.

5.3 Article 3

Atomistic molecular dynamics simulations of nine lipid bilayer systems were performed in this study. Three of the simulated systems contained dopamine, three contained L-dopa, and three were reference systems (pure membranes). The bilayers had different lipid compositions: three of them were composed of 128 molecules of dilineoylphosphatidylcholine (DLPC, di-18:2-DLPC; PC bilayer); three were composed of 48 sphingomyelin (SM), 48 dioleoylphosphatidylcholine (DOPC), and 32 cholesterol molecules (SM-PC-CHOL bilayer), and the remaining three systems contained a mixture of 44 DLPC, 60 dilineoylphosphatidylethanolamine (DLPE, di-18:2-PE), and 24 dilineoylphosphatidylserine (DLPS, di-18:2-PS, negatively charged) molecules (PC-PE-PS bilayer). The systems were hydrated with ~11 500 water molecules, and in six of them 20 dopamine or L-dopa molecules were randomly inserted into the water phase. 160- or 210-ns long MD simulations of each bilayer were performed at a constant pressure (1 bar) and temperature (310 K) using the OPLS-AA force field.

5.4 Unpublished results

The unpublished results (see List of Publications) discussed in Section 6.2.2 were found using a simulation protocol as follows. Atomistic molecular dynamics simulations were performed for two systems comprised of different lipid bilayers with 4 identical transmembrane LW21 (K2W2L8AL8W2K2) peptides. Systems were constructed by replicating and translating (in a 2x2 manner in the membrane plane) the end structure of the membrane containing one LW21 peptide and cholesterol from the simulations performed in Article 2. Therefore, the resulting lipid bilayers were composed of about 494 lipids, either di-16:1 phosphatidylcholine (PC) or di-24:1 PC. The number of cholesterol molecules was about 124, thus its concentration was ~20 mol%. The transmembrane peptide used in the simulations was LW21 (K2W2L8AL8W2K2). The systems were hydrated with ~14 000 water molecules and the OPLS-AA force field was used in the simulations. Systems were simulated for ~2 μs at constant temperature (310 K) and pressure (1 bar).

6 Core research findings

6.1 Membrane is a unique environment for protein function

The reason for the specific kinetic activity of the membrane bound form of COMT protein (MB-COMT) was investigated using the atomistic MD simulations in Articles 1 and 3. Taking into consideration that very little is known about the additional 50 residues of MB-COMT, the results of this study shed new light on the structure of this fragment and its interactions with lipids. The resulting data can help to understand the role of this fragment in catalytic activity of MB-COMT. On the other hand, it can also be speculated that the reason of different enzymatic activity of COMT forms is related to the affinity of some of the COMT's ligands to membranes, and therefore the role of the membrane-binding fragment of MB-COMT might be to proximate its catalytic part to the membrane—where the concentration of some of the ligands is higher. In Article 3, this hypothesis was tested by running simulations of two COMT ligands (dopamine and L-dopa), which have different enzymatic characteristics for MB- and S-COMT, together with the lipid bilayers of different compositions. Importantly, the results showing that affinity of these compounds to membranes were validated experimentally. These results are not surprising because the structures of dopamine and L-dopa are similar to those of aromatic amino acids shown to preferentially locate to the membrane-water interface (MacCallum et al. 2008). The same amino acids often occupy those positions on the membrane protein surface that are located within the membrane-water interface (Ulmschneider et al. 2005). However, the interactions of lipid bilayers with four other neurotransmitters (glutamate, acetylcholine, c-aminobutyric acid, glycine (Wang et al. 2011) and enkephaline (Chandrasekhar et al. 2006)) have been reported earlier. Nevertheless, in Article 3 the interactions between the neurotransmitters and the membrane lipids are shown to be strongly dependent on the lipid type, the chemical structure of the neurotransmitter, and particularly the charge carried by the neurotransmitter. Neurotransmitters' membrane binding has also more practical implications, which are described in more detail thereafter.

6.1.1 Role of the membrane-binding fragment of the COMT protein

Results of the simulations in Article 1 were grouped into seven sections: peptide structure, peptide location, peptide-lipid interactions, peptide intramolecular interactions, peptide-ion interactions, hydrophobic mismatch, and peptide sequence. As described earlier, the structure of the membrane-bound fragment of MB-COMT is not known. Thus, the secondary structure of the peptide was examined in all of the simulations. While the transmembrane helix is rather stable during the simulation, the linker fragment does not fold into any stable structure (Figure 16).

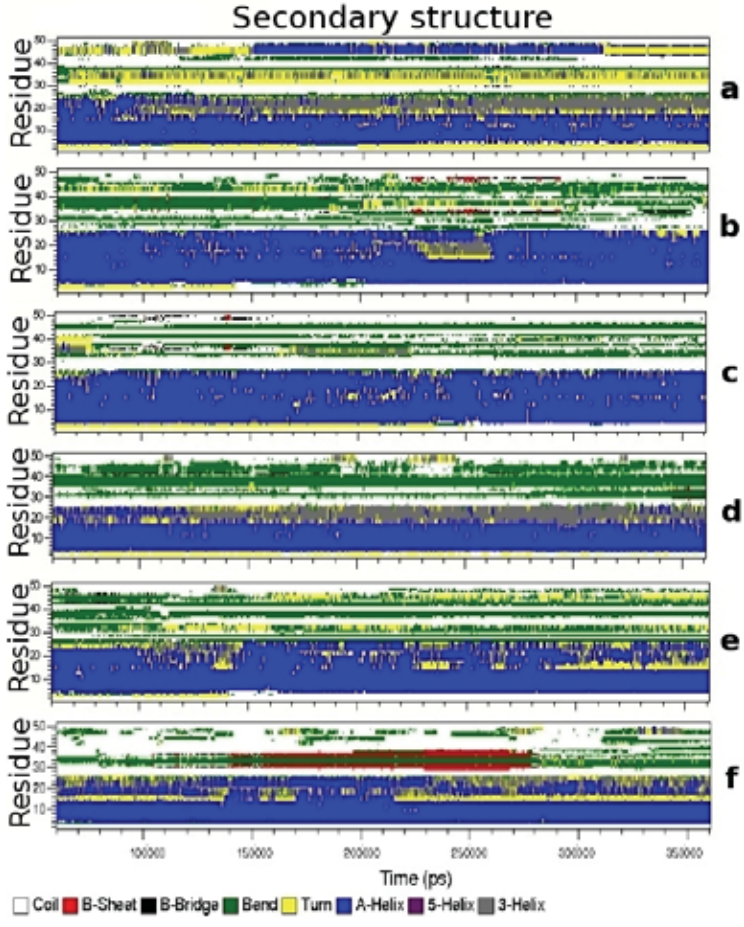

FIGURE 16. Time evolution of the secondary structure of the MB-COMT protein's membrane binding fragment given by six independent simulations (a-f).

Nonetheless, the time scale of the simulations might not be long enough to observe folding (Lindahl & Sansom 2008; Seibert et al. 2005) which additionally can be slower in the environment of the water-membrane interface. However, the lack of the main protein unit (catalytic part) also can

play a role here. In some of the simulations, formation of a helical structure, which was predicted in the previous bioinformatics study (Bai 2007), was observed (Figure 17).

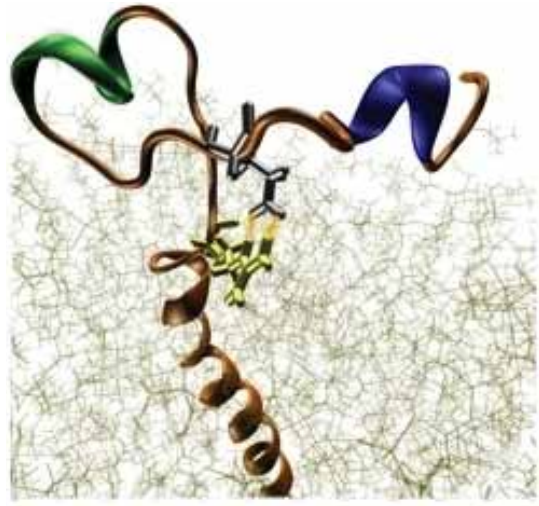

FIGURE 17. Helical structures (green and blue) of the MB-COMT linker part with the salt bridge between the residues ARG27 (yellow) and GLU40 (silver). Membrane lipids are depicted as tan lines and MB-COMT in gold as a “new cartoon” representation. Picture made using VMD (Humphrey et al. 1996).

Position of the linker region in relation to the membrane was calculated, and it showed clearly that the linker is associated closely with the membrane, and that there is a clear tendency of the middle part of the linker (residues 38–40) to interact with the lipid headgroups. This results from the hydrogen bonds and charge pairs established between the amino acid residues and lipid headgroup atoms. The most interesting finding in this study regarding the internal structure of the linker fragment was the observation of the specific salt bridge between the residues ARG27 and GLU40 (Figure 17). This interaction resulted in a 13-residue long loop at the membrane-water interface established on a linker. Importantly, this salt bridge seems to be the major reason for maintaining the close proximity of the peptide to the membrane. Strikingly, it was also calculated that such a loop might be a general fold for other membrane proteins of a similar structure, which is also consistent with the computational study of Phospholamban (PLB) protein (Kim e al. 2009). It was also shown previously that the preferential formation of a salt bridge could occur in an environment of ~30% exposure of the residue surface to water (Sarakatsannis & Duan 2005), which is indeed likely to occur at the water-membrane interface.

Altogether, results from the simulations in Article 1 highlighted that the additional membrane-binding fragment existing in MB-COMT shows specific behavior toward lipids in the membrane. Even more, the membrane-water interface seems to create conditions that enhance probability of salt bridge formation, and that was found to be a universal rule for proteins similar to COMT. It can

therefore be postulated that the role of this fragment is to proximate the catalytic domain to the membrane, since the linker part revealed high affinity to the membrane interface. Due to this reason, it seems to be worth checking whether this proximity of the catalytic domain of MB-COMT to a membrane can enhance its enzymatic activity through the uptake of these ligands closely associated with a lipid bilayer. Therefore, the next paragraph discusses the results of Article 3, where interactions of two molecules with membranes were studied using MD simulations that were later validated experimentally.

6.1.2 Importance of binding of dopamine and L-dopa to membrane

Simulation results from Article 3 can be concluded through a simple visual inspection of the simulation trajectory (Figure 18). Namely, dopamine and L-dopa molecules, which were initially placed in the water phase, tended to associate with the membrane surface along the time of the simulation. The effect was significantly stronger for L-dopa than for dopamine and was also enhanced for the mixed PC-PE-PS bilayer and the SM-PC-CHOL membrane compared to the PC bilayer (Figure 18).

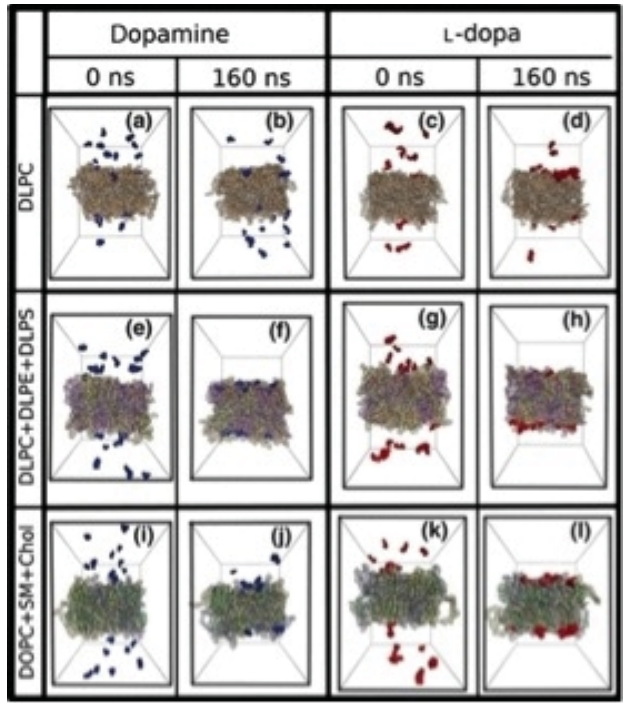

FIGURE 18. Snapshots showing simulated systems (a, c, e, g, i, k) at the beginning, and (b, d, f, h, j, e) at the end of simulations (a, b, e, f, i, j). Dopamine molecules are shown in blue, and (c, d, g, h, k, l) L-dopa molecules in red. Lipid molecules depicted here are (a, b, c, d) PC and (e, f, g, h) PC-PE-PS, and (i, j, k, l) SM-PC-CHOL. Water is not shown for clarity. Snapshots were prepared using the VMD package (Humphrey et al. 1996).

This was further confirmed by the calculation of the density profiles of chosen groups of atoms in the system (Figure 19).

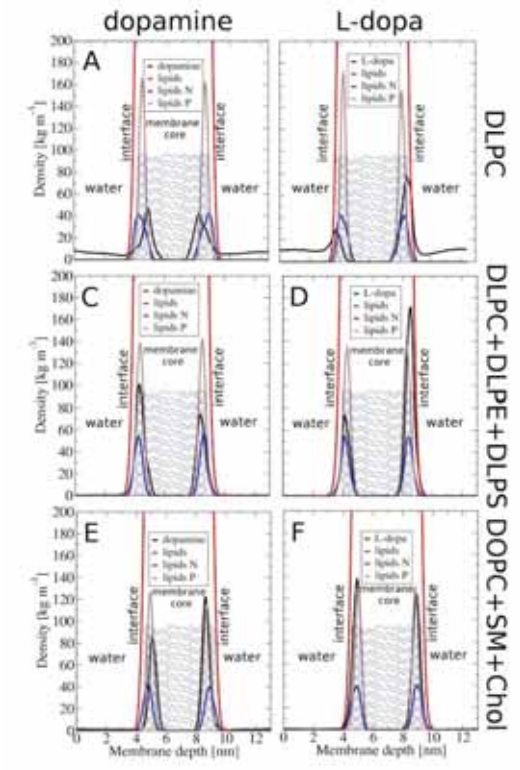

FIGURE 19. Density profiles of dopamine (a, c, e) and (b, d, f) L-dopa (black line), lipids' nitrogen (blue line), lipids' phosphate (pink line), and all lipid atoms (red line). Data corresponds to (a, b) PC, (c, d) PC-PE-PS bilayers, and (e, f) SM-PC-CHOL. Position of the lipid bilayer is shown schematically.

Dopamine's peaks of the density are lower than for L-dopa, indicating that it has slightly less attraction to lipids, but at the same time these peaks are a bit shifted toward the membrane core, compared to L-dopa, which is caused by deeper membrane penetration by dopamine molecules. Detailed analysis of hydrogen bonds revealed the specifics of the interactions that occurred between the molecules and particular lipid types. Hydrogen bonds were formed mainly with lipid phosphate oxygen atoms and to a less extent with lipid carbonyl groups, which are more frequent for dopamine. Since the interaction of anesthetics with lipids has been suggested to be one of the mechanisms for their functions (Frangopol & Mihăilescu 2001) and that neurotransmitters are believed to analogously share this feature (Cantor 2003), changes of membrane properties were measured in all of the systems simulated in Article 3. The effect of dopamine and L-dopa on the bilayer properties is not large, but it is consistent and depends on the lipid composition of the bilayer—with the

largest effect on the PC-PE-PS membrane. Worth noting is the impact of cholesterol, which seems to play a significant role in preserving the bilayer properties from neurotransmitters effect on it. Interestingly, dopamine interacts with lipids less strongly than in the case of L-dopa; however, it can still exert a greater effect on the membrane properties. This is most likely a result of its deeper penetration to the bilayer and the positive charge that it carries. Most likely, the deeper binding of dopamine into a membrane leads to accumulation of positive charge at the interface, which results in an expansion of the bilayer surface.

One of the very important implications of the results from Article 3 is related to the alterations of lipid composition that have been found in several neurodegenerative diseases (Fenton et al. 2000; Adibhatla et al. 2006; Adibhatla & Hatcher 2007; Schmitt et al. 2004; Harrison & Weinberger 2005). Not difficult to imagine is that disturbance in lipid composition may lead to an increased or decreased binding of important neurotransmitters, the altered diffusion of them, and hence to diseases. On the other hand, high membrane association of dopamine and L-dopa enhances the availability of these compounds for cell membrane uptake processes, and the importance of membrane-bound metabolizing enzymes over soluble enzymes (such as MB-COMT over S-COMT) is enhanced. Equally as important, it can be speculated that the role of such membrane-bound enzymes is to neutralize molecules from affecting the membrane in a way that could impact membrane protein function.

6.1.3 Conclusions

Motivation for the research shown in the two articles (1 and 3) came from the intriguing role of the membrane-binding part of the COMT protein, which changes the enzymatic characteristic of that important enzyme. Taking into consideration the identical enzymatic part for both forms (soluble and membrane-bound) of the protein, it is tempting to propose that membranes play a significant role in this phenomenon. Membranes can indeed interact with the protein, but they can also affect the behavior and the availability of the protein ligands. Therefore, two of these approaches were validated. In Article 1, the membrane-binding part of COMT was investigated in the atomistic MD simulations. The results revealed the characteristic of the TM and the linker parts of MB-COMT, shedding some light on how it can possibly look and behave in regards to a membrane. The second approach presented in Article 3 was based on the idea that if COMT ligands have different enzymatic characteristics for MB- and S-COMT, they might interact differently with a lipid membrane and thus their availability might vary. The data presented in these two articles does not give a clear answer for the mechanism of MB- and S-COMT discrimination between their ligands. However, it gives important clues for that, and even more, it shows some more general rules that might be applied to other membrane proteins and physiological processes related to them. In Article 1, the characteristic fold motif for the membrane-water interface protein part was found and further demonstrated to be a possible characteristic motif for membrane proteins similar to COMT. Importantly, the membrane-water interface environment enhances the existence of this salt bridge. As for COMT, it is clear from the results of the simulations that the membrane-binding part will

keep the protein in close distance to the membrane. Thus, the data from Article 3 show that the two ligands for COMT (dopamine and L-dopa) have a different affinity to membranes, and this might be relevant for the distinction between MB- and S-COMT kinetics. Additionally, this observation has some practical implications. Dopamine as an important neurotransmitter and L-dopa as its precursor used in Parkinson's disease treatment, were never shown before to interact with lipids. Surprisingly, textbooks' view on how these molecules diffuse in cells is simplified and shown as a point-to-point travel where neurotransmitters do not interact with other molecules and lipid membranes. It can have significance for the physiological processes, which were broadly discussed in Article 3. Altogether, these two articles showed that membranes provide a special environment for protein functions that needs to be taken into account in membrane protein research.

6.2 Cholesterol and hydrophobic mismatch of peptides

Article 2 emphasizes the role of cholesterol in protein sorting under negative hydrophobic mismatch conditions. Further simulations show that cholesterol maintains a specific geometry around the negatively mismatched peptide.

6.2.1 Cholesterol modulates hydrophobic mismatch and sorting of peptides

Simulations from Article 2 show that under positive mismatch conditions (peptide longer than the bilayer), the increase in acyl chain order and bilayer thickness around the TM helix is less pronounced in the presence of cholesterol (Figure 20), while in the case of negative mismatch (peptide shorter than the bilayer), the lipids around the TM helix were markedly less ordered and thinner than the rest of the lipids in the membrane, which also caused the peptide to be slightly stretched (Figure 20). Under such circumstances, cholesterol counteracts these bilayer deformations and forces them to take place in the close vicinity of the TM helix (Figure 20). This molecular level description can serve as a molecular mechanism for the role of cholesterol in hydrophobic matching of peptides. Namely, based on the simulation results, lateral sorting of peptides in the mismatched bilayers as observed in experiments (Article 2) can be explained as resulting from the increasing significance of negative mismatch mediated by cholesterol, which in turn results in peptide clustering to minimize the exposure to such unfavorable conditions.

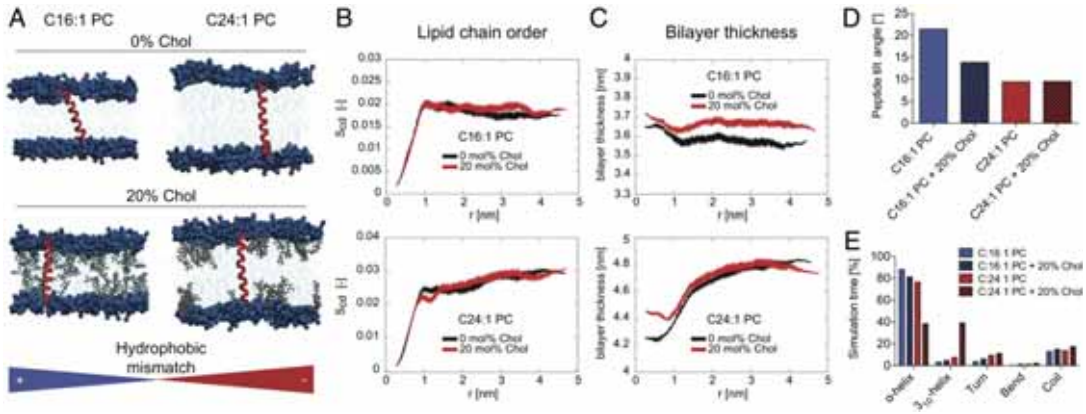

FIGURE 20. Hydrophobic mismatch between a transmembrane peptide and a lipid bilayer determines bilayer structure, helix orientation, and fold. (A) Snapshots from the MD simulations with LW21 TM peptide (red) embedded in C16:1 and C24:1 PC (headgroups are depicted in dark blue, chains in light blue) in the presence and absence of cholesterol (gray). Positive and negative mismatch are indicated by blue and red color, respectively. (B) Distance profiles of lipid chain order (S_{cd} order parameter of the *sn*-1 chain) with respect to the helix backbone at 0 nm (t = 500 ns) for C16：1 and C24：1. Black denotes 0% cholesterol, red 20% cholesterol. The S_{cd} parameter shown here represents the average value of the S_{cd} profile along the hydrocarbon chain. (C) Membrane thickness (P-P distance in units of nanometers) with respect to the helix backbone at 0 nm (t = 500 ns) for C16:1 and C24:1. Black stands for 0% cholesterol, red 20% cholesterol. (D) Bar graph of the average tilt angle of LW21 in the four simulations in units of degrees (see axis). (E) Fold adopted by LW21 over the simulation time in percent (see legend).

6.2.2 Orientation of cholesterol varies in the vicinity of the mismatched peptide

The simulations from Article 2 were extended to consider two different bilayer systems with four identical transmembrane LW21 (K2W2L8AL8W2K2) peptides. The systems were constructed by replicating and translating (2x2 – in the membrane plane) the final structure of the membrane containing one LW21 peptide and cholesterol using the simulations performed in Article 2. Therefore, the resulting lipid bilayers were composed of ~494 lipids, either di-16:1 phosphatidylcholine (PC) or di-24:1 PC. The number of cholesterol molecules was ~124, thus its concentration was ~20 mol%. The transmembrane peptide used in the simulations was LW21 (K2W2L8AL8W2K2). The systems were hydrated with ~14,000 water molecules. Systems were simulated with the OPLS-AA force field for ~2 μs at constant temperature (310 K) and pressure (1 bar). The simulations demonstrated that both direct (through single lipids) and indirect (through bulk properties of membrane) types of the lipid-protein interaction are related.

The RDF of cholesterol molecules with respect to the peptide was computed, and a slight but very clear difference between the two oppositely mismatched membranes was observed (see Figure

21). Namely, under negative mismatch the cholesterol distribution is concentrated closer to the peptide (black line – PC24), and the difference compared to positive mismatch (PC16 – red line) is present up to a distance of 2 nm. Then, the average number of cholesterol molecules that were observed up to varying distances (0.5, 1, 1.5, 2, 2.5, 3 nm) from the peptide was calculated. Table 3 shows that on average there is at least one cholesterol molecule more (per each leaflet) in the vicinity of the negatively mismatched peptide compared to the positively mismatched peptide (2.20 vs. 3.19 at a distance of 1.5 nm). This is consistent with the RDF plots shown in Figure 21. The difference in the number of cholesterol molecules between the positively and negatively mismatched systems is found to be substantial, up to a distance of about 2 nm from the peptide. Beyond this distance it decreases gradually. Additionally, there are more PC lipids in the vicinity of the positively mismatched peptide compared to the negatively mismatched one, while in the latter case there is more cholesterol around the peptide. The cholesterol-to-lipid ratio is higher under negative than positive mismatch. This clearly indicates that under negative mismatch, the peptide attracts cholesterol specifically to its vicinity.

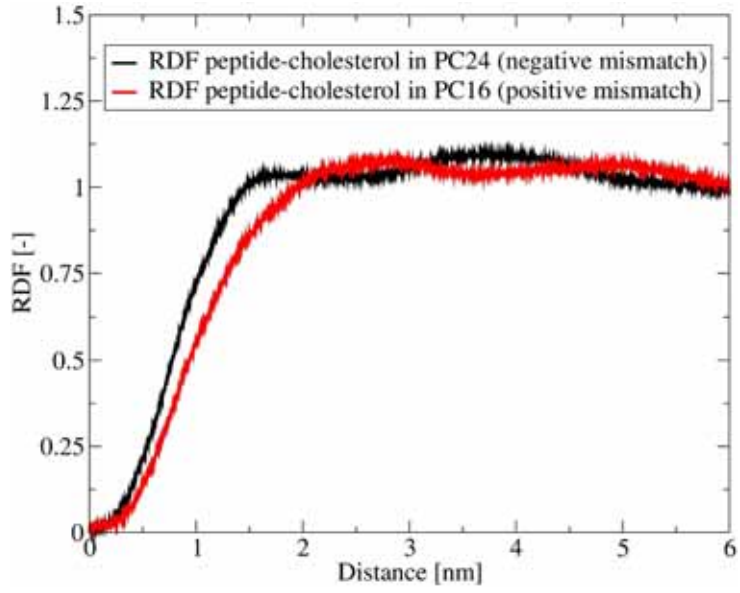

FIGURE 21. Radial distribution function of the center of mass (COM) of cholesterol molecules around the peptide's COM projected on the membrane plane, averaged over four peptides present in each system: black – PC24 (negative mismatch) and red – PC16 (positive mismatch).

TABLE 3. Average number of lipids for varying distances from the peptide center of mass, and the percentage of cholesterol among all lipids at that distance. The fixed total value of Nchol/(NPC+NChol) in each system is 20%.

Dist. (nm)	N_{Chol} in PC16	N_{Chol} in PC24	N_{PC16}	N_{PC24}	$N_{Chol}/(N_{PC16}+N_{Chol})$	$N_{Chol}/(N_{PC24}+N_{Chol})$
0.5	0.31 (+/-0.004)	0.28 (+/- 0.002)	1.45 (+/- 0.007)	1.37 (+/- 0.007)	17.61 %	16.97 %
1.0	0.58 (+/-0.004)	0.87 (+/- 0.004)	7.28 (+/- 0.01)	7.50 (+/- 0.01)	7.38 %	19.39 %
1.5	2.20 (+/-0.008)	3.19 (+/- 0.007)	18.10 (+/- 0.01)	17.57 (+/- 0.01)	10.84 %	15.20 %
2.0	5.25 (+/-0.01)	6.48 (+/- 0.009)	32.62 (+/- 0.02)	30.97 (+/- 0.02)	13.86 %	17.30 %
2.5	9.59 (+/-0.02)	10.67 (+/-0.01)	51.14 (+/- 0.02)	48.17 (+/- 0.02)	15.79 %	18.13 %
3.0	15.06 (+/-0.02)	15.81 (+/- 0.02)	73.84 (+/- 0.02)	69.41 (+/- 0.02)	16.94 %	21.32 %

Due to the asymmetry cholesterol (two distinctly different sides), the orientation of cholesterol around the peptide was determined. It has been shown previously that the rough β-face can be decomposed into two subfaces and that cholesterol has triangular symmetry (Martinez-Seara et al. 2010). To elucidate if cholesterol orientation is somehow specific around the peptide, two-dimensional density plots were calculated (similarly to calculations in (Martinez-Seara et al. 2010)). The results shown in Figure 22 indicate that not only is cholesterol preferentially attracted to the peptide under negative mismatch, but in this case it also shows a preferential orientation around the peptide. Namely, the negative mismatch causes cholesterol to orientate its rough β-face towards the peptide in its close vicinity. The increase in density (yellow color) seen on the right side (x>0) in panels E and G in Figure 22 correspond to the elevated density observed in the RDF in Figure 21. One possible explanation for this peculiar behavior of cholesterol is its different effects on the α- and β-faces. It has previously been shown that the α-face increases the order of neighboring saturated chains more than the β-face, while in the case of monounsaturated chains the situation is the opposite (Róg & Pasenkiewicz-Gierula 2001; Róg & Pasenkiewicz-Gierula 2006). Here, for lipids with unsaturated chains, one can expect that their interaction with the α-face leads to lower chain order and thus lower membrane thickness, thereby locally reducing the mismatch between the peptides and cholesterol around its smooth α-face.

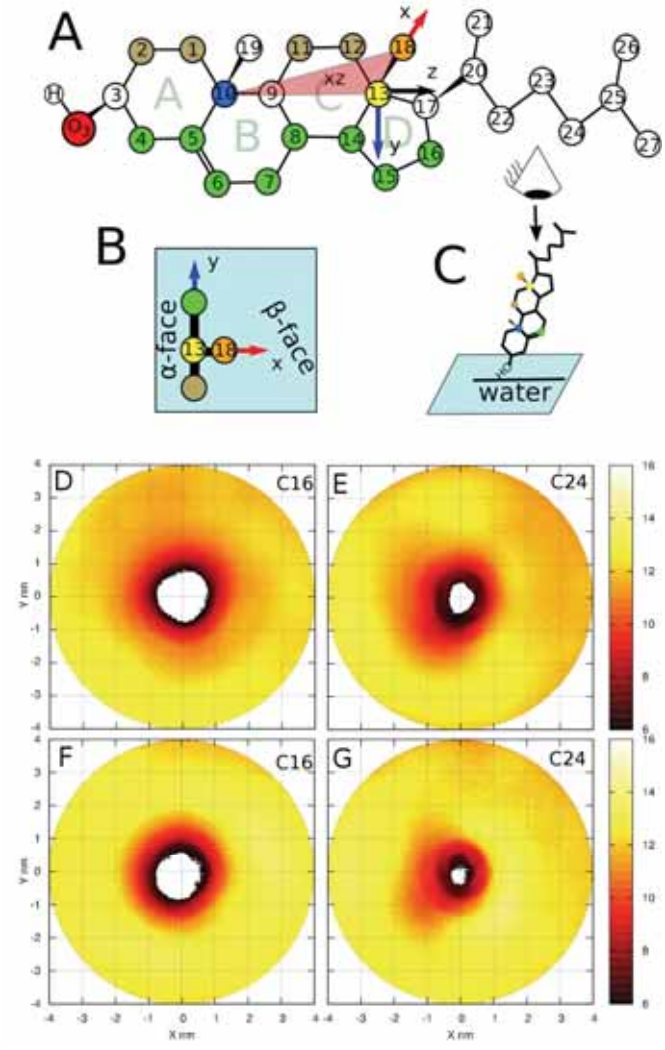

FIGURE 22. Panel A shows the reference axes used in the two-dimensional density distribution calculations shown in panels D–G. The origin of the axis is C13 colored in yellow. The vector between C13 (yellow) and C18 (orange) points along the x-axis. The triangle between C18 (orange), C13 (yellow), and C10 (blue) is in the xz-plane and is depicted in red. Panel B shows a schematic view of cholesterol as a projection in the reference xy-plane from the terminal acyl chain toward the head as shown in Panel C by the arrow. Two-dimensional density distributions in (D, F – upper and lower layer) positive mismatch and (E, G – upper and lower layer) negative mismatch for the peptides around a tagged cholesterol molecule. The different faces of cholesterol can be distinguished in panels D–G: the smooth α-face corresponds to the region x<0 and the rough β-face to x>0.

In order to elucidate the specific cholesterol-peptide interactions under different mismatch conditions, the average number of hydrogen bonds between cholesterol and peptides was calculated.

The average number of hydrogen bonds was 0.66 (+/- 0.007) for negative mismatch (PC24) and 0.30 (+/- 0.005) for positive mismatch (PC16). Although the number is low for both systems, there is a clear difference between positive and negative mismatch, indicating that negative mismatch favors the cholesterol-protein hydrogen bond existence. There are at least three possible explanations for this observation, none of which can explain this observation on its own. First of all, the lower number of hydrogen bonds in positive mismatch results from the lower number of cholesterol molecules in peptide vicinity. Second, the major decrease in the number of hydrogen bonds was due to interactions with terminal tryptophan residues (0.35 +/- 0.005 in PC24 and 0.13; +/- 0.004 in PC16). That can be explained by the position of these residues which under negative mismatch are more buried in the membrane than under positive mismatch. Third, the preferential orientation of cholesterol with its β-face pointing toward the peptide under negative mismatch promotes hydrogen bonding with the peptide, as a hydroxyl group sticks out from the β-face (3β OH), thus promoting chances for hydrogen bonding.

In summation, the results from the simulations have shown that direct cholesterol-protein interactions and cholesterol's geometry in a membrane can be influenced by the hydrophobic mismatch (Figure 23). Importantly, this is the first report of such phenomenon. It was described earlier in the thesis that there are differences in membrane thickness and cholesterol content along the cell compartments and organelles, and that cholesterol can regulate functions of many proteins. Thereby, the presented data indicates that the membrane-protein hydrophobic mismatch can control protein function via modulation of cholesterol-protein interactions. Thus it can have many implications for the membrane protein function in this indirect manner. The role of such a mutual effect (direct lipid-protein interaction strengthened by hydrophobic mismatch) can be to enhance the influence of unspecific factors (like hydrophobic mismatch) for only these proteins that are sensitive to cholesterol (of which examples were given earlier in the thesis). Importantly, this is the first evidence of such cooperation between the specific lipid-protein interaction and membrane physical property (hydrophobic mismatch); as well as for the first time the specific cholesterol orientation of cholesterol around the negatively mismatched peptide was observed. Further studies should evaluate the significance of these observations for the membrane proteins' function.

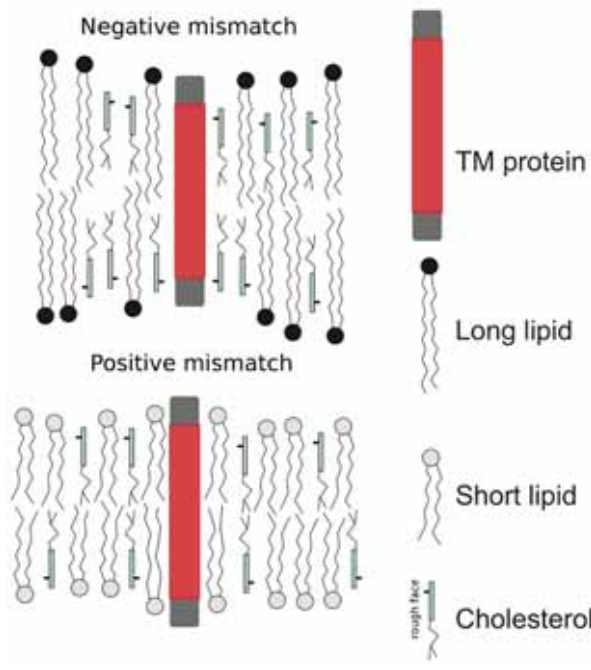

FIGURE 23. Schematic picture of cholesterol behavior under negative (upper scheme) and positive (lower scheme) mismatch. In case of negative mismatch, cholesterol tends to orientate its rough face toward the peptide and concentrate closer to it, while the behavior is opposite in positive mismatch.

6.2.3 Conclusions

Hydrophobic thickness is one of the important physical features of membranes. Cholesterol in turn has a huge impact on the properties of many lipids and membrane types. Therefore, and not surprisingly, cholesterol and hydrophobic length of a membrane are associated and can have an impact on each other. Transmembrane proteins embedded in a lipid bilayer are obviously affected by the length of the hydrophobic core of a membrane. In Article 2, these three ingredients (lipid bilayer, cholesterol, and transmembrane peptides) were shown to affect each other in a sophisticated way, which as it has been shown earlier has physiological relevance (Munro 1995). Experimental data in Article 2 suggested the sorting of peptides to take place under negative mismatch and presence of cholesterol, which was not observed under the positive mismatch, or absence of cholesterol. Molecular dynamics simulations revealed the molecular mechanism underlying this phenomenon and demonstrated that cholesterol increases the significance of negative hydrophobic mismatch, therefore suggesting this to be the mechanism for the sorting of peptides. Extended MD simulations explained more deeply the molecular events that occur under negative hydrophobic mismatch. It was shown that under such conditions cholesterol will behave in a special manner in the vicinity of

the mismatched peptide, and it will undergo a specific geometrical reorientation. These adaptations suggest that negative mismatch is indeed a special case for transmembrane peptides under the presence of cholesterol. Results from these two articles show that a lipid membrane is a complicated multicomponent environment where physical properties can have an impact on peptides embedded in it. The micro-environment in the vicinity of transmembrane peptides can also be controlled through hydrophobic mismatch. Most importantly, the complexity of membranes in cells is enormous, and the hydrophobic length of lipids can be one of the mechanisms controlling lipid-protein interactions.

Concluding remarks

This thesis demonstrates that the atomistic molecular dynamics simulations can be successfully used to explore molecular mechanisms of the biologically relevant processes, such as the lipid-protein interactions. What is even more important in that particular case is that this methodology is highly valued for studies of the lipid-protein systems where experimental methods may have many limitations. In case of the COMT protein-related research in this thesis, the outcome indicates that the lipid bilayer can affect both protein and its ligands. Therefore, lipid bilayer is a specific environment for the enzymatic processes that differs from the standard situation of soluble proteins. MD simulations from that study suggested more general principles that can possibly govern very important physiological processes, such as neurotransmission. Importantly, these findings were also validated with experimental procedures that confirmed its validity. Quite the opposite of that situation (experimental results leading to simulations) led to the simulation data presented in Article 2, where molecular mechanisms governing the experimental observations of clustering of peptides according to their hydrophobic length were revealed. In-depth analyses and an extension of this simulation allowed for more light to be shed on very specific cholesterol-protein interactions under negative hydrophobic mismatch.

What is common for all the articles in this thesis is that they emphasize the role of the membrane as a unique environment for proteins. Anyone who wants to understand how membrane proteins function has to first understand the membrane involvement in their function, but this is not trivial due to the complexity and dynamics of the lipid-protein interactions. Experimental methods together with molecular dynamics simulations can fulfill each other, as it is shown in the articles of this thesis. They can complement each other and provide us with a more precise picture of the main rules governing biochemistry of cells. Exponentially growing computational resources and methods available for MD simulations signify a bright future for studies of more complex

systems that are necessary to give more insight into the lipid-protein interactions. Therefore, it is also very important to evolve the understanding between the experimental and computational researchers. Within this thesis, it is also shown that this is feasible, and moreover it can lead to a very novel insight into investigated problems and large benefits for both parties.

References

Adibhatla, R.M. & Hatcher, J.F. 2007. Role of lipids in brain injury and diseases. *Future Lipidology*. 2:403–422.

Adibhatla, R.M., Hatcher, J.F., & Dempsey, R.J. 2006. Lipids and lipidomics in brain injury and diseases. *AAPS Journal*. 8:E314–E321.

Aktas, M., Danne, L., Möller, P., & Narberhaus, F. 2014. Membrane lipids in Agrobacterium tumefaciens: biosynthetic pathways and importance for pathogenesis. *Frontiers in Plant Science*. 5:109.

Albert, A.D., Young, J.E., & Yeagle, P.L. 1996. Rhodopsin-cholesterol interactions in bovine rod outer segment disk membranes. *Biochimica et Biophysica Acta (BBA) - Biomembranes*. 1285:47–55.

Albert, A.D. & Boesze-Battaglia, K. 2005. The role of cholesterol in rod outer segment membranes. *Progress in Lipid Research*. 44:99–124.

Alder, B.J. & Wainwright, T.E. 1957. Phase transition for a hard sphere system. *Journal of Chemical Physics*. 27:1208–1209.

Anderson, R.G.W. & Jacobson, K. 2002. A role for lipid shells in targeting proteins to caveolae, rafts, and other lipid domains. *Science*. 296:1821–1825.

Arias-Cartin, R., Grimaldi, S., Pommier, J., Lanciano, P., Schaefer, C., Arnoux, P., Giordano, G., Guigliarelli, B., & Magalon, A. 2011. Cardiolipin-based respiratory complex activation in bacteria. *Proceedings of the National Academy of Sciences*. 108:7781–7786.

Arunan, E., Desiraju, G. R., Klein, R. A., Sadlej, J., Scheiner, S., Alkorta, I., Clary, D. C., Crabtree, R. H., Dannenberg, J. J., Hobza, P., Kjaergaard, H. G., Legon, A. C., Mennucci, B. & Nesbitt, D. J. 2011. Defining the hydrogen bond: An account (IUPAC Technical Report). *Pure and Applied Chemistry.* 83:1619–1636.

Bagatolli, L.A., Ipsen, J.H., Simonsen, A.C., & Mouritsen, O.G. 2010. An outlook on organization of lipids in membranes: Searching for a realistic connection with the organization of biological membranes. *Progress in Lipid Research*. 49:378–389.

Bagatolli, L.A. & Mouritsen, O.G. 2013. Is the fluid mosaic (and the accompanying raft hypothesis) a suitable model to describe fundamental features of biological membranes? What may be missing? *Frontiers in Plant Science*. 4:457.

Bai, H.W., Shim, J.Y., Yu, J., & Zhu, B.T. 2007. Biochemical and molecular modeling studies of the O-methylation of various endogenous and exogenous catechol substrates catalyzed by recombinant human soluble and membrane-bound catechol-O-methyltransferases. *Chemical Research in Toxicology*. 20:1409–1425.

Bao, H. & Duong, F. 2013. Phosphatidylglycerol directs binding and inhibitory action of EIIAGlc protein on the maltose transporter. *Journal of Biological Chemistry*. 288:23666–23674.

Barrett, P.J., Song, Y., Horn, W.D.V., Hustedt, E.J., Schafer, J.M., Hadziselimovic, A., Beel, A.J., & Sanders, C.R. 2012. The amyloid precursor protein has a flexible transmembrane domain and binds cholesterol. *Science*. 336:1168–1171.

Basu, I., Chattopadhyay, A., & Mukhopadhyay, C. 2014. Ion channel stability of Gramicidin A in lipid bilayers: Effect of hydrophobic mismatch. *Biochimica et Biophysica Acta (BBA) - Biomembranes*. 1838:328–338.

Bechinger, B. & Seelig, J. 1991. Conformational changes of the phosphatidylcholine headgroup due to membrane dehydration. A 2H-NMR study. *Chemistry and Physics of Lipids*. 58:1–5.

Berendsen, H.J.C., van der Spoel, D., & van Drunen, R. 1995. GROMACS: A message-passing parallel molecular dynamics implementation. *Computer Physics Communications*. 91:43–56.

Berman, H.M., Westbrook, J., Feng, Z., Gilliland, G., Bhat, T.N., Weissig, H., Shindyalov, I.N., & Bourne, P.E. 2000. The Protein Data Bank. *Nucleic Acids Research*. 28:235–242.

Berridge, M.J., Lipp, P., & Bootman, M.D. 2000. The versatility and universality of calcium signalling. *Nature Reviews Molecular Cell Biology*. 1:11–21.

Bill, R.M., Henderson, P.J.F., Iwata, S., Kunji, E.R.S., Michel, H., Neutze, R., Newstead, S., Poolman, B., Tate, C.G., & Vogel, H. 2011. Overcoming barriers to membrane protein structure determination. *Nature Biotechnology*. 29:335–340.

Binder, M.D., Hirokawa, N., & Windhorst, U. 2008. Encyclopedia of Neuroscience. *Springer*, Berlin, Heidelberg.

Bini, L., Pacini, S., Liberatori, S., Valensin, S., Pellegrini, M., Raggiaschi, R., Pallini, V., & Baldari, C.T. 2003. Extensive temporally regulated reorganization of the lipid raft proteome following T-cell antigen receptor triggering. *Biochemical Journal*. 369:301–309.

Bittman, R., Clejan, S., Lund-Katz, S., & Phillips, M.C. 1984. Influence of cholesterol on bilayers of ester- and ether-linked phospholipids Permeability and 13C-nuclear magnetic resonance measurements. *Biochimica et Biophysica Acta (BBA) - Biomembranes*. 772:117–126.

Bockmann, R.A., Hac, A., Heimburg, T., & Grubmuller, H. 2003. Effect of sodium chloride on a lipid bilayer. *Biophysical Journal*. 85:1647–1655.

Bogdanov, M. & Dowhan, W. 1998. Phospholipid-assisted protein folding: phosphatidylethanolamine is required at a late step of the conformational maturation of the polytopic membrane protein lactose permease. *EMBO Journal*. 17:5255–5264.

Bogdanov, M. & Dowhan, W. 1999. Lipid-assisted protein folding. *Journal of Biological Chemistry*. 274:36827–36830.

Bogdanov, M., Xie, J., Heacock, P., & Dowhan, W. 2008. To flip or not to flip: lipid-protein charge interactions are a determinant of final membrane protein topology. *Journal of Cell Biology*. 182:925–935.

Borchman, D., Foulks, G.N., Yappert, M.C., Tang, D., & Ho, D.V. 2007. Spectroscopic evaluation of human tear lipids. *Chemistry and Physics of Lipids*. 147:87–102.

Bremer, E.G., Schlessinger, J., & Hakomori, S. 1986. Ganglioside-mediated modulation of cell growth. Specific effects of GM3 on tyrosine phosphorylation of the epidermal growth factor receptor. *Journal of Biological Chemistry*. 261:2434–2440.

Bretscher, M.S. 1973. Membrane structure: some general principles. *Science*. 181:622– 629.

Bretscher, M.S. & Munro, S. 1993. Cholesterol and the Golgi apparatus. *Science*. 261:1280–1281.

Brown, M.F. 1994. Modulation of rhodopsin function by properties of the membrane bilayer. *Chemistry and Physics of Lipids*. 73:159–180.

Brown, D.A. & London, E. 1998. Functions of lipid rafts in biological membranes. *Annual Review of Cell and Developmental Biology*. 14:111–136.

Bussi, G., Donadio, D., & Parrinello, M. 2007. Canonical sampling through velocity rescaling. *Journal of Chemical Physics*. 126:014101.

Cantor, R.S. 1997. Lateral pressures in cell membranes: A mechanism for modulation of protein function. *Journal of Physical Chemistry B*. 101:1723–1725.

Cantor, R.S. 1998. The lateral pressure profile in membranes: a physical mechanism of general anesthesia. *Toxicology Letters*. 100–101:451–458.

Cantor, R.S. 1999. The influence of membrane lateral pressures on simple geometric models of protein conformational equilibria. *Chemistry and Physics of Lipids*. 101:45–56.

Cantor, R.S. 2003. Receptor desensitization by neurotransmitters in membranes: are neurotransmitters the endogenous anesthetics? *Biochemistry*. 42:11891–11897.

Cevc, G. 1990. Membrane electrostatics. *Biochimica et Biophysica Acta (BBA)*. 1031:311–382.

Chandrasekhar, I., van Gunsteren, W.F., Zandomeneghi, G., Williamson, P.T.F., & Meier, B.H. 2006. Orientation and conformational preference of leucine-enkephalin at the surface of a hydrated dimyristoylphosphatidylcholine bilayer: NMR and MD simulation. *Journal of the American Chemical Society*. 128:159–170.

Chen, I.A. 2006. The emergence of cells during the origin of life. *Science*. 314:1558–1559.

Chen, J., Song, J., Yuan, P., Tian, Q., Ji, Y., Ren-Patterson, R., Liu, G., Sei, Y., & Weinberger, D.R. 2011. Orientation and cellular distribution of membrane-bound

Catechol-O-methyltransferase in cortical neurons implications for drug development. *Journal of Biological Chemistry*. 286:34752–34760.

Cherezov, V., Rosenbaum, D.M., Hanson, M.A., Rasmussen, S.G.F., Thian, F.S., Kobilka, T.S., Choi, H.-J., Kuhn, P., Weis, W.I., Kobilka, B.K., & Stevens, R.C. 2007. High-resolution crystal structure of an engineered human beta2-adrenergic G protein-coupled receptor. *Science*. 318:1258–1265.

Chong, P.L. 1994. Evidence for regular distribution of sterols in liquid crystalline phosphatidylcholine bilayers. *Proceedings of the National Academy of Sciences*. 91:10069–10073.

Chong, P.L.-G., Zhu, W., & Venegas, B. 2009. On the lateral structure of model membranes containing cholesterol. *Biochimica et Biophysica Acta (BBA)*. 1788:2–11.

Cole, N.B., Ellenberg, J., Song, J., DiEuliis, D., & Lippincott-Schwartz, J. 1998. Retrograde transport of Golgi-localized proteins to the ER. *Journal of Cell Biology*. 140:1–15.

Contreras, F.X., Ernst, A.M., Haberkant, P., Björkholm, P., Lindahl, E., Gönen, B., Tischer, C., Elofsson, A., von Heijne, G., Thiele, C., Pepperkok, R., Wieland, F., & Brügger, B. 2012. Molecular recognition of a single sphingolipid species by a protein/'s transmembrane domain. *Nature*. 481:525–529.

Coskun, Ü. & Simons, K. 2011. Cell membranes: The lipid perspective. *Structure*. 19:1543–1548.

Danielli, J.F. & Davson, H. 1935. A contribution to the theory of permeability of thin films. *Journal of Cellular and Comparative Physiology*. 5:495–508.

De Kruyff, B., De Greef, W.J., Van Eyk, R.V.W., Demel, R.A., & Van Deene, L.L.M. 1973. The effect of different fatty acid and sterol composition on the erythritol flux through the cell membrane of Acholeplasma laidlawii. *Biochimica et Biophysica Acta (BBA) - Biomembranes*. 298:479–499.

Demel, R.A., Jansen, J.W., van Dijck, P.W., & van Deenen, L.L. 1977. The preferential interaction of cholesterol with different classes of phospholipids. *Biochimica et Biophysica Acta (BBA)*. 465:1–10.

Dickson, C.J., Madej, B.D., Skjevik, Å.A., Betz, R.M., Teigen, K., Gould, I.R., & Walker, R.C. 2014. Lipid14: The Amber lipid force field. *Journal of Chemical Theory and Computation*. 10:865–879.

Dowhan, W. 1997. Molecular basis for membrane phospholipid diversity: why are there so many lipids? *Annual Review of Biochemistry*. 66:199–232.

Dowhan, W. & Bogdanov, M. 2009. Lipid-dependent membrane protein topogenesis. *Annual Review of Biochemistry*. 78:515–540.

Dowhan, W. & Bogdanov, M. 2012. Molecular genetic and biochemical approaches for defining lipid-dependent membrane protein folding. *Biochimica et Biophysica Acta (BBA) - Biomembranes, Protein Folding in Membranes*. 1818:1097–1107.

Dror, R.O., Arlow, D.H., Maragakis, P., Mildorf, T.J., Pan, A.C., Xu, H., Borhani, D.W., & Shaw, D.E. 2011. Activation mechanism of the β2-adrenergic receptor. *Proceedings of the National Academy of Sciences*. 108:18684–18689.

Dror, R.O., Dirks, R.M., Grossman, J.P., Xu, H., & Shaw, D.E. 2012. Biomolecular simulation: a computational microscope for molecular biology. *Annual Review of Biophysics*. 41:429–452.

Duan, Y. & Kollman, P.A. 1998. Pathways to a protein folding intermediate observed in a 1-microsecond simulation in aqueous solution. *Science*. 282:740–744.

Edidin, M. 2003. The state of lipid rafts: from model membranes to cells. *Annual Review of Biophysics and Biomolecular Structure*. 32:257–283.

Eichacker, L.A., Granvogl, B., Mirus, O., Müller, B.C., Miess, C., & Schleiff, E. 2004. Hiding behind hydrophobicity. Transmembrane segments in mass spectrometry. *Journal of Biological Chemistry*. 279:50915–50922.

Ejsing, C.S., Sampaio, J.L., Surendranath, V., Duchoslav, E., Ekroos, K., Klemm, R.W., Simons, K., & Shevchenko, A. 2009. Global analysis of the yeast lipidome by quantitative shotgun mass spectrometry. *Proceedings of the National Academy of Sciences*. 106:2136–2141.

El-Sayed, M.Y., Guion, T.A., & Fayer, M.D. 1986. Effect of cholesterol on viscoelastic properties of dipalmitoylphosphatidylcholine multibilayers as measured by a laser-induced ultrasonic probe. *Biochemistry*. 25:4825–4832.

Epand, R.M. & Epand, R.F. 1994. Calorimetric detection of curvature strain in phospholipid bilayers. *Biophysical Journal*. 66:1450–1456.

Epand, R.M., Sayer, B.G., & Epand, R.F. 2005. Caveolin scaffolding region and cholesterol- rich domains in membranes. Journal of Molecular Biology. 345(2):339–350.

Ernst, A.M., Contreras, F.X., Brügger, B., & Wieland, F. 2010. Determinants of specificity at the protein–lipid interface in membranes. *FEBS Letters, Frontiers in Membrane Biochemistry*. 584:1713–1720.

Essmann, U., Perera, L., Berkowitz, M.L., Darden, T., Lee, H., & Pedersen, L.G. 1995. A smooth particle mesh Ewald method. *Journal of Chemical Physics*. 103:8577–8593.

Estep, T.N., Mountcastle, D.B., Barenholz, Y., Biltonen, R.L., & Thompson, T.E. 1979. Thermal behavior of synthetic sphingomyelin-cholesterol dispersions. *Biochemistry*. 18:2112–2117.

Fahy, E., Subramaniam, S., Brown, H.A., Glass, C.K., Merrill, A.H., Jr, Murphy, R.C., Raetz, C.R.H., Russell, D.W., Seyama, Y., Shaw, W., Shimizu, T., Spener, F., van Meer, G., VanNieuwenhze, M.S., White, S.H., Witztum, J.L., & Dennis, E.A. 2005. A comprehensive classification system for lipids. *Journal of Lipid Research*. 46:839–861.

Feller, S.E. & MacKerell, A.D. 2000. An improved empirical potential energy function for molecular simulations of phospholipids. *Journal of Physical Chemistry B*. 104:7510–7515.

Fenton, W.S., Hibbeln, J., & Knable, M. 2000. Essential fatty acids, lipid membrane abnormalities, and the diagnosis and treatment of schizophrenia. *Biological Psychiatry*. 47:8–21.

Foster, L.J., De Hoog, C.L., & Mann, M. 2003. Unbiased quantitative proteomics of lipid rafts reveals high specificity for signaling factors. *Proceedings of the National Academy of Sciences*. 100:5813–5818.

Frangopol, P.T. & Mihăilescu, D. 2001. Interactions of some local anesthetics and alcohols with membranes. *Colloids and Surfaces B: Biointerfaces*. 22:3–22.

Fry, M. & Green, D.E. 1980. Cardiolipin requirement by cytochrome oxidase and the catalytic role of phospholipid. *Biochemical and Biophysical Research Communications*. 93:1238–1246.

Gebhardt, C., Gruler, H., & Sackmann, E. 1977. On domain structure and local curvature in lipid bilayers and biological membranes. *Zeitschrift für Naturforschung C - A Journal of Biosciences*. 32:581–596.

Geest, M. van & Lolkema, J.S. 2000. Membrane topology and insertion of membrane proteins: Search for topogenic signals. *Microbiology and Molecular Biology Reviews*. 64:13–33.

Gimpl, G., Burger, K., & Fahrenholz, F. 1997. Cholesterol as modulator of receptor function. *Biochemistry*. 36:10959–10974.

Gimpl, G., Burger, K., & Fahrenholz, F. 2002. A closer look at the cholesterol sensor. *Trends in Biochemical Sciences*. 27:596–599.

Gomez, B. & Robinson, N.C. 1999. Phospholipase digestion of bound cardiolipin reversibly inactivates bovine cytochrome bc1. *Biochemistry*. 38:9031–9038.

Gorter, E. & Grendel, F. 1925. On bimolecular layers of lipoids on the chromocytes of the blood. *Journal of Experimetal Medicine*. 41:439–443.

Grant, C.W. 1975. Lipid lateral phase separations. Spin label freeze-fracture electron microscopy studies. *Biophysical Journal*. 15:949–952.

Grossman, M.H., Creveling, C.R., Rybczynski, R., Braverman, M., Isersky, C., & Breakefield, X.O. 1985. Soluble and particulate forms of rat Catechol-O-methyltransferase distinguished by gel electrophoresis and immune fixation. *Journal of Neurochemistry*. 44:421–432.

Guldberg, H.C. & Marsden, C.A. 1975. Catechol-O-methyl transferase: pharmacological aspects and physiological role. *Pharmacological Reviews*. 27:135–206.

Hamill, O.P. & Martinac, B. 2001. Molecular basis of mechanotransduction in living cells. *Physiological Reviews*. 81:685–740.

Hansen, S.B., Tao, X., & MacKinnon, R. 2011. Structural basis of PIP2 activation of the classical inward rectifier K+ channel Kir2.2. *Nature*. 477:495–498.

Hanson, M.A., Cherezov, V., Griffith, M.T., Roth, C.B., Jaakola, V.-P., Chien, E.Y.T., Velasquez, J., Kuhn, P., & Stevens, R.C. 2008. A specific cholesterol binding site is established by the 2.8 Å structure of the human β2-adrenergic receptor. *Structure*. 16:897–905.

Harris, T.J.C. & Siu, C.H. 2002. Reciprocal raft-receptor interactions and the assembly of adhesion complexes. *Bioessays*. 24:996–1003.

Harrison, P.J. & Weinberger, D.R. 2005. Schizophrenia genes, gene expression, and neuropathology: on the matter of their convergence. *Molecular Psychiatry*. 10:40–68.

Heerklotz, H. 2002. Triton promotes domain formation in lipid raft mixtures. Biophysical *Journal*. 83:2693–2701.

Heo, W.D., Inoue, T., Park, W.S., Kim, M.L., Park, B.O., Wandless, T.J., & Meyer, T. 2006. PI(3,4,5)P3 and PI(4,5)P2 lipids target proteins with polybasic clusters to the plasma membrane. *Science*. 314:1458–1461.

Hess, B., Bekker, H., Berendsen, H.J.C., & Fraaije, J.G.E.M. 1997. LINCS: A linear constraint solver for molecular simulations. *Journal of Computational Chemistry*. 18:1463–1472.

Hessa, T., Meindl-Beinker, N.M., Bernsel, A., Kim, H., Sato, Y., Lerch-Bader, M., Nilsson, I., White, S.H., & von Heijne, G. 2007. Molecular code for transmembrane-helix recognition by the Sec61 translocon. *Nature*. 450:1026–1030.

Hilgemann, D.W. 2003. Getting ready for the decade of the lipids. *Annual Review of Physiology*. 65:697–700.

Hoover, W.G. 1985. Canonical dynamics: Equilibrium phase-space distributions. *Physical Review A*. 31:1695–1697.

Huang, J. & Feigenson, G.W. 1999. A microscopic interaction model of maximum solubility of cholesterol in lipid bilayers. *Biophysical Journal*. 76:2142–2157.

Humphrey, W., Dalke, A., & Schulten, K. 1996. VMD: visual molecular dynamics. *Journal of Molecular Graphics*. 14:33–38.

Hunte, C. & Richers, S. 2008. Lipids and membrane protein structures. *Current Opinion in Structural Biology*. 18:406–411.

Ikonen, E. 2008. Cellular cholesterol trafficking and compartmentalization. *Nature Reviews Molecular Cell Biology*. 9:125–138.

Ipsen, J.H., Karlström, G., Mourtisen, O.G., Wennerström, H., & Zuckermann, M.J. 1987. Phase equilibria in the phosphatidylcholine-cholesterol system. *Biochimica et Biophysica Acta (BBA) - Biomembranes*. 905:162–172.

Jafurulla, M., Tiwari, S., & Chattopadhyay, A. 2011. Identification of cholesterol recognition amino acid consensus (CRAC) motif in G-protein coupled receptors. *Biochemical and Biophysical Research Communications*. 404:569–573.

Jain, M.K. & White, H.B., 3rd. 1977. Long-range order in biomembranes. *Advances in lipid research*. 15:1–60.

Jämbeck, J.P.M. & Lyubartsev, A.P. 2012. Derivation and systematic validation of a refined all-atom force field for phosphatidylcholine lipids. *Journal of Physical Chemistry B*. 116:3164–3179.

Jodko-Piorecka, K. & Litwinienko, G. 2013. First experimental evidence of dopamine interactions with negatively charged model biomembranes. *ACS Chemical Neuroscience*. 4:1114–1122.

Jójárt, B. & Martinek, T.A. 2007. Performance of the general amber force field in modeling aqueous POPC membrane bilayers. *Journal of Computational Chemistry*. 28:2051–2058.

Jorgensen, W.L., Maxwell, D.S., & Tirado-Rives, J. 1996. Development and testing of the OPLS all-atom force field on conformational rnergetics and properties of organic liquids. *Journal of the American Chemical Society*. 118:11225–11236.

Jorgensen, W.L. 2004. The many roles of computation in drug discovery. *Science*. 303:1813–1818.

Jormakka, M., Törnroth, S., Byrne, B., & Iwata, S. 2002. Molecular basis of proton motive force generation: structure of formate dehydrogenase-N. *Science*. 295:1863–1868.

Kaczanowski, S. & Zielenkiewicz, P. 2010. Why similar protein sequences encode similar three-dimensional structures? *Theoretical Chemistry Accounts*. 125:643–650.

Käenmäki, M., Tammimäki, A., Myöhänen, T., Pakarinen, K., Amberg, C., Karayiorgou, M., Gogos, J.A., & Männistö, P.T. 2010. Quantitative role of COMT in dopamine clearance in the prefrontal cortex of freely moving mice. *Journal of Neurochemistry*. 114:1745–1755.

Kaminski, G.A., Friesner, R.A., Tirado-Rives, J., & Jorgensen, W.L. 2001. Evaluation and reparametrization of the OPLS-AA force field for proteins via comparison with accurate quantum chemical calculations on peptides. *Journal of Physical Chemistry B*. 105:6474–6487.

Karnovsky, M.J., Kleinfeld, A.M., Hoover, R.L., & Klausner, R.D. 1982. The concept of lipid domains in membranes. *Journal of Cell Biology*. 94:1–6.

Kelkar, D.A. & Chattopadhyay, A. 2007. Modulation of gramicidin channel conformation and organization by hydrophobic mismatch in saturated phosphatidylcholine bilayers. *Biochimica et Biophysica Acta (BBA) - Biomembranes*. 1768:1103–1113.

Kenworthy, A. 2002. Peering inside lipid rafts and caveolae. *Trends in Biochemical Sciences*. 27:435– 437.

Killian, J.A. 1998. Hydrophobic mismatch between proteins and lipids in membranes. *Biochimica et Biophysica Acta (BBA) - Reviews on Biomembranes*. 1376:401–416.

Killian, J.A. & Nyholm, T.K.M. 2006. Peptides in lipid bilayers: the power of simple models. *Current Opinion in Structural Biology*. 16:473–479.

Kim, C., Schmidt, T., Cho, E.G., Ye, F., Ulmer, T.S., & Ginsberg, M.H. 2012. Basic amino-acid side chains regulate transmembrane integrin signalling. *Nature*. 481:209–213.

Kim, T., Lee, J., & Im, W. 2009. Molecular dynamics studies on structure and dynamics of phospholamban monomer and pentamer in membranes. *Proteins*. 76:86–98.

Klauda, J.B., Venable, R.M., Freites, J.A., O'Connor, J.W., Tobias, D.J., Mondragon-Ramirez, C., Vorobyov, I., MacKerell, A.D., & Pastor, R.W. 2010. Update of the CHARMM all-atom additive force field for lipids: validation on six lipid types. *Journal of Physical Chemistry B*. 114:7830–7843.

Kovbasnjuk, O., Edidin, M., & Donowitz, M. 2001. Role of lipid rafts in Shiga toxin 1 interaction with the apical surface of Caco-2 cells. *Journal of Cell Science*. 114:4025–4031.

Krogh, A., Larsson, B., von Heijne, G., & Sonnhammer, E.L. 2001. Predicting transmembrane protein topology with a hidden Markov model: application to complete genomes. *Journal of Molecular Biology*. 305:567–580.

Lagerström, M.C. & Schiöth, H.B. 2008. Structural diversity of G protein-coupled receptors and significance for drug discovery. *Nature Reviews Drug Discovery*. 7:339–357.

Lange, C., Nett, J.H., Trumpower, B.L., & Hunte, C. 2001. Specific roles of protein–phospholipid interactions in the yeast cytochrome bc1 complex structure. *The EMBO Journal*. 20:6591–6600.

Laursen, M., Yatime, L., Nissen, P., & Fedosova, N.U. 2013. Crystal structure of the high-affinity Na+,K+-ATPase–ouabain complex with Mg2+ bound in the cation binding site. *Proceedings of the National Academy of Sciences*. 110:10958–10963.

Lee, A.G. 2003. Lipid-protein interactions in biological membranes: a structural perspective. *Biochimica et Biophysica Acta (BBA)*. 1612:1–40.

Lee, A.G. 2004. How lipids affect the activities of integral membrane proteins. *Biochimica et Biophysica Acta (BBA)*. 1666:62–87.

Lee, A.G. 2011. Lipid-protein interactions. *Biochemical Society Transactions*. 39:761–766.

Lee, A.G., Birdsall, N.J.M., Metcalfe, J.C., Toon, P.A., & Warren, G.B. 1974. Clusters in lipid bilayers and the interpretation of thermal effects in biological membranes. *Biochemistry*. 13:3699–3705.

Lentz, B.R., Barenholz, Y., & Thompson, T.E. 1976. Fluorescence depolarization studies of phase transitions and fluidity in phospholipid bilayers. 2. Two-component phosphatidylcholine liposomes. *Biochemistry*. 15:4529–4537.

Li, H. & Papadopoulos, V. 1998. Peripheral-type benzodiazepine receptor function in cholesterol transport. Identification of a putative cholesterol recognition/interaction amino acid sequence and consensus pattern. *Endocrinology*. 139:4991–4997.

Li, L., Shi, X., Guo, X., Li, H., & Xu, C. 2014. Ionic protein–lipid interaction at the plasma membrane: what can the charge do? *Trends in Biochemical Sciences*. 39:130–140.

Lingwood, D. & Simons, K. 2010. Lipid rafts as a membrane-organizing principle. *Science*. 327:46–50.

Lingwood, D., Binnington, B., Róg, T., Vattulainen, I., Grzybek, M., Coskun, Ü., Lingwood, C.A., & Simons, K. 2011. Cholesterol modulates glycolipid conformation and receptor activity. *Nature Chemical Biology*. 7:260–262.

Lindahl, E. & Sansom, M.S.P. 2008. Membrane proteins: molecular dynamics simulations. *Current Opinion in Structural Biology*. 18:425–431.

Lindorff-Larsen, K., Piana, S., Dror, R.O., & Shaw, D.E. 2011. How fast-folding proteins fold. *Science*. 334:517–520.

Lippincott-Schwartz, J. & Phair, R.D. 2010. Lipids and cholesterol as regulators of traffic in the endomembrane system. *Annual Review of Biophysics*. 39:559–578.

Liu, W., Chun, E., Thompson, A.A., Chubukov, P., Xu, F., Katritch, V., Han, G.W., Roth, C.B., Heitman, L.H., IJzerman, A.P., Cherezov, V., & Stevens, R.C. 2012. Structural basis for allosteric regulation of GPCRs by sodium ions. *Science*. 337:232–236.

Llorente, A., Skotland, T., Sylvänne, T., Kauhanen, D., Róg, T., Orłowski, A., Vattulainen, I., Ekroos, K., & Sandvig, K. 2012. Molecular lipidomics of exosomes released by PC-3 prostate cancer cells. *Biochimica et Biophysica Acta (BBA)*. 1831:1302–1309.

Lundbaek, J.A. & Andersen, O.S. 1994. Lysophospholipids modulate channel function by altering the mechanical properties of lipid bilayers. *Journal of General Physiology*. 104:645–673.

Lundbaek, J.A., Maer, A.M., & Andersen, O.S. 1997. Lipid bilayer electrostatic energy, curvature stress, and assembly of gramicidin channels. *Biochemistry*. 36:5695–5701.

Lundbaek, J.A., Andersen, O.S., Werge, T., & Nielsen, C. 2003. Cholesterol-induced protein sorting: an analysis of energetic feasibility. *Biophysical Journal*. 84:2080–2089.

MacCallum, J.L., Bennett, W.F.D., & Tieleman, D.P. 2008. Distribution of amino acids in a lipid bilayer from computer simulations. *Biophysical Journal*. 94:3393–3404.

Maciejewski, A., Pasenkiewicz-Gierula, M., Cramariuc, O., Vattulainen, I., & Rog, T. 2014. Refined OPLS all-atom force field for saturated phosphatidylcholine bilayers at full hydration. *Journal of Physical Chemistry B*. 118:4571–4581.

Manglik, A., Kruse, A.C., Kobilka, T.S., Thian, F.S., Mathiesen, J.M., Sunahara, R.K., Pardo, L., Weis, W.I., Kobilka, B.K., & Granier, S. 2012. Crystal structure of the μ-opioid receptor bound to a morphinan antagonist. *Nature*. 485:321–326.

Männistö, P.T. & Kaakkola, S. 1999. Catechol-O-methyltransferase (COMT): biochemistry, molecular biology, pharmacology, and clinical efficacy of the new selective COMT inhibitors. *Pharmacological Reviews*. 51:593–628.

Marcelja, S. 1976. Lipid-mediated protein interaction in membranes. *Biochimica et Biophysica Acta (BBA)*. 455:1–7.

Marrink, S.J., Risselada, H.J., Yefimov, S., Tieleman, D.P., & de Vries, A.H. 2007. The MARTINI force field: coarse grained model for biomolecular simulations. *Journal of Physical Chemistry B*. 111:7812–7824.

Marsh, D. 1990. Lipid-protein interactions in membranes. *FEBS Letters*. 268:371–375.

Marsh, D. & Horváth, L.I. 1998. Structure, dynamics and composition of the lipid-protein interface. Perspectives from spin-labelling. *Biochimica et Biophysica Acta (BBA)*. 1376:267–296.

Martí-Renom, M.A., Stuart, A.C., Fiser, A., Sánchez, R., Melo, F., & Sali, A. 2000. Comparative protein structure modeling of genes and genomes. *Annual Review of Biophysics and Biomolecular Structure*. 29:291–325.

Martinez-Seara, H., Róg, T., Karttunen, M., Vattulainen, I., & Reigada, R. 2010. Cholesterol induces specific spatial and orientational order in cholesterol/phospholipid membranes. *PLoS ONE*. 5:e11162.

Matsumoto, M., Weickert, C.S., Akil, M., Lipska, B.K., Hyde, T.M., Herman, M.M., Kleinman, J.E., & Weinberger, D.R. 2003. Catechol O-methyltransferase mRNA expression in human and rat brain: evidence for a role in cortical neuronal function. *Neuroscience*. 116:127–137.

Maulik, P.R. & Shipley, G.G. 1996. Interactions of N-stearoyl sphingomyelin with cholesterol and dipalmitoylphosphatidylcholine in bilayer membranes. *Biophysical Journal*. 70:2256–2265.

McCammon, J.A., Gelin, B.R., & Karplus, M. 1977. Dynamics of folded proteins. *Nature*. 267:585–590.

McDonald, T.G. & Van Eyk, J.E. 2003. Mitochondrial proteomics. Undercover in the lipid bilayer. *Basic Research in Cardiology*. 98:219–227.

McIntosh, T.J. & Simon, S.A. 2006. Roles of bilayer material properties in function and distribution of membrane proteins. Annual Review of Biophysics and Biomolecular *Structure*. 35:177–198.

Meuillet, E.J., Kroes, R., Yamamoto, H., Warner, T.G., Ferrari, J., Mania-Farnell, B., George, D., Rebbaa, A., Moskal, J.R., & Bremer, E.G. 1999. Sialidase gene transfection enhances epidermal growth factor receptor activity in an epidermoid carcinoma cell line, A431. *Cancer Ressearch*. 59:234–240.

Meyer-Lindenberg, A., Kohn, P.D., Kolachana, B., Kippenhan, S., McInerney-Leo, A., Nussbaum, R., Weinberger, D.R., & Berman, K.F. 2005. Midbrain dopamine and prefrontal function in humans: interaction and modulation by COMT genotype. *Nature Neuroscience*. 8:594–596.

Miettinen, M.S., Gurtovenko, A.A., Vattulainen, I., & Karttunen, M. 2009. Ion dynamics in cationic lipid bilayer systems in saline solutions. *Journal of Physical Chemistry B*. 113:9226–9234.

Mikhalyov, I., Gretskaya, N., Bergström, F., & Johansson, L.B.-Å. 2002. Electronic ground and excited state properties of dipyrrometheneboron difluoride (BODIPY): Dimers with application to biosciences. *Physical Chemistry Chemical Physics*. 4:5663–5670.

Mobashery, N., Nielsen, C., & Andersen, O.S. 1997. The conformational preference of gramicidin channels is a function of lipid bilayer thickness. *FEBS Letters*. 412:15–20.

Monnard, P.-A., Apel, C.L., Kanavarioti, A., & Deamer, D.W. 2002. Influence of ionic inorganic solutes on self-assembly and polymerization processes related to early forms of life: implications for a prebiotic aqueous medium. *Astrobiology*. 2:139–152.

Mouritsen, O.G. & Bloom, M. 1984. Mattress model of lipid-protein interactions in membranes. *Biophysical Journal*. 46:141–153.

Mouritsen, O.G. & Jørgensen, K. 1998. A new look at lipid-membrane structure in relation to drug research. *Pharmaceutical Research*. 15:1507–1519.

Mouritsen, O.G. 2013. Physical chemistry of curvature and curvature stress in membranes. *Current Physical Chemistry*. 3:17–26.

Mukhopadhyay, P., Monticelli, L., & Tieleman, D.P. 2004. Molecular dynamics simulation of a palmitoyl-oleoyl phosphatidylserine bilayer with Na+ counterions and NaCl. *Biophysical Journal*. 86:1601–1609.

Muller, P. 1994. Glossary of terms used in physical organic chemistry (IUPAC Recommendations 1994). *Pure and Applied Chemistry*. 66.

Munro, S. 1991. Sequences within and adjacent to the transmembrane segment of alpha-2,6-sialyltransferase specify Golgi retention. *EMBO Journal*. 10:3577–3588.

Munro, S. 1995. An investigation of the role of transmembrane domains in Golgi protein retention. *EMBO Journal*. 14:4695–4704.

Munro, S. 2003. Lipid rafts: elusive or illusive? *Cell*. 115:377–388.

Myöhänen, T.T., Schendzielorz, N., & Männistö, P.T. 2010. Distribution of catechol-O-methyltransferase (COMT) proteins and enzymatic activities in wild-type and soluble COMT deficient mice. *Journal of Neurochemistry*. 113:1632–1643.

M'Baye, G., Mély, Y., Duportail, G., & Klymchenko, A.S. 2008. Liquid ordered and gel phases of lipid bilayers: fluorescent probes reveal close fluidity but different hydration. *Biophysical Journal*. 95:1217–1225.

Nicolaides, N. & Santos, E.C. 1985. The di- and triesters of the lipids of steer and human meibomian glands. *Lipids*. 20:454–467.

Nielsen, C., Goulian, M., & Andersen, O.S. 1998. Energetics of inclusion-induced bilayer deformations. *Biophysical Journal*. 74:1966–1983.

Niemelä, P.S., Ollila, S., Hyvönen, M.T., Karttunen, M., & Vattulainen, I. 2007. Assessing the nature of lipid raft membranes. *PLoS Computational Biology*. 3:e34.

Niemelä, P.S., Miettinen, M.S., Monticelli, L., Hammaren, H., Bjelkmar, P., Murtola, T., Lindahl, E., & Vattulainen, I. 2010. Membrane proteins diffuse as dynamic complexes with lipids. *Journal of the American Chemical Society*. 132:7574–7575.

Nilsson, I., Ohvo-Rekilä, H., Slotte, J.P., Johnson, A.E., & von Heijne, G. 2001. Inhibition of protein translocation across the endoplasmic reticulum membrane by sterols. *Journal of Biological Chemistry*. 276:41748–41754.

Nosé, S. & Klein, M.L. 1983. Constant pressure molecular dynamics for molecular systems. *Molecular Physics*. 50:1055–1076.

Nosé, S. 1984. A molecular dynamics method for simulations in the canonical ensemble. *Molecular Physics*. 52:255–268.

Nunes, T., Machado, R., Rocha, J.F., Fernandes-Lopes, C., Costa, R., Torrão, L., Loureiro, A.I., Falcão, A., Vaz-da -Silva, M., Wright, L., Almeida, L., & Soares-da-Silva, P. 2009. Pharmacokinetic—pharmacodynamic interaction between nebicapone and controlled-release levodopa/benserazide: A single-center, phase I, double-blind, randomized, placebo-controlled, four-way crossover study in healthy subjects. *Clinical Therapeutics*. 31:2258–2271.

Ollila, S.H., Róg, T., Karttunen, M., & Vattulainen, I. 2007. Role of sterol type on lateral pressure profiles of lipid membranes affecting membrane protein functionality:

Comparison between cholesterol, desmosterol, 7-dehydrocholesterol and ketosterol. *Journal of Structural Biology, 3rd International Conference on Structure, Dynamics and Function of Proteins in Biological Membranes*. 159:311–323.

Ollila, S.H., Louhivuori, M., Marrink, S.J., & Vattulainen, I. 2011. Protein shape change has a major effect on the gating energy of a mechanosensitive channel. *Biophysical Journal*. 100:1651–1659.

Ono, A. & Freed, E.O. 2005. Role of lipid rafts in virus replication. *Advances in Virus Research*. 64:311– 358.

Onsager, L. 1936. Electric Moments of Molecules in Liquids. *Journal of the American Chemical Society*. 58:1486–1493.

Overton CE (1901). "Studien über die Narkose zugleich ein Beitrag zur allgemeinen Pharmakologie". Gustav Fischer, Jena, Switzerland.

Pabst, G., Hodzic, A., Štrancar, J., Danner, S., Rappolt, M., & Laggner, P. 2007. Rigidification of neutral lipid bilayers in the presence of salts. *Biophysical Journal*. 93:2688–2696.

Paddock, C., Lytle, B.L., Peterson, F.C., Holyst, T., Newman, P.J., Volkman, B.F., & Newman, D.K. 2011. Residues within a lipid-associated segment of the PECAM-1 cytoplasmic domain are susceptible to inducible, sequential phosphorylation. *Blood*. 117:6012–6023.

Paila, Y.D. & Chattopadhyay, A. 2009. The function of G-protein coupled receptors and membrane cholesterol: specific or general interaction? *Glycoconjugate Journal*. 26:711–720.

Pandit, S.A., Bostick, D., & Berkowitz, M.L. 2003. Molecular Dynamics Simulation of a Dipalmitoylphosphatidylcholine Bilayer with NaCl. *Biophysical Journal*. 84:3743–3750.

Pang, L., Graziano, M., & Wang, S. 1999. Membrane cholesterol modulates galanin-GalR2 interaction. *Biochemistry*. 38:12003–12011.

Papaleo, F., Crawley, J.N., Song, J., Lipska, B.K., Pickel, J., Weinberger, D.R., & Chen, J. 2008. Genetic dissection of the role of Catechol-O-methyltransferase in cognition and stress reactivity in mice. *Journal of Neuroscience*. 28:8709–8723.

Parrinello, M. & Rahman, A. 1981. Polymorphic transitions in single crystals: A new molecular dynamics method. *Journal of Applied Physics*. 52:7182–7190.

Palsdottir, H. & Hunte, C. 2004. Lipids in membrane protein structures. *Biochimica et Biophysica Acta (BBA) - Biomembranes, Lipid-Protein Interactions*. 1666:2–18.

Parl, F.F., Dawling, S., Roodi, N., & Crooke, P.S. 2009. Estrogen metabolism and breast cancer. *Annals of the New York Academy of Sciences*. 1155:68–75.

Patel, A.J., Lazdunski, M., & Honoré, E. 2001. Lipid and mechano-gated 2P domain K(+) channels. *Current Opinion in Cell Biology*. 13:422–428.

Patra, M., Karttunen, M., Hyvönen, M.T., Falck, E., Lindqvist, P., & Vattulainen, I. 2003. Molecular dynamics simulations of lipid bilayers: major artifacts due to truncating electrostatic interactions. *Biophysical Journal*. 84:3636–3645.

Payandeh, J., Scheuer, T., Zheng, N., & Catterall, W.A. 2011. The crystal structure of a voltage- gated sodium channel. *Nature*. 475:353–358.

Peters, G.H., Wang, C., Cruys-Bagger, N., Velardez, G.F., Madsen, J.J., & Westh, P. 2013. Binding of serotonin to lipid membranes. *Journal of the American Chemical Society*. 135:2164–2171.

Petrache, H.I., Dodd, S.W., & Brown, M.F. 2000. Area per lipid and acyl length distributions in fluid phosphatidylcholines determined by (2)H NMR spectroscopy. *Biophysical Journal*. 79:3172–3192.

Phillips, M.C., Ladbrooke, B.D., & Chapman, D. 1970. Molecular interactions in mixed lecithin systems. Biochimica et Biophysica Acta (BBA) - Biomembranes. 196(1):35–44.

Phillips, R., Ursell, T., Wiggins, P., & Sens, P. 2009. Emerging roles for lipids in shaping membrane-protein function. *Nature*. 459:379–385.

Pike, L.J. & Casey, L. 2002. Cholesterol levels modulate EGF receptor-mediated signaling by altering receptor function and trafficking. *Biochemistry*. 41:10315–10322.

Pizzo, P., Giurisato, E., Tassi, M., Benedetti, A., Pozzan, T., & Viola, A. 2002. Lipid rafts and T cell receptor signaling: a critical re-evaluation. *European Journal of Immunology*. 32:3082–3091.

Poveda, J.A., Giudici, A.M., Renart, M.L., Molina, M.L., Montoya, E., Fernández-Carvajal, A., Fernández-Ballester, G., Encinar, J.A., & González-Ros, J.M. 2014. Lipid modulation of ion channels through specific binding sites. *Biochimica et Biophysica Acta (BBA) - Biomembranes, Membrane Structure and Function: Relevance in the Cell's Physiology, Pathology and Therapy*. 1838:1560–1567.

Pöyry, S., Cramariuc, O., Postila, P.A., Kaszuba, K., Sarewicz, M., Osyczka, A., Vattulainen, I., & Róg, T. 2013. Atomistic simulations indicate cardiolipin to have an integral role in the structure of the cytochrome bc1 complex. *Biochimica et Biophysica Acta (BBA) - Bioenergetics*. 1827:769–778.

Pronk, S., Páll, S., Schulz, R., Larsson, P., Bjelkmar, P., Apostolov, R., Shirts, M.R., Smith, J.C., Kasson, P.M., Spoel, D. van der, Hess, B., & Lindahl, E. 2013. GROMACS 4.5: a high-throughput and highly parallel open source molecular simulation toolkit. *Bioinformatics*. 29:845–854.

Pucadyil, T.J. & Chattopadhyay, A. 2006. Role of cholesterol in the function and organization of G-protein coupled receptors. *Progress in Lipid Research*. 45:295–333.

Radhakrishnan, A. & McConnell, H. 2005. Condensed complexes in vesicles containing cholesterol and phospholipids. *Proceedings of the National Academy of Sciences*. 102:12662–12666.

Raman, P., Cherezov, V., & Caffrey, M. 2006. The Membrane Protein Data Bank. *Cellular and Molecular Life Sciences*. 63:36–51.

Raunser, S. & Walz, T. 2009. Electron crystallography as a technique to study the structure on membrane proteins in a lipidic environment. *Annual Review of Biophysics*. 38:89–105.

Reenilä, I. & Männistö, P.T. 2001. Catecholamine metabolism in the brain by membrane-bound and soluble catechol-o-methyltransferase (COMT) estimated by enzyme kinetic values. *Medical Hypotheses*. 57:628–632.

Róg, T., Pasenkiewicz-Gierula, M., Vattulainen, I., & Karttunen, M. 2009. Ordering effects of cholesterol and its analogues. *Biochimica et Biophysica Acta (BBA) - Biomembranes, Lipid Interactions, Domain Formation, and Lateral Structure of Membranes*. 1788:97–121.

Róg, T. & Pasenkiewicz-Gierula, M. 2001. Cholesterol effects on the phosphatidylcholine bilayer nonpolar region: a molecular simulation study. *Biophysical Journal*. 81:2190–2202.

Róg, T. & Pasenkiewicz-Gierula, M. 2006. Cholesterol effects on a mixed-chain phosphatidylcholine bilayer: a molecular dynamics simulation study. *Biochimie*. 88:449–460.

Robertson, J.D. 1959. The ultrastructure of cell membranes and their derivatives. *Biochemical Society Symposia*. 16:3–43.

Robertson, J.D. 1960. The molecular structure and contact relationships of cell membranes. *Progress in Biophysics and Molecular Biology*. 10:343–418.

Rosenbaum, D.M., Rasmussen, S.G.F., & Kobilka, B.K. 2009. The structure and function of G- protein-coupled receptors. *Nature*. 459:356–363.

Ruprecht, J.J., Mielke, T., Vogel, R., Villa, C., & Schertler, G.F. 2004. Electron crystallography reveals the structure of metarhodopsin I. *EMBO Journal*. 23:3609–3620.

Sachs, J.N., Nanda, H., Petrache, H.I., & Woolf, T.B. 2004. Changes in phosphatidylcholine headgroup tilt and water order induced by monovalent salts: molecular dynamics simulations. *Biophysical Journal*. 86:3772–3782.

Sackmann, E. 1984. Physical basis of trigger processes and membrane structures. *Biological Membranes*. 5:105–143.

Saffarian, S., Li, Y., Elson, E.L., & Pike, L.J. 2007. Oligomerization of the EGF receptor investigated by live cell fluorescence intensity distribution analysis. *Biophysical Journal*. 93:1021– 1031.

Sanbonmatsu, K.Y. & Tung, C.-S. 2007. High performance computing in biology: multimillion atom simulations of nanoscale systems. *Journal of Structural Biology*. 157:470–480.

Sarakatsannis, J.N. & Duan, Y. 2005. Statistical characterization of salt bridges in proteins. *Proteins*. 60:732–739.

Schäfer, L.V., Jong, D.H. de, Holt, A., Rzepiela, A.J., Vries, A.H. de, Poolman, B., Killian, J.A., & Marrink, S.J. 2011. Lipid packing drives the segregation of transmembrane helices into disordered lipid domains in model membranes. *Proceedings of the National Academy of Sciences*. 108:1343–1348.

Schlame, M. & Ren, M. 2009. The role of cardiolipin in the structural organization of mitochondrial membranes. *Biochimica et Biophysica Acta (BBA) - Biomembranes, Includes Special Section: Cardiolipin*. 1788:2080–2083.

Schmidt, C.F., Barenholz, Y., & Thompson, T.E. 1977. A nuclear magnetic resonance study of sphingomyelin in bilayer systems. *Biochemistry*. 16:2649–2656.

Schmidt, U., Guigas, G., & Weiss, M. 2008. Cluster formation of transmembrane proteins due to hydrophobic mismatching. *Physical Review Letters*. 101:128104.

Schmidt, U. & Weiss, M. 2010. Hydrophobic mismatch-induced clustering as a primer for protein sorting in the secretory pathway. *Biophysical Chemistry*. 151:34–38.

Schmitt, A., Wilczek, K., Blennow, K., Maras, A., Jatzko, A., Petroianu, G., Braus, D.F., & Gattaz, W.F. 2004. Altered thalamic membrane phospholipids in schizophrenia: a postmortem study. *Biological Psychiatry*. 56:41–45.

Schreier, S., Malheiros, S.V.P., & de Paula, E. 2000. Surface active drugs: self-association and interaction with membranes and surfactants. Physicochemical and biological aspects. *Biochimica et Biophysica Acta (BBA) - Biomembranes, Detergents in Biomembrane Studies*. 1508:210–234.

Scolari, S., Müller, K., Bittman, R., Herrmann, A., & Müller, P. 2010. Interaction of mammalian seminal plasma protein PDC-109 with cholesterol: implications for a putative CRAC domain. *Biochemistry*. 49:9027–9031.

Seibert, M.M., Patriksson, A., Hess, B., & van der Spoel, D. 2005. Reproducible polypeptide folding and structure prediction using molecular dynamics simulations. *Journal of Molecular Biology*. 354:173–183.

Shan, Y., Kim, E.T., Eastwood, M.P., Dror, R.O., Seeliger, M.A., & Shaw, D.E. 2011. How does a drug molecule find its target binding site? *Journal of the American Chemical Society*. 133:9181–9183.

Sharpe, H.J., Stevens, T.J., & Munro, S. 2010. A comprehensive comparison of transmembrane domains reveals organelle-specific properties. *Cell*. 142:158–169.

Shevchenko, A. & Simons, K. 2010. Lipidomics: coming to grips with lipid diversity. *Nature Reviews Molecular Cell Biology*. 11:593–598.

Shi, X., Bi, Y., Yang, W., Guo, X., Jiang, Y., Wan, C., Li, L., Bai, Y., Guo, J., Wang, Y., Chen, X., Wu, B., Sun, H., Liu, W., Wang, J., & Xu, C. 2013. Ca2+ regulates T-cell receptor activation by modulating the charge property of lipids. *Nature*. 493:111–115.

Shimshick, E.J. & McConnell, H.M. 1973. Lateral phase separation in phospholipid membranes. *Biochemistry*. 12:2351–2360.

Simons, K. & Van Meer, G. 1988. Lipid sorting in epithelial cells. *Biochemistry*. 27:6197–6202.

Simons, K. & Ikonen, E. 1997. Functional rafts in cell membranes. *Nature*. 387:569–572.

Simons, K. & Toomre, D. 2000. Lipid rafts and signal transduction. *Nature Reviews Molecular Cell Biology*. 1:31–39.

Simons, K. & Vaz, W.L.C. 2004. Model systems, lipid rafts, and cell membranes. *Annual Review of Biophysics and Biomolecular Structure*. 33:269–295.

Singer, S.J. & Nicolson, G.L. 1972. The fluid mosaic model of the structure of cell membranes. *Science*. 175:720–731.

Sivasubramanian, N. & Nayak, D.P. 1987. Mutational analysis of the signal-anchor domain of influenza virus neuraminidase. *Proceedings of the National Academy of Sciences*. 84:1–5.

Skjevik, Å.A., Madej, B.D., Walker, R.C., & Teigen, K. 2012. LIPID11: A modular framework for lipid simulations using amber. *Journal of Physical Chemistry B*. 116:11124–11136.

Smart, E.J., Graf, G.A., McNiven, M.A., Sessa, W.C., Engelman, J.A., Scherer, P.E., Okamoto, T., & Lisanti, M.P. 1999. Caveolins, liquid-ordered domains, and signal transduction. *Molecular and Cellular Biology*. 19:7289–7304.

Smith, A.W. 2012. Lipid–protein interactions in biological membranes: A dynamic perspective. *Biochimica et Biophysica Acta (BBA) - Biomembranes, Membrane protein structure and function*. 1818:172–177.

Soares-da-Silva, P., Vieira-Coelho, M.A., & Parada, A. 2003. Catechol-O-methyltransferase inhibition in erythrocytes and liver by BIA 3-202 (1-[3,4-dibydroxy-5-nitrophenyl]-2-phenyl-ethanone). *Pharmacology & Toxicology*. 92:272–278.

Sperotto, M.M., Ipsen, J.H., & Mouritsen, O.G. 1989. Theory of protein-induced lateral phase separation in lipid membranes. *Cell Biophysics*. 14:79–95.

Starling, A.P., East, J.M., & Lee, A.G. 1995a. Effects of gel phase phospholipid on the Ca2+-ATPase. *Biochemistry*. 34:3084–3091.

Starling, A.P., East, J.M., & Lee, A.G. 1995b. Evidence that the effects of phospholipids on the activity of the Ca(2+)-ATPase do not involve aggregation. *Biochemical Journal*. 308:343–346.

Stillwell, W. 2013. An Introduction to Biological Membranes: From Bilayers to Rafts. *Elsevier*. San Diego.

Stoeckenius, W. & Engelman, D.M. 1969. Current models for the structure of biological membranes. *Journal of Cell Biology*. 42:613–646.

Strandberg, E., Esteban-Martín, S., Ulrich, A.S., & Salgado, J. 2012. Hydrophobic mismatch of mobile transmembrane helices: Merging theory and experiments. *Biochimica et Biophysica Acta (BBA) - Biomembranes*. 1818:1242–1249.

Stroud, R.M. 2011. New tools in membrane protein determination. *F1000 Biology Reports*. 3.

Sugita, Y. & Okamoto, Y. 1999. Replica-exchange molecular dynamics method for protein folding. *Chemical Physics Letters*. 314:141–151.

Szostak, J.W., Bartel, D.P., & Luisi, P.L. 2001. Synthesizing life. *Nature*. 409:387–390.

Tan, H.-Y., Callicott, J.H., & Weinberger, D.R. 2009. Prefrontal cognitive systems in schizophrenia : Towards human genetic brain mechanisms. *Cognitive Neuropsychiatry*. 14:277–298.

Tang, D., Dean, W.L., Borchman, D., & Paterson, C.A. 2006. The influence of membrane lipid structure on plasma membrane Ca2+-ATPase activity. *Cell Calcium*. 39:209–216.

Triano, I., Barrera, F.N., Renart, M.L., Molina, M.L., Fernández-Ballester, G., Poveda, J.A., Fernández, A.M., Encinar, J.A., Ferrer-Montiel, A.V., Otzen, D., & González-Ros, J.M. 2010. Occupancy of nonannular lipid binding sites on KcsA greatly increases the stability of the tetrameric protein. *Biochemistry*. 49:5397–5404.

Tsui-Pierchala, B.A., Encinas, M., Milbrandt, J., & Johnson, E.M., Jr. 2002. Lipid rafts in neuronal signaling and function. *Trends in Neuroscience*. 25:412–417.

Tupper, P. 2005. Ergodicity and the Numerical Simulation of Hamiltonian Systems. *SIAM Journal on Applied Dynamical Systems*. 4:563–587.

Ulmanen, I. & Lundström, K. 1991. Cell-free synthesis of rat and human catechol O-methyltransferase. *European Journal of Biochemistry*. 202:1013–1020.

Ulmschneider, M.B., Sansom, M.S.P., & Di Nola, A. 2005. Properties of integral membrane protein structures: derivation of an implicit membrane potential. *Proteins*. 59:252–265.

Urbina, J.A., Pekerar, S., Le, H., Patterson, J., Montez, B., & Oldfield, E. 1995. Molecular order and dynamics of phosphatidylcholine bilayer membranes in the presence of cholesterol, ergosterol and lanosterol: a comparative study using 2H-, 13C- and 31P-NMR spectroscopy. *Biochimica et Biophysica Acta (BBA) - Biomembranes*. 1238:163–176.

Van den Bogaart, G., Meyenberg, K., Risselada, H.J., Amin, H., Willig, K.I., Hubrich, B.E., Dier, M., Hell, S.W., Grubmüller, H., Diederichsen, U., & Jahn, R. 2011. Membrane protein sequestering by ionic protein-lipid interactions. *Nature*. 479:552–555.

Van Klompenburg, W., Nilsson, I., von Heijne, G., & de Kruijff, B. 1997. Anionic phospholipids are determinants of membrane protein topology. *EMBO Journal*. 16:4261–4266.

Van Meer, G. 1989. Lipid traffic in animal cells. *Annual Review of Cell Biology*. 5:247–275.

Van Meer, G., Voelker, D.R., & Feigenson, G.W. 2008. Membrane lipids: where they are and how they behave. *Nature Reviews Molecular Cell Biology*. 9:112–124.

Vermeer, L.S., de Groot, B.L., Réat, V., Milon, A., & Czaplicki, J. 2007. Acyl chain order parameter profiles in phospholipid bilayers: computation from molecular dynamics simulations and comparison with 2H NMR experiments. *European Biophysical Journal*. 36:919–931.

Vidgren, J., Svensson, L.A., & Liljas, A. 1994. Crystal structure of catechol O-methyltransferase. *Nature*. 368:354–358.

Vincent, N., Genin, C., & Malvoisin, E. 2002. Identification of a conserved domain of the HIV- 1 transmembrane protein gp41 which interacts with cholesteryl groups. *Biochimica et Biophysica Acta (BBA)*. 1567:157–164.

Wacker, D., Wang, C., Katritch, V., Han, G.W., Huang, X.-P., Vardy, E., McCorvy, J.D., Jiang, Y., Chu, M., Siu, F.Y., Liu, W., Xu, H.E., Cherezov, V., Roth, B.L., & Stevens, R.C. 2013. Structural features for functional selectivity at serotonin receptors. *Science*. 340:615–619.

Wang, C., Ye, F., Velardez, G.F., Valardez, G.F., Peters, G.H., & Westh, P. 2011. Affinity of four polar neurotransmitters for lipid bilayer membranes. *Journal of Physical Chemistry B*. 115:196–203.

Warne, T., Moukhametzianov, R., Baker, J.G., Nehmé, R., Edwards, P.C., Leslie, A.G.W., Schertler, G.F.X., & Tate, C.G. 2011. The structural basis for agonist and partial agonist action on a β1-adrenergic receptor. *Nature*. 469:241–244.

Weinberger, D.R. 2005. Genetic mechanisms of psychosis: In vivo and postmortem genomics. *Clinical Therapeutics, Schizophrenia: Genetics and Treatment*. 1:S8–S15.

Whorton, M.R. & MacKinnon, R. 2011. Crystal structure of the mammalian GIRK2 K+ channel and gating regulation by G proteins, PIP2, and sodium. *Cell*. 147:199–208.

Wunderlich, F., Kreutz, W., Mahler, P., Ronai, A., & Heppeler, G. 1978. Thermotropic fluid ordered “discontinuous” phase separation in microsomal lipids of Tetrahymena. An x-ray diffraction study. *Biochemistry*. 17:2005–2010.

Wunderlich, F., Ronai, A., Speth, V., Seelig, J., & Blume, A. 1975. Thermotropic lipid clustering in tetrahymena membranes. *Biochemistry*. 14:3730–3735.

Xu, C., Gagnon, E., Call, M.E., Schnell, J.R., Schwieters, C.D., Carman, C.V., Chou, J.J., & Wucherpfennig, K.W. 2008. Regulation of T Cell receptor activation by dynamic membrane binding of the CD3ε cytoplasmic tyrosine-based motif. *Cell*. 135:702–713.

Yeagle, P.L. 1985. Cholesterol and the cell membrane. *Biochimica et Biophysica Acta (BBA) - Reviews on Biomembranes*. 822:267–287.

Yeagle, P.L., Young, J., & Rice, D. 1988. Effects of cholesterol on sodium-potassium ATPase ATP hydrolyzing activity in bovine kidney. *Biochemistry*. 27:6449–6452.

Yeagle, P.L. 2014. Non-covalent binding of membrane lipids to membrane proteins. *Biochimica et Biophysica Acta (BBA) - Biomembranes, Membrane Structure and Function: Relevance in the Cell’s Physiology, Pathology and Therapy*. 1838:1548–1559.

Yetukuri, L., Ekroos, K., Vidal-Puig, A., & Oresic, M. 2008. Informatics and computational strategies for the study of lipids. *Molecular Biosystems*. 4:121–127.

Zhou, Q., Hakomori, S., Kitamura, K., & Igarashi, Y. 1994. GM3 directly inhibits tyrosine phosphorylation and de-N-acetyl-GM3 directly enhances serine phosphorylation of epidermal growth factor receptor, independently of receptor-receptor interaction. *Journal of Biological Chemistry*. 269:1959–1965.

ORIGINAL PAPERS

I

PROPERTIES OF THE MEMBRANE BINDING COMPONENT OF CATECHOL-O-METHYLTRANSFERASE REVEALED BY ATOMISTIC MOLECULAR DYNAMICS SIMULATIONS

by
Orłowski, A., St-Pierre, J.-F., Magarkar, A., Bunker, A., Pasenkiewicz-Gierula, M., Vattulainen, I., & Róg, T. 2011

Journal of Physical Chemistry B vol. 115, 13541-13550

THE JOURNAL OF PHYSICAL CHEMISTRY B

ARTICLE

pubs.acs.org/JPCB

Properties of the Membrane Binding Component of Catechol-*O*-methyltransferase Revealed by Atomistic Molecular Dynamics Simulations

Adam Orłowski,[†,‡] Jean-François St-Pierre,[§] Aniket Magarkar,[∥] Alex Bunker,[∥,⊥] Marta Pasenkiewicz-Gierula,[†] Ilpo Vattulainen,[‡,#,▽] and Tomasz Róg*[,‡]

[†]Department of Computational Biophysics and Bioinformatics, Faculty of Biotechnology, Biochemistry and Biophysics, Jagiellonian University, Gronostajowa 7, Poland

[‡]Department of Physics, Tampere University of Technology, P.O. Box 692, FI-33101 Tampere, Finland

[§]Departement de Physique and Regroupement Quebecois sur les Materiaux de Pointe, Universite de Montreal, C.P. 6128, Succursale Centre-ville, Montreal (Quebec), Canada

[∥]Centre for Drug Research, Faculty of Pharmacy, University of Helsinki, P.O. Box 56, FI-00014, University of Helsinki, Finland

[⊥]Department of Chemistry, Aalto University School of Science, P.O. Box 6100, FI-02015, AALTO, Espoo, Finland

[#]Department of Applied Physics, Aalto University School of Science, Finland

[▽]MEMPHYS—Center for Biomembrane Physics, University of Southern Denmark, Odense, Denmark

Supporting Information

ABSTRACT: We used atomistic simulations to study the membrane-bound form of catechol-*O*-methyltransferase (MB-COMT). In particular we investigated the 26-residue transmembrane α-helical segment of MB-COMT together with the 24-residue fragment that links the transmembrane component to the main protein unit that was not included in our model. In numerous independent simulations we observed the formation of a salt bridge between ARG27 and GLU40. The salt bridge closed the flexible loop that formed in the linker and kept it in the vicinity of the membrane-water interface. All simulations supported this conclusion that the linker has a clear affinity for the interface and preferentially arranges its residues to reside next to the membrane, without a tendency to relocate into the water phase. Furthermore, an extensive analysis of databases for sequences of membrane proteins that have a single transmembrane helical segment brought about an interesting view that the flexible loop observed in our work can be a common structural element in these types of proteins. In the same spirit we close the article by discussing the role of salt bridges in the formation of three-dimensional structures of membrane proteins that exhibit a single transmembrane helix.

1. INTRODUCTION

About 30% of the genome codes for *membrane proteins*, which function in a number of ways, including diverse tasks such as signaling, recognition, and transport. Membrane proteins come in two varieties: *peripheral proteins*, which are loosely associated with the membrane, and *integral proteins*, which are embedded in a cell membrane. The domain anchoring the integral protein to a membrane is typically a highly symmetric structure composed of one or more transmembrane helices, which are discussed in this work.

The three-dimensional (3D) structure of proteins is usually determined by techniques that are based on X-ray or electron scattering. As the main principles of these techniques are well established, the challenge associated with protein structure determination is closely related to the crystallization of proteins, a crucial step prior to conducting scattering measurements. Despite many related difficulties, the progress in the determination of water-soluble protein structures has nonetheless been substantial. The situation is much more complicated with membrane proteins, the main reason being that protein structure should in this case be determined under conditions where the protein is solvated by and crystallized in a lipid membrane. This is a major challenge, and while some techniques to this end have been developed,[1,2] the number of solved 3D structures of membrane proteins has remained modest. The cases where the complete protein structure is known are particularly limited in number, as quite a few reported protein structures refer to incomplete systems where the structures of only a subset of the domains that make up the protein have been determined.

Received: July 27, 2011
Revised: October 9, 2011
Published: October 11, 2011

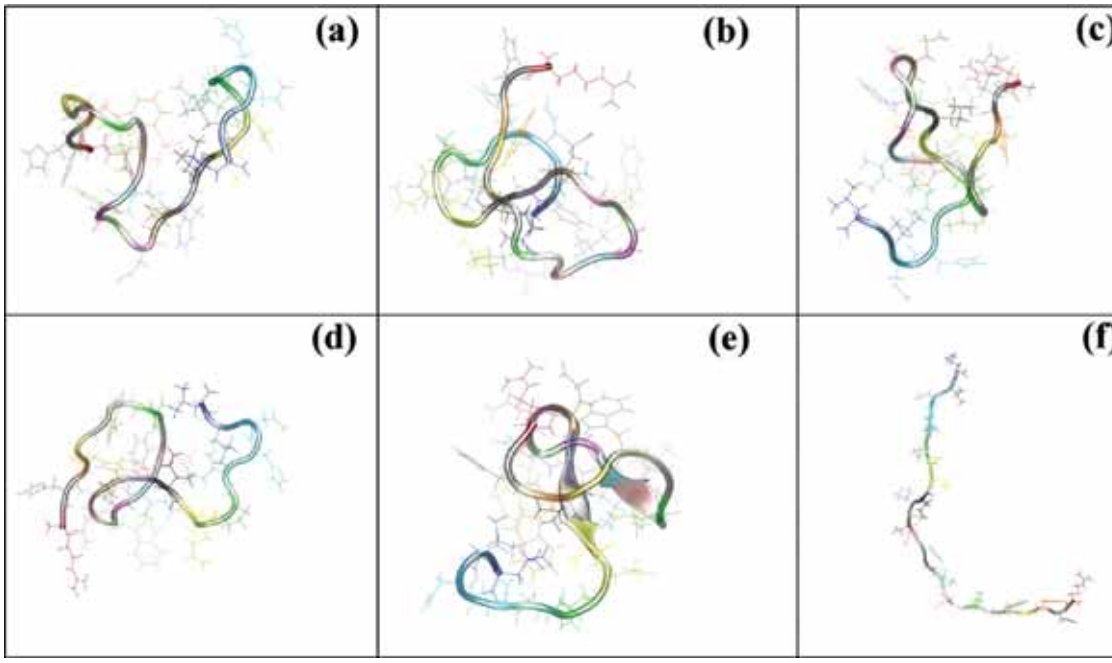

Figure 1. Initial structures of the linker fragments. Structures a−e originate from replica exchange simulation, while structure f is an extended conformation. Figures were generated with the VMD program.[49]

These concerns are exemplified by catechol-*O*-methyltransferase (COMT), a protein of significant pharmaceutical interest: it has an important role in neurochemistry, where one of its main functions is the inactivation, through O-methylation, of catecholamine neurotransmitters such as dopamine, epinephrine, norepinephrine, and catechol steroids.[3] It is also known to methylate a wide variety of xenobiotics that contain the catechol group. Among these xenobiotics is the leading drug for treatment of Parkinson's disease,[3] L-Dopa, and it is this activity that drives the development of inhibitors for COMT (for a recent review, see the work of Männistö et al.[4]).

COMT is known to exist in two forms: the water-soluble (S) form known as S-COMT, and the membrane-bound (MB) form known as MB-COMT. S-COMT is essentially a catalytic domain since it is identical in sequence and structure to the catalytic domain of MB-COMT. The difference between the two forms lies in the additional 50-residue fragment that is covalently attached to the N-terminus of the catalytic domain of MB-COMT. A sequence analysis of this additional fragment clearly indicates that its 26 N-terminal residues form a single transmembrane helix, while the remaining 24 residues constitute a linker segment that connects the helix to the catalytic domain. Interestingly, while the water-soluble and membrane-bound forms of COMT have an identical catalytic domain, enzymatic kinetics of the two forms are different.[5] It can be hypothesized that the cause of this difference lies in the interaction of the protein with a membrane, possibly mediated by the linker segment.

The 3D structure of S-COMT has been determined,[6] but the structure of the entire MB-COMT remains unclear. There is data in favor of a helical structure for the transmembrane part (see, e.g., ref 7), but finding the structure of the linker segment has turned out to be more complicated. While bioinformatics tools have been used to reconstruct the structure of the whole protein,[7] the relevance of this approach can be debated: almost all of the templates used in protein structure prediction through sequence identity are structures of water-soluble proteins. This is not the case for the COMT linker segment, which is instead located at a water−membrane interface.

In this study, we use atomistic molecular dynamics (MD) simulations to predict the behavior of the linker segment of MB-COMT at a water−membrane interface. This study is an extension of our previous work, which focused mainly on methodological issues of rat S-COMT,[8] where the Apo enzyme was simulated for 70 ns starting from a structure crystallized with an inhibitor.

2. METHODS

We performed MD simulations of a lipid bilayer with the 50-residue fragment that differentiates MB-COMT from S-COMT. As described above, the fragment consists of a 26-residue transmembrane helix and a 24-residue linker segment that connects the helix to the catalytic domain (S-COMT).

The lipid bilayer was composed of 124 dilinoleylphosphatidylcholine (2-18:2c9 PC) (DLPC) molecules symmetrically distributed in the two leaflets. Its initial structure was that of our previous study[9,10] from which four lipid molecules were removed to create a void for the transmembrane helix. The initial structure of the 26-amino acid transmembrane helix (MPEAPPLLLAAVLLGLVLLVVLLLLL) was chosen to be α-helical. As for the 24-amino acid linker segment (RHWGWGLCLIGWNEFILQPIHNLL), its 3D structure was not known. Therefore, five

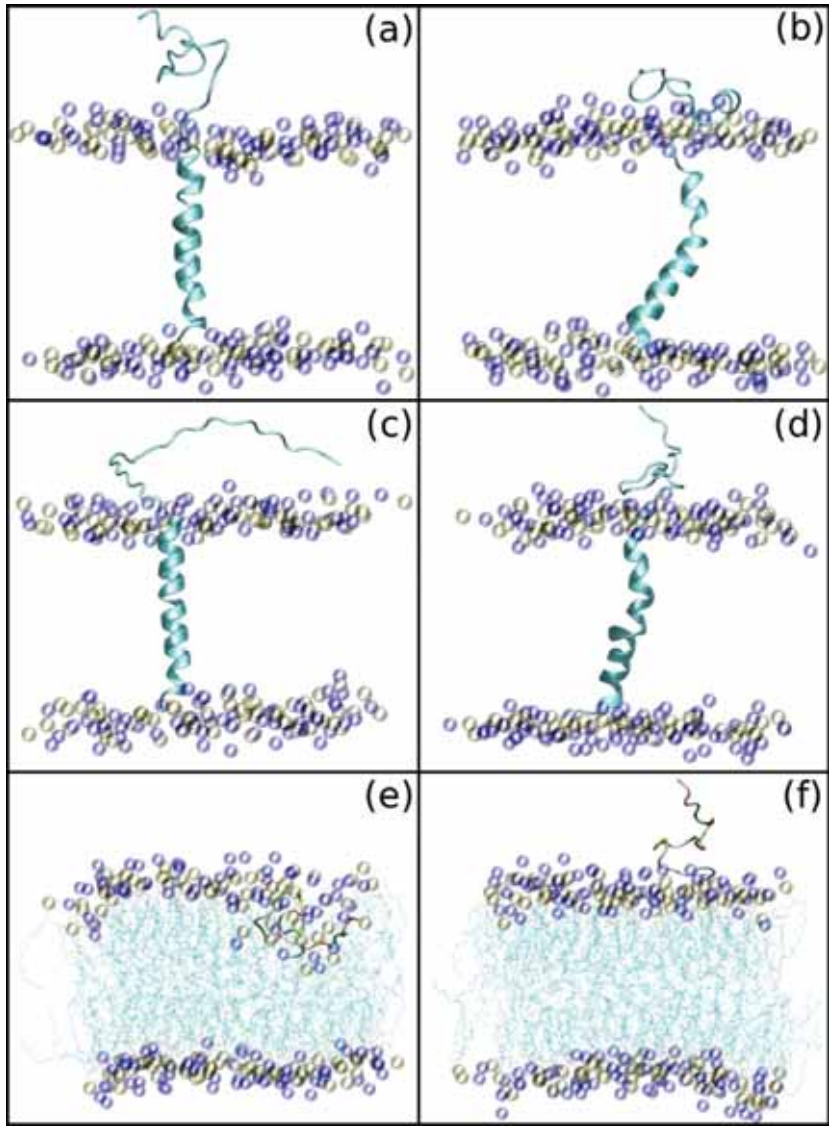

Figure 2. Initial (a,c,e) and final (b,d,f) structures of lipid bilayers with a transmembrane helix and a linker. While the peptide is shown in full, only the phosphorus atoms are shown for the lipids, and water is not shown for clarity. Panels a and b represent the simulation initiated using the initial peptide structure configuration shown in Figure 1a; panels c and d correspond to the structure depicted in Figure 1f. Panel e shows the initial structure of the system where the peptide was pulled into the hydrocarbon region of the bilayer (based on Figure 1e), and panel f shows this structure after a simulation of 40 ns. The figure was generated using VMD.[49]

initial conformations were generated (Figure 1) for the linker using replica exchange molecular dynamics (REMD) in conjunction with the optimized potential for efficient structure prediction (OPEP).[11] REMD simulations were executed at 16 temperatures ranging from 222.5 to 525 K. The simulation was executed for 100 ns at a 1.5 fs time step, and temperature exchange was attempted every 15 ps. In each of these conformations, the linker segment was covalently attached to the transmembrane helix. A similar procedure was performed for an extended conformation (Figure 1) that was the sixth case considered in our work, and all of these six conformations were finally inserted into the DLPC bilayer. Examples of system structures are shown in Figure 2.

To further study the linker segment in particular, we constructed six additional systems where the linker in each of the above conformations was placed at the water−bilayer interface (without the transmembrane helix).

Altogether, 12 systems were constructed, each hydrated with ∼8000 water molecules. The systems also had 20 K^+ and 20 Cl^-

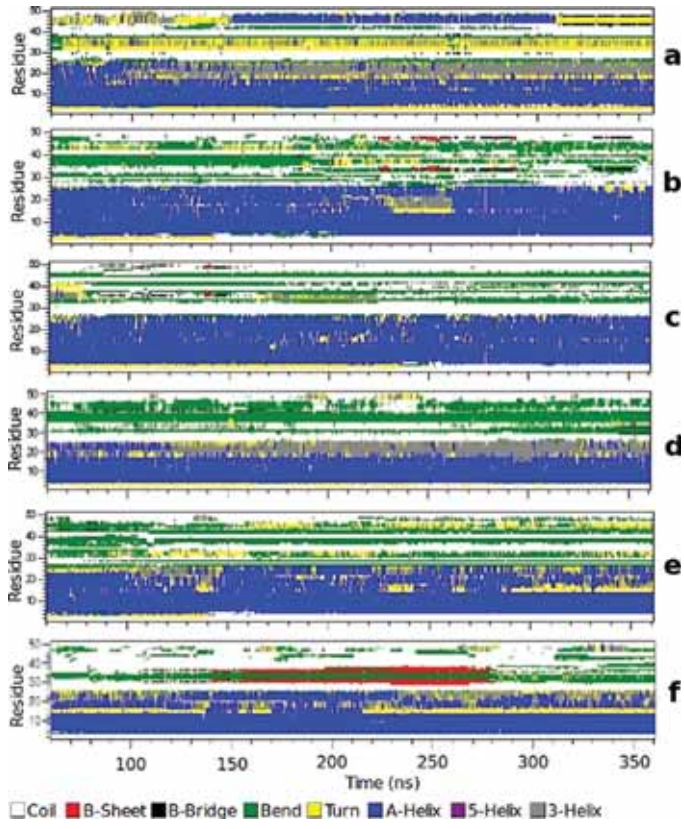

Figure 3. Secondary structure elements of a transmembrane helix (residues 1−26) and a linker (residues 27−50) shown as a function of time determined with DSSP.[29] Panels a−f correspond to simulations started using as the initial configuration the structures shown in Figure 1 labeled a−f, respectively.

ions that were added to the water phase to mimic the KCl concentration of 140 mM in the intracellular environment.

For the lipids, peptides, and ions, we used the all-atom OPLS force field.[12−15] Details of the parametrization are discussed in our previous articles.[9,10,16] Partial charges on the PC head groups were taken from Takaoka et al.[17] as they were derived in compliance with the OPLS methodology. Definitions of the charge groups are given in our previous work.[16] For water, we employed the TIP3 model.[18]

Prior to MD simulations, the structures of the systems were optimized to remove van der Waals contacts between atoms. Energy minimizations and MD simulations were performed using the GROMACS 4 software package.[19,20] The simulations of the six bilayer systems with the transmembrane helix and the linker were carried out for 360 ns. The last 300 ns fragment of each trajectory was used for analysis. The remaining six bilayer systems with the linker segment placed at the water−bilayer interface were simulated for 100 ns each, and of these simulations the last 60 ns were used for analysis. Periodic boundary conditions were employed in all three directions. The LINCS algorithm was used to preserve covalent bond lengths.[21] The time step was set to 2 fs. The temperature (300 K) and pressure (1 bar) were controlled using the Nosé−Hoover[22,23] and Parrinello−Rahman methods,[24] respectively. The temperatures of the solute and the solvent were controlled independently. For pressure, a semi-isotropic control was used. The Lennard-Jones interactions were cut off at 1.0 nm, and the electrostatic interactions were calculated using the particle mesh Ewald method with a real space cutoff of 1.0 nm.[25,26] This protocol was successfully used in our previous studies.[9,27,28]

3. RESULTS

3.1. Characteristics of the Peptide Structure. To characterize the conservation of the 50-residue peptide structure in the bilayer systems, we monitored the temporary secondary structure of both fragments (the helix and the linker) using the DSSP program.[29] Results are shown in Figures 3 and 4. As can be seen from Figure 3, the structure of the transmembrane helix is generally preserved; however, there are short periods when the helicity is temporarily either lost or altered from an α-helix to a more extended 3−10 helix. The spatial structure of the linker was not stable in any of the simulated systems. The dominant structural motives of the linker segment covalently attached to the transmembrane helix were bends, coils, and turns; however, the formation of a helical fragment was also observed in one of the simulations. In the systems where the linker was loosely associated with the bilayer, the dominant structural motives were

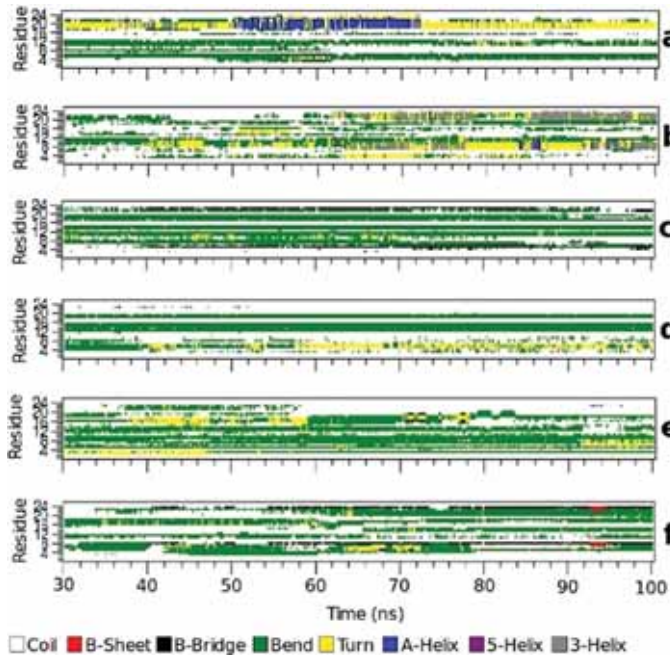

Figure 4. Secondary structure elements of a linker loosely associated with a membrane (without the transmembrane part) shown as a function of time determined with DSSP.[29] Panels a−f correspond to simulations started using as the initial configuration the structures shown in Figure 1 labeled a−f, respectively.

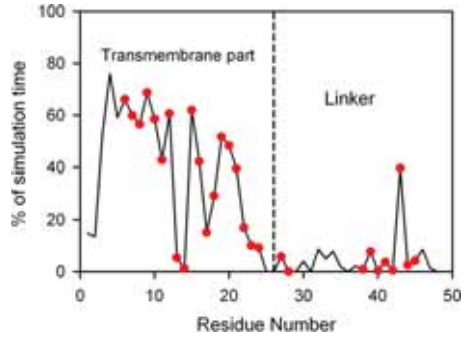

Figure 5. Percentage of simulation time for which a given residue adopts helical conformation (data averaged over all 6 runs and time). In red are marked points whose conformation is predicted to be helical in the studies of Bui et al.[7]

transient bends and turns (Figure 4). The percentage of the simulation time for which a given residue participates in a particular local conformation is given in Tables S1 and S2 presented in the Supporting Information (SI).

The structures of the helix and the linker segment have been previously analyzed using bioinformatics tools by Bai et al.[7] They predicted, for each peptide residue, the probability of its participation in the helical structure and found that residues 38−45 of the 50-residue fragment (residues 12−19 of the 24-residue linker) can adopt a helical structure. We thus, for each residue, recorded cases when the residue is an element of a helical structure during the simulation (Figure 5). Red points in Figure 5 indicate the residues for which a helical structure was predicted by ref 7. Our analyses indeed indicate that residues 38−45 have a tendency to form a helix, but residues 30−35 also display the same tendency, albeit less apparent. Examples of the helical conformations in the linker segment are shown in Figure 6.

3.2. Peptide Location. To assess the location of the linker segment relative to the bilayer surface, we first calculated the average position of the phosphorus atoms in the membrane leaflet from which the linker protrudes, and then we computed the time averaged position of each Cα atom of the linker relative to the average phosphorus atom position (Figure 7). Figure 7a shows large variations in the linker behavior but also some common characteristics. The ensemble-averaged (over six linker segments) distance profile is as follows: for residues 27−35, there is a gradual increase of the distance from 0.15 to 1.3 nm followed by a decrease to 0.9 nm for the three next residues, 38−40. For the remaining 10 residues, the distance increases to 1.6 nm. Meanwhile, the ensemble-averaged distance profile for the systems where the linker is loosely associated with the bilayer gradually increases from 0.9 to 1.7 nm with an increasing residue number (Figure 7b). No dip is observed in this profile. It is interesting to note that in each system the linker segment remains associated with the water−membrane interface for the whole simulation run, even though initially it was placed randomly in the water phase near the bilayer surface.

Figure 2e shows the initial conformation of the additional starting structure, which was obtained by pulling the peptide down (we used the structure shown in Figure 1e) into the interface. This initial structure was generated to find out whether the linker could

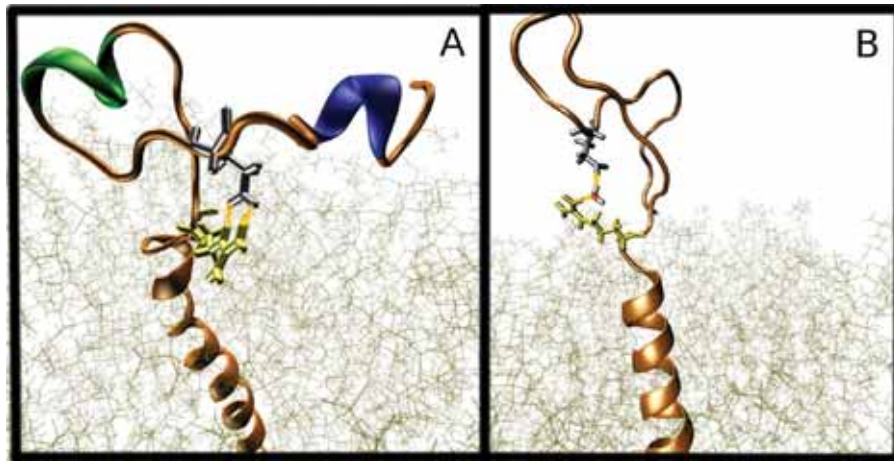

Figure 6. (A) Structure of the peptide at the end of simulation (structure a from Figure 1) with a salt bridge between GLU40 (silver) and ARG27 (yellow). Residues 33−36 (green) and 44−47 (blue) have helical structure. Water is not shown for clarity. (B) Illustration of a water bridge within the linker region; see text for discussion.

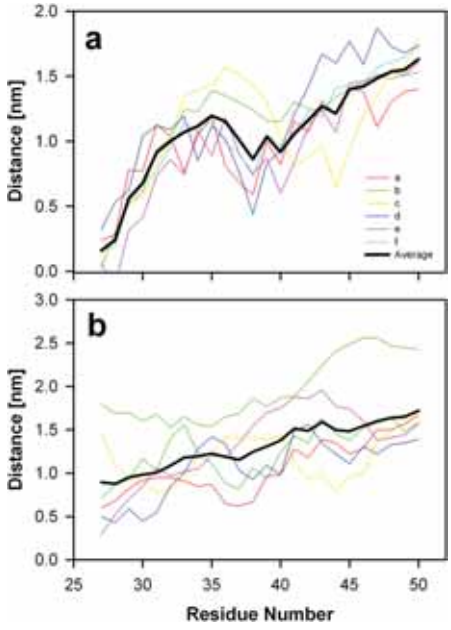

Figure 7. Distance between the membrane−water interface and Cα atoms of each linker residue: (a) the linker connected to a transmembrane part and (b) the linker loosely associated with a membrane. Average position of a phosphorus atom at the interface is set to zero. Residue 25 is the first one after the transmembrane helix. Lines a−f correspond to simulations started using as the initial configuration the structures shown in Figure 1 labeled a−f, respectively.

possibly relocate closer to the membrane core in a stable fashion. However, as shown in Figure 2f, the peptide left the bilayer core region relatively quickly and remained associated with the membrane interface in a way similar to that observed in other simulations.

3.3. Peptide−Lipid Interactions. To characterize interactions between peptide and lipids, we evaluated the number of the peptide-lipid hydrogen bonds and charge pairs. In these calculations, we used geometrical criteria established in our previous studies: hydrogen bonds exist if the distance between donor (D) and acceptor (A) is less than 0.325 nm and the angle between a chemical bond D−H and a hydrogen bond D−A is less than 35°.[30] Charge pairs are electrostatic interactions between the positively charged methyl groups in the choline moiety of PC and the negatively charged oxygen atoms of neighboring groups of the same or other molecule. These interactions are defined by a distance cutoff of 0.4 nm. The numbers of these peptide−lipid interactions per peptide are given in Table 1. In general, the data indicate that there are more peptide−lipid hydrogen bonds and charge pairs when the linker is covalently attached to the transmembrane helix than otherwise.

Since the carboxyl group of the peptide is not present when a whole protein is attached, we performed additional analysis to estimate how its presence can affect the observed results. As the carboxyl group is negatively charged, it can interact with the positively charged choline group via the charge pairs. Thus first we calculated the frequency of the occurrence of charge pairs (measured as a percentage of simulation time during which any given pair exists). For the case of the covalently bonded peptide, the charge pairs exist over 7.3% of the simulation time, while for the case of the loosely associated peptide, it was 2.5% of the simulation time. Next we calculated the average distance between any atom of lipids and the carboxyl group. The distance is 1.1 and 1.3 nm for the case of covalently bonded and loosely associated peptide, respectively. In Supporting Information Table S3, the values obtained in each MD run are given. Obtained results suggest that the interactions of the C-terminal carboxyl group with the membrane are rather weak and do not affect the observed results. This is consistent with data presented in Figure 7, which indicate that the C-terminus is located further away than other residues from the membrane and does not indicate a specific interaction with lipids.

3.4. Peptide Intramolecular Interactions. Although we did not observe any specific and stable secondary structure elements

Table 1. Average Numbers of Hydrogen Bonds and Charge Pairs between Peptide and Bilayer Lipids Per Peptide Molecule

	hydrogen bonds			charge pairs
structure number	helix 1−25	linker 26−50	whole 1−50	linker 26−50
Linker Covalently Attached to Helix				
1	1.6	1.5	3.1	6.37
2	1.3	4.0	5.3	5.00
3	1.2	2.5	3.7	6.20
4	1.7	2.0	3.7	6.43
5	1.8	4.9	6.7	7.00
6	2.6	2.1	4.7	3.75
average	1.7	2.8	4.5	5.79
Loosely Associated Linker				
1		2.5		2.62
2		0.15		0.73
3		1.5		3.02
4		1.9		3.05
5		2.5		4.78
6		0.15		3.48
average		1.45		2.95

in the linker segment, we found a tendency to form a specific salt bridge between ARG27 located at the end of the transmembrane helix and GLU40 of the linker segment (Figure 6). This salt bridge was predicted in four selected initial structures regarding the peptides with a transmembrane part. Figure 8a shows the time development of the distance between a nitrogen atom in the ARG27 side chain (N^{η}) and an ε oxygen atom in the GLU40 side chain (O^{ε}) (the shortest distance between possible $N^{\eta}-O^{\varepsilon}$ pairs is ~0.3 nm). As can be seen in Figure 8a, the above-mentioned salt bridge is observed in all simulations, including the two where it was not present in the initial structures of the peptide. The salt bridge displays a dynamic behavior: although it is present in all simulation systems, it frequently breaks for long periods of time.

The salt bridge is also formed between ARG27 and GLU40 of the linker segment loosely associated with the bilayer. The time profiles of distance between the N^{η} and O^{ε} of these two amino acids are shown in Figure 8b. The salt bridge is, however, created less frequently than in the case of the linker bonded to the transmembrane helix (Figure 8a).

A salt bridge is commonly defined as an interaction between two charged residues when they are hydrogen bonded, thus the distance between nitrogen and oxygen is below 0.3 nm.[31] In our simulations, we observed two very stable distances for the $N^{\eta}-O^{\varepsilon}$ pair, one of about 0.27 nm, which corresponds to the presence of a hydrogen bond, and the second of about 0.5 nm (see, e.g., the gray curve on Figure 8b, first 20 ns). In these situations the classically understood salt bridge is broken; however, the residues still interact via a water bridge-type interaction (a water molecule is simultaneously hydrogen bonded with two different residues[30]). As can be seen in Figure 8b, these water bridges are stable. A snapshot of such a water-mediated salt bridge is shown in Figure 6b.

Since this salt bridge seems to be an important structural element, we analyzed its environment more carefully, calculating the solvent-accessible surface area (SASA) as a percentage of the

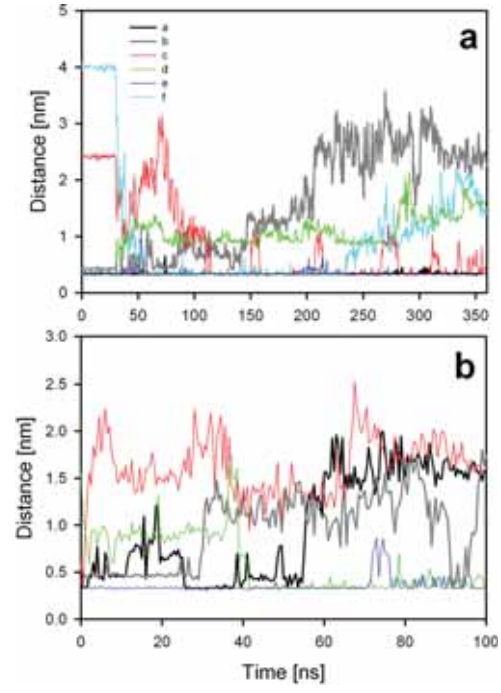

Figure 8. Time development of the distance between nitrogen N^{η} in ARG27 and oxygen O^{ε} in GLU40 in (a) a linker bonded with transmembrane helix and (b) the loosely associated linker. Structure names (a−f) refer to the initial structures shown in Figure 1. Lines a−f correspond to simulations started using as the initial configuration the structures shown in Figure 1 labeled a−f, respectively.

total surface areas of these two groups. We found that the exposure of ARG27 to the water is (36 ± 2)% and (63 ± 4)% in the bonded and free linker, respectively, and for GLU40 the values are (40 ± 4)% and (49 ± 5)% in the bonded and free linker, respectively.

3.5. Peptide−Ion Interactions. Ions are known to affect the properties of macromolecules and the interactions between them. Thus, we also analyzed the interactions of K^+ and Cl^- ions with the peptide in addition to their interactions with the bilayer lipids. The analysis of the distribution of both ion types along the bilayer normal revealed that both ions are almost evenly distributed in the water phase and thus do not interact strongly with the lipids headgroups. This behavior is in sharp contrast to that of Na^+ and Cl^- of NaCl, as Na^+ binds strongly to the PC headgroup, while Cl^- remains loosely associated with the membrane.[28] This difference between Na^+ and K^+ interactions with the bilayer was previously observed in MD simulation studies where different force field parameters were used.[32,33]

We next analyzed interactions of K^+ ions with the peptide oxygen atoms. We considered that an ion and an oxygen create a "bonded pair" when the distance between them is less than 0.325 nm, which corresponds to the position of the first minimum of the radial distribution function of ions and such oxygen atoms.[34] Our analysis revealed that, on average, there are only 0.20 K^+ ions bound to the entire peptide molecule (transmembrane helix and linker segment) and 0.10 with the loosely attached linker segment.

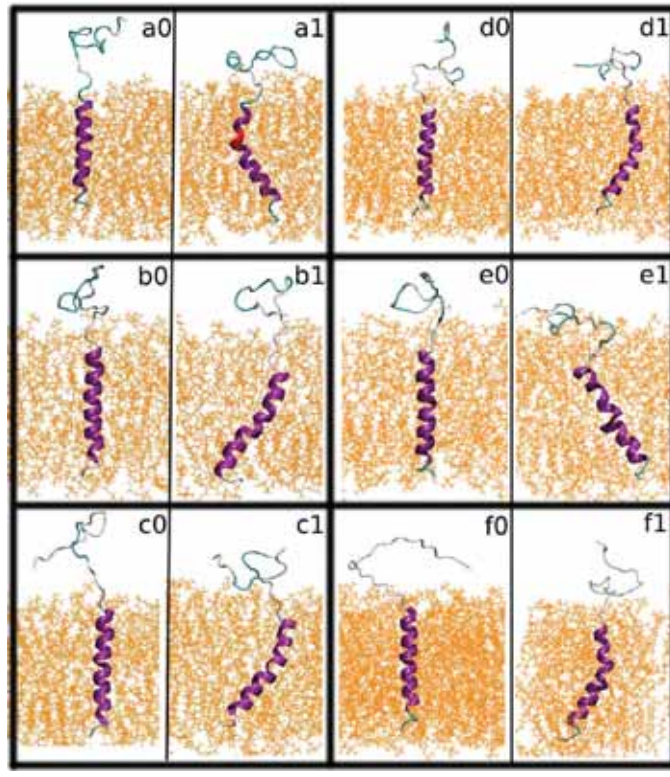

Figure 9. Snapshots of the initial (a0, b0, c0, d0, e0, f0) and final (a1, b1, c1, d1, e1, f1) simulation structures of the tilted transmembrane helix and linker. The kink at ALA17 is shown in red. Panels a−f correspond to simulations started using as the initial configuration the structures shown in Figure 1 labeled a−f, respectively.

Obviously, ions bind to residues located outside the membrane hydrophobic core, and somewhat preferentially to acidic residues: GLU3, GLU40, and LEU50 (C-terminal). However, the number of K^+ ions bound to these residues is small: a maximum of 0.03 K^+ per residue. In summary, we did not find strong interactions of K^+ and Cl^- with either the peptide or the bilayer lipids.

3.6. Hydrophobic Mismatch. The difference between the thickness of the hydrophobic core of the bilayer and the transmembrane peptide length predispose the peptide considered here to undergo positive hydrophobic mismatch as described in several prior studies.[35−37] In all of the present simulations, we observed tilting of the transmembrane helix of 18−30° relative to the bilayer normal. The second, parallel effect of the mismatch was the presence of a kink in the helix around the residue GLY15 in four cases, and in the other two, around ALA17 (Figure 9). It is possible that the presence of the linker segment covalently attached to the transmembrane helix and its interactions with the lipids can affect hydrophobic mismatch adjustments. In systems where the linker is located closer to the bilayer surface (Figure 7a in runs a−d), the kink is observed closer to the end of the transmembrane helix at ALA17 and thus closer to the linker.

3.7. Sequence Analysis. The above-discussed results for COMT indicate the formation of a loop at the water−membrane interface. To investigate whether such a loop appears frequently in membrane proteins in general, we analyzed databases for membrane proteins that have a single transmembrane helix. Of particular interest in this analysis were those sequences that were next to the transmembrane helix. For the sequence analysis, we used the data set created by Sharpe et al.,[38] which includes proteins of humans taken from the RefSeq database.[39] Information about transmembrane domains was extracted from the literature and the TopDb database.[40] For those proteins whose transmembrane domain is not known, it was predicted using the TMHMM program.[41] The data set obtained in this fashion consists of 223 protein sequences. To estimate the probability of loop formation in a given peptide sequence, we focused on a 20 amino acid long sequence that followed the transmembrane helix and computed the probability for finding oppositely charged amino acids in the sequence. In the analysis, the linker was divided into five regions, which included amino acids 1−4, 5−7, 7−10, 10−15, and 15−20, counting away from the membrane. The analysis shows that positively charged residues are preferentially placed in the first region. In agreement with Sharpe et al.[38] we observed them in 71% of the analyzed sequences. Table 2 shows the probabilities for finding a residue of the opposite charge in fragments 7−10, 7−15, and 7−20 under a condition that in region 1−4 there is a charged residue. As the occurrence of such sequences is high, we conclude that a loop at the interface region can be a common structural element of transmembrane proteins in general.

Table 2. Probability of the Presence of the Oppositely Charged Amino Acids in the Various Fragments of the Transmembrane Protein Sequence

amino acid fragments	occurrence of oppositely charged amino acid [%]
1−3 and 7−10	22.45
1−3 and 7−15	33.97
1−3 and 7−20	44.10

4. DISCUSSION

COMT can exist in two forms: cytosolic (S-COMT) and membrane bound (MB-COMT). In MB-COMT, the catalytic domain (which is equivalent to the S-COMT structure) is anchored to a membrane by a 26-residue transmembrane helix and connected to the helix through a 24-residue linker segment. In the present study, we performed six MD simulations of a membrane with the transmembrane helix and linker segment of MB-COMT, and six MD simulations of a membrane with the linker segment only. These simulations were designed to show the difference in the behavior of the linker either bonded to the transmembrane helix or loosely placed in the water phase near the bilayer surface.

The simulations showed that the linker has a clear affinity for the membrane−water interface and preferentially arranges its residues next to it without a tendency to relocate into the water phase. Such a trend was observed for the linker both bonded with the transmembrane helix and loosely placed at the bilayer surface.

The results of the linker secondary structure analysis carried out in our study are not entirely conclusive. While we observed transient helical structures in the linker, we did not find any *consistent* pattern of the secondary structure that could suggest some specific folding of the linker. This might be interpreted as an absence of stable secondary structure in the linker. However, there are two grounds on which an argument can be made that this conclusion is incorrect: (1) the time scale of the simulation, and (2) the lack of the main protein unit, that is, the catalytic domain, S-COMT. Our simulations, although long in terms of current possibilities (360 ns), may be too short to observe peptide folding,[42,43] which additionally can be slower in the environment of the water−membrane interface.[42,43] The presence of the catalytic domain can also influence conditions of folding through altering the local environment, e.g., the hydration level, as well as by excluding some conformations that are observed in the current simulations where the end of the peptide is directed toward the bilayer. At the same time, in a subset of the simulations, we observed the formation of a helical structure (Figure 5), which was predicted in the previous bioinformatics study by Bai et al.[7] The fact that the membrane interface can stabilize helical structures was documented in another MD simulation study of different peptides[44] and is known, e.g., for antimicrobial peptides such as magainin.[45,46] Considering the above, one can hypothesize that the linker segment adopts the structure shown in Figure 6a, with a short helical fragment in the loop that is closed by a salt bridge. To confirm this hypothesis, future studies that include the entire COMT protein are needed.

Although we could not provide a final description of the secondary structure of the linker segment, we were able to observe the presence of a salt bridge between ARG27 located at the end of the transmembrane helix and GLU40 closing a 13-residue long loop. This salt bridge was present in all simulations of the linker for some period of time. In some structures, it was present in the initial structure but in some it was formed during the simulation. The behavior of the salt bridge was dynamic; it could be broken and reformed periodically. In some cases it could be replaced by a water-mediated interaction known as a water bridge.[30] The same type of a salt bridge was occasionally also present in the structure of the linker loosely associated with the bilayer; however, the probability of its formation was clearly lower. This salt bridge seems to be a key element of maintaining the close proximity of the peptide to the membrane. It is possible that this interaction is the cause of a characteristic dip around residue GLU40 in Figure 6, and is also the reason why the rest of the peptide remains in close proximity to the membrane.

In the study of phospholamban, a small 52-residue protein composed of a transmembrane helix and a short peptide outside the membrane, which in many respects resembles the MB-COMT fragment simulated in this study, the formation of a similar salt bridge was observed.[47] In that case the loop formed was shorter and included only six residues. That observation, together with the results of our simulations, can be connected with an extensive statistical analysis of salt bridges in proteins.[48] This statistical analysis of known protein structures has shown the preferential formation of salt bridges in an environment of ∼30% exposure of the residue surface to the water. This level of partial exposure being found to be optimal has been hypothesized to result from two competing factors: (a) the insertion of charged residues into the hydrophobic core of the protein is energetically unfavorable due to the cost of charge group dehydration, and (b) full exposure to the water might decrease the probability of salt bridging due to the competition for hydrogen bonding with water.[48] The water-membrane interface in fact creates conditions that lead to lower hydration for the residues located at the end of the transmembrane helix, thus conditions for the formation of a salt bridge seem to be optimal. This lower hydration is documented by our analysis of the SASA that shows exposure of these two residues to the water at a level of 36−40%. At the same time, water exposure of the same residues in a freely placed linker is higher, and thus the frequency of the salt bridge formation is lower. In our present simulations, the main part of the protein was not present, thus we can expect that when it is present it can decrease the number of water molecules in the linker neighborhood to make the formation of the salt bridge more favorable.

An interesting question remains: Is the formation of similar loops stabilized by salt bridges a common phenomenon in the case of transmembrane proteins? As we have discussed above, the water−membrane interface creates an optimal condition for the salt bridge formation between charged residues, and such a salt bridge has been observed in two different MD simulation studies.[47] Additionally, it is known that positively charged residues, arginine or lysine, are preferentially located at the end of transmembrane peptides in membrane proteins.[38] Our additional analysis of the sequences of the single-helix transmembrane proteins showed that in 44% of cases when a charged residue is located at the end of a transmembrane helix, a residue of opposite charge is present at the position 7−20. This indicates that a similar loop might be a common structural element of the transmembrane proteins.

■ ASSOCIATED CONTENT

Ⓢ Supporting Information. Percentage of simulation time over which a given type of secondary structure was observed in

the system with the linker attached to a transmembrane helix and loosely attached to the bilayer surface. Average shortest distance between the carboxyl group of C-terminus and lipids atoms, the frequency of the contacts between carboxyl group lipids atoms, and the frequency of charge pairs between carboxyl group and lipids choline groups. This material is available free of charge via the Internet at http://pubs.acs.org.

AUTHOR INFORMATION

Corresponding Author
*E-mail: tomasz.rog@tut.fi; tomasz.rog@gmail.com.

ACKNOWLEDGMENT

Computational resources were provided by the Finnish IT Centre for Science (CSC) and the SharcNet grid computing facility (www.sharcnet.ca). We wish to thank the Academy of Finland, the Natural Sciences and Engineering Research Council of Canada (NSERC), the Erasmus program, and the Emil Aaltonen (A.B.) and CIMO (A.B.) foundations for financial support.

REFERENCES

(1) Vinothkumar, K. R.; Henderson, R. *Q. Rev. Biophys.* **2010**, *43*, 65–158.
(2) McLuskey, K.; Roszak, A. W.; Zhu, Y.; Isaacs, N. W. *Eur. Biophys. J.* **2009**, *39*, 723–755.
(3) Guldberg, H. C.; Marsden, C. A. *Pharmacol. Rev.* **1975**, *27*, 135–206.
(4) Männistö, P. T.; Kaakkola, S. *Pharmacol. Rev.* **1999**, *51*, 593–628.
(5) Reenilä, I.; Männistö, P. T. *Med. Hypotheses* **2001**, *57*, 628–632.
(6) Vidgren, J.; Svensson, L. A.; Liljas, A. *Nature* **1994**, *368*, 354–358.
(7) Bai, H.-W.; Shim, J.-Y.; Yu, J.; Zhu, B. T. *Chem. Res. Toxicol.* **2007**, *20*, 1409–1425.
(8) Bunker, A.; Männistö, P.; St Pierre, J.-F.; Róg, T.; Pomorski, P.; Stimson, L.; Karttunen, M. *SAR QSAR Environ. Res.* **2008**, *19*, 179–189.
(9) Róg, T.; Martinez-Seara, H.; Munck, N.; Orešič, M.; Karttunen, M.; Vattulainen, I. *J. Phys. Chem. B* **2009**, *113*, 3413–3422.
(10) Pöyry, S.; Róg, T.; Karttunen, M.; Vattulainen, I. *J. Phys. Chem. B* **2009**, *113*, 15513–15521.
(11) Derreumaux, P. *J. Chem. Phys.* **1999**, *111*, 2301–2310.
(12) Jorgensen, W. L.; Maxwell, D. S.; Tirado-Rives, J. *J. Am. Chem. Soc.* **1996**, *118*, 11225–11236.
(13) Rizzo, R. C.; Jorgensen, W. L. *J. Am. Chem. Soc.* **1999**, *121*, 4827–4836.
(14) Price, M. L. P.; Ostrovsky, D.; Jorgensen, W. L. *J. Comput. Chem.* **2001**, *22*, 1340–1352.
(15) Kaminski, G. A.; Friesner, R. A.; Tirado-Rives, J.; Jorgensen, W. L. *J. Phys. Chem. B* **2001**, *105*, 6474–6487.
(16) Stepniewski, M.; Bunker, A.; Pasenkiewicz-Gierula, M.; Karttunen, M.; Róg, T. *J. Phys. Chem. B* **2010**, *114*, 11784–11792.
(17) Takaoka, Y.; Pasenkiewicz-Gierula, M.; Miyagawa, H.; Kitamura, K.; Tamura, Y.; Kusumi, A. *Biophys. J.* **2000**, *79*, 3118–3138.
(18) Jorgensen, W. L.; Chandrasekhar, J.; Madura, J. D.; Impey, R. W.; Klein, M. L. *J. Chem. Phys.* **1983**, *79*, 926.
(19) Lindahl, E.; Hess, B.; van der Spoel, D. *J. Mol. Model.* **2001**, *7*, 306–317.
(20) van der Spoel, D.; Lindahl, E.; Hess, B.; Groenhof, G.; Mark, A. E.; Berendsen, H. J. C. *J. Comput. Chem.* **2005**, *26*, 1701–1718.
(21) Hess, B.; Bekker, H.; Berendsen, H.; Fraaije, J. *J. Comput. Chem.* **1997**, *18*, 1463–1472.
(22) Nosé, S. *J. Chem. Phys.* **1984**, *81*, 511.
(23) Hoover, W. G. *Phys. Rev. A* **1985**, *31*, 1695.
(24) Parrinello, M. *J. Appl. Phys.* **1981**, *52*, 7182.
(25) Essmann, U.; Perera, L.; Berkowitz, M.; Darden, T.; Lee, H.; Pedersen, L. *J. Chem. Phys.* **1995**, *103*, 8577–8593.
(26) Patra, M.; Karttunen, M.; Hyvönen, M. T.; Falck, E.; Vattulainen, I. *J. Phys. Chem. B* **2004**, *108*, 4485–4494.
(27) Kaszuba, K.; Róg, T.; St. Pierre, J.-F.; Männistö, P. T.; Karttunen, M.; Bunker, A. *SAR QSAR Environ. Res.* **2009**, *20*, 595–609.
(28) Hall, A.; Róg, T.; Karttunen, M.; Vattulainen, I. *J. Chem. Phys. B* **2010**, *114*, 7797–7807.
(29) Kabsch, W.; Sander, C. *Biopolymers* **1983**, *22*, 2577–2637.
(30) Róg, T.; Murzyn, K.; Milchoud, J.; Karttunen, M.; Pasenkiewicz-Gierula, M. *J. Phys. Chem. B* **2009**, *113*, 2378–2387.
(31) Kumar, S.; Nussinov, R. *J. Mol. Biol.* **1999**, *293*, 1241–1255.
(32) Vácha, R.; Berkowitz, M. L.; Jungwirth, P. *Biophys. J.* **2009**, *96*, 4493–4501.
(33) Gurtovenko, A. A.; Vattulainen, I. *J. Chem. Phys.* **2009**, *130*, 215107.
(34) Zhao, W.; Rog, T.; Gurtovenko, A.; Vattulainen, I.; Karttunen, M. *Biophys. J.* **2007**, *92*, 1114–1124.
(35) Killian, J. A. *FEBS Lett.* **2003**, *555*, 134–138.
(36) Gil, T.; Ipsen, J. H.; Mouritsen, O. G.; Sabra, M. C.; Sperotto, M. M.; Zuckermann, M. J. *Biochim. Biophys. Acta* **1998**, *1376*, 245–266.
(37) Róg, T.; Murzyn, K.; Karttunen, M.; Pasenkiewicz-Gierula, M. *J. Pept. Sci.* **2008**, *14*, 374–382.
(38) Sharpe, H. J.; Stevens, T. J.; Munro, S. *Cell* **2010**, *142*, 158–169.
(39) Pruitt, K. D.; Tatusova, T.; Klimke, W.; Maglott, D. R. *Nucleic Acids Res.* **2009**, *37*, D32–36.
(40) Tusnady, G. E.; Kalmar, L.; Simon, I. *Nucleic Acids Res.* **2007**, *36*, D234–D239.
(41) Krogh, A.; Larsson, B.; von Heijne, G.; Sonnhammer, E. L. *J. Mol. Biol.* **2001**, *305*, 567–580.
(42) Lindahl, E.; Sansom, M. S. *Curr. Opin. Struct. Biol.* **2008**, *18*, 425–431.
(43) Seibert, M. M.; Patriksson, A.; Hess, B.; van der Spoel, D. *J. Mol. Biol.* **2005**, *354*, 173–183.
(44) Polverini, E.; Coll, E. P.; Tieleman, D. P.; Harauz, G. *Biochim. Biophys. Acta* **2011**, *1808*, 674–683.
(45) Khandelia, H.; Ipsen, J. H.; Mouritsen, O. G. *Biochim. Biophys. Acta* **2008**, *1778*, 1528–1536.
(46) Murzyn, K.; Róg, T.; Pasenkiewicz-Gierula, M. In *Computational Science - ICCS 2004*; Bubak, M., Albada, G. D., Sloot, P. M. A., Dongarra, J., Eds.; Springer: Berlin/Heidelberg, 2004; Vol. 3037, pp 325−331.
(47) Kim, T.; Lee, J.; Im, W. *Proteins* **2009**, *76*, 86–98.
(48) Sarakatsannis, J. N.; Duan, Y. *Proteins* **2005**, *60*, 732–739.
(49) Humphrey, W.; Dalke, A.; Schulten, K. *J. Mol. Graphics* **1996**, *14*, 33–38.

II

LATERAL SORTING IN MODEL MEMBRANES BY CHOLESTEROL-MEDIATED HYDROPHOBIC MATCHING

by

II. Kaiser, H.-J., Orłowski, A., Róg, T., Nyholm, T.K.M., Chai, W., Feizi, T., Lingwood, D., Vattulainen, I., & Simons, K. 2011.

Proceedings of the National Academy of Sciences vol. 108, 16628-16633

Lateral sorting in model membranes by cholesterol-mediated hydrophobic matching

Hermann-Josef Kaiser[a,1], Adam Orłowski[b], Tomasz Róg[b], Thomas K. M. Nyholm[c], Wengang Chai[d], Ten Feizi[d], Daniel Lingwood[a], Ilpo Vattulainen[b,e,f], and Kai Simons[a,2]

[a]Max Planck Institute for Molecular Cell Biology and Genetics, Pfotenhauerstr. 108, 01307 Dresden, Germany; [b]Department of Physics, Tampere University of Technology, Korkeakoulunkatu 10, FI-33720 Tampere, Finland; [c]Department of Biosciences, Biochemistry, Åbo Akademi University, Tykistökatu 6, FIN-20520 Turku, Finland; [d]Department of Medicine, Imperial College London, Northwick Park & St. Mark's Campus, Harrow, HA1 3UJ, United Kingdom; [e]Department of Applied Physics, Aalto University School of Science and Technology, FI-00076 Aalto, Finland; and [f]Department of Physics and Chemistry, MEMPHYS—Center for Biomembrane Physics, University of Southern Denmark, Campusvej 55, DK-5230 Odense M, Denmark

Edited by Stephen H. White, University of California, Irvine, CA, and accepted by the Editorial Board August 16, 2011 (received for review March 7, 2011)

Theoretical studies predict hydrophobic matching between transmembrane domains of proteins and bilayer lipids to be a physical mechanism by which membranes laterally self-organize. We now experimentally study the direct consequences of mismatching of transmembrane peptides of different length with bilayers of different thicknesses at the molecular level. In both model membranes and simulations we show that cholesterol critically constrains structural adaptations at the peptide-lipid interface under mismatch. These constraints translate into a sorting potential and lead to selective lateral segregation of peptides and lipids according to their hydrophobic length.

mattress model | membrane domain | protein–lipid interaction | self-assembly | annular lipid

Hydrophobicity is the key criterion for lipids and proteins to integrate into membranes (1). This self-assembly is driven by the minimization of hydrophobic surface area exposed to the aqueous phase (2). Next to sterols, eukaryotic membranes contain a variety of phospholipids with different chain length (3) and proteins with a variety of transmembrane (TM) domain lengths (4). Why cell membranes contain so many lipids is still enigmatic. But one reason could be membrane sorting due to grouping of TM proteins and lipids with similar hydrophobic length.

The "mattress model" predicts that the embedding of a rigid, helical TM protein into a fluid bilayer causes the lipids to adapt locally to a mismatch (5). In this way exposure of hydrophobic surface area is minimized. The adaptive flexing and straightening of the lipids can also be accompanied by a tilting of the protein (6). Because of these strain-causing adaptations of the bilayer, selective association of matching lipids with TM proteins as well as macroscopic sorting processes according to hydrophobic length have been predicted by theory and simulation (7, 8). Membrane properties such as elasticity—modulated by cholesterol—were also predicted as crucial parameters (9). Such mismatch-dependent, cholesterol-induced sorting has indeed been proposed as a retention mechanism for the Golgi-resident proteins in the secretory pathway (10).

Due to the complexity of cell membranes, model membranes have proven a valuable system to investigate hydrophobic matching (11–13). Hydrophobic peptides of the poly-leucine type have been used as generic TM proteins because of the ease of their organic solvent-based reconstitution (14, 15). From these experiments, it has become clear that TM proteins indeed tolerate moderate mismatch with the bilayer (13, 14, 16). However, large mismatch as well as cholesterol have been found to reduce efficiency of TM peptide incorporation into bilayers, suggesting that there are energetic limitations to mismatch buffering (12).

Despite indication for selective protein–lipid interactions and hydrophobic matching (17, 18), actual sorting of TM proteins and accompanying lipid cosorting has not been reconstituted in vitro. Therefore, it remains unclear whether hydrophobic mismatch is a significant parameter in the organization of proteinacious membranes.

Using TM peptides and lipids of defined acyl chain length in atomistic molecular dynamics (MD) simulations and reconstituted proteo-liposomes we have investigated hydrophobic mismatching with respect to (*i*) the structural impact of mismatched helices on lipid bilayers; and (*ii*) its consequences on the lateral distribution of peptides and lipids.

Our results suggest that cholesterol severely strains the peptide–lipid interface under mismatch if the bilayer is thicker than the TM segment. Moreover, it enforces a redistribution of TM peptides and lipids according to hydrophobic length. We propose that cholesterol reduces the adaptability of the lipids to mismatched proteins and therefore makes hydrophobic mismatch energetically more relevant. Our data thus provide a molecular basis for the role of TM domain (TMD) length and cholesterol in protein and lipid sorting in the secretory pathway.

Results

First we investigated the structure of the protein–lipid interface in model systems under conditions of hydrophobic mismatch. We carried out atomistic MD simulations pcarallel to organic solvent reconstitution of bilayers containing LW19 ($K_2W_2L_7AL_7W_2K_2$), LW21 ($K_2W_2L_8AL_8W_2K_2$), or LW29 ($K_2W_2L_{12}AL_{12}W_2K_2$) peptides (Fig. S1*A*). To vary hydrophobic mismatch we used a series of monounsaturated phosphatidylcholines (PC), having different fatty acid lengths from C16:1 to C24:1 (13, 19) and defined positive mismatch as $\text{length}_{\text{protein}} > \text{thickness}_{\text{bilayer}}$ and negative mismatch as $\text{length}_{\text{protein}} < \text{thickness}_{\text{bilayer}}$ (Table S1).

Atomistic MD Simulations. In the 500 ns atomistic MD simulations we used the two extreme conditions of LW21 in C16:1 PC and C24:1 PC in the absence and presence of 20 mol% cholesterol (Fig. 1*A* and Movies S1–S4). In the C16:1 PC membranes the radial profiles and average maps showed increased acyl chain order and bilayer thickness around the TM helix (Fig. 1 *B* and *C* and Fig. S2). This became less pronounced with cholesterol (Fig. 1 *B* and *C* and Fig. S2). In addition the peptide tilted in the membrane, being more prominent without cholesterol (Fig. 1*D*). This suggested that the mismatch adaption (bilayer thickening

Author contributions: H.-J.K., A.O., T.R., T.K.M.N., D.L., I.V., and K.S. designed research; H.-J.K., A.O., T.R., and T.K.M.N. performed research; W.C. and T.F. contributed new reagents/analytic tools; H.-J.K., A.O., T.R., T.K.M.N., D.L., I.V., and K.S. analyzed data; and H.-J.K. and K.S. wrote the paper.

The authors declare no conflict of interest.

This article is a PNAS Direct Submission. S.H.W. is a guest editor invited by the Editorial Board.

[1]Present address: Max-Delbrück-Centrum für Molekulare Medizin, Robert-Rössle-Strasse 10, 13125 Berlin, Germany

[2]To whom correspondence should be addressed. E-mail: simons@mpi-cbg.de.

This article contains supporting information online at www.pnas.org/lookup/suppl/doi:10.1073/pnas.1103742108/-/DCSupplemental.

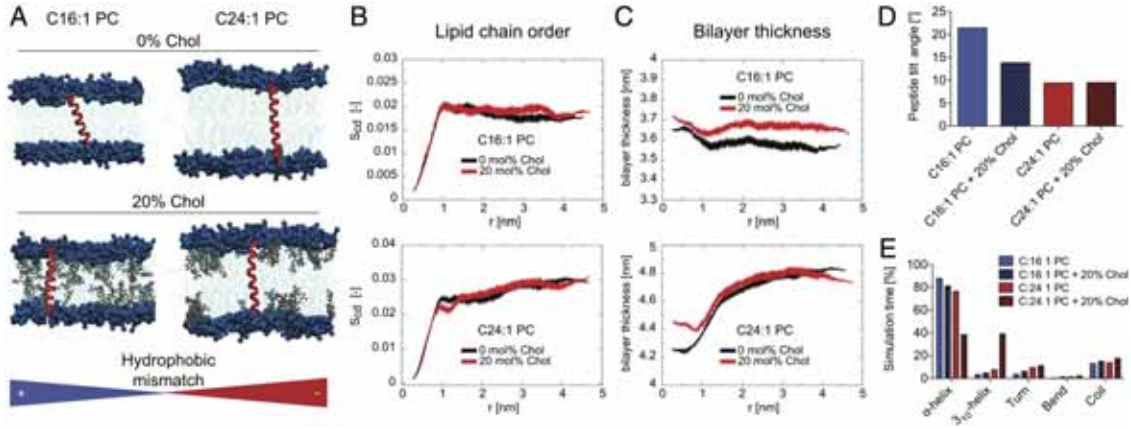

Fig. 1. Hydrophobic mismatch between transmembrane peptide and lipid determines bilayer structure, helix orientation, and fold. (*A*) Snapshots from the MD simulations with LW21 TM peptide (red) embedded in C16:1 and C24:1 PC (headgroups dark blue, chains light blue) in the presence and absence of cholesterol (gray). Positive hydrophobic mismatch ($length_{TMD} > thickness_{bilayer}$) and negative mismatch ($length_{TMD} < thickness_{bilayer}$) is indicated by the blue/red color bar. (*B*) Distance profiles of lipid chain order (S_{cd} of Sn1) with respect to the helix backbone at 0 nm ($t = 500$ ns) for C16:1 and C24:1. Black trace is 0% cholesterol, red trace is 20% cholesterol. The S_{cd} parameter shown here represents the average value of the S_{cd} profile along the hydrocarbon chain. (*C*) Membrane thickness (P-P distance in units of nanometers) with respect to the helix backbone at 0 nm ($t = 500$ ns) for C16:1 and C24:1. Black trace is 0% cholesterol, red trace is 20% cholesterol. (*D*) Bar graph of the average tilt angle of LW21 in the four simulations in degrees (see axis). (*E*) Fold adopted by LW21 over the simulation time in percent (see legend).

and tilt) became less in the presence of cholesterol. Peptide length measured from N- to C-terminal Cα remained unaffected, being 3.80 ± 0.12 nm without cholesterol and 3.90 ± 0.14 nm with cholesterol. In the C24:1 PC system, the bilayer around the peptide was markedly less ordered and thinner. In the presence of cholesterol this region localized closer to the peptide (Fig. 1*C* and Fig. S2) and was associated with a marked stretching of the helix from 4.08 ± 0.12 nm to 4.42 ± 0.13 nm and a conversion from the α into the longer 3_{10} form (Fig. 1*E*). These data indicated that the strongest protein-induced bilayer deformation occurred under negative mismatch. Cholesterol counteracted bilayer adaptation by shifting the deformation closer to the peptide surface and by forcing the helix to stretch.

Reconstitution in Large Unilamellar Vesicles. To test predictions from the simulation studies, we reconstituted peptides of two different lengths (3 mol% of LW21 and LW19 peptides) into large unilamellar vesicles (LUVs) by organic solvent reconstitution and extrusion (100 nm pore size). Incorporation of the peptides into LUVs could be measured by intrinsic Trp fluorescence (Fig. 2*A* and Fig. S3*A*) or by coomassie staining (Fig. S3*B*). We also validated integral membrane association by protection from proteinase K digestion (Fig. S1*B*) and their predominately helical structure (>85%) by circular dichroism (CD) measurements (Fig. S1*C* and Table S2). We found that 30 mol% cholesterol greatly reduced incorporation of LW21 into negatively mismatched bilayers (Fig. 2*A*; full spectra in Fig. S3*A*). The unincorporated peptide could be recovered from the extruder membrane and did not remain on the vesicles (Fig. S3*B*). Also the shorter LW19 showed this trend (Fig. S4*A*). In the absence of cholesterol, incorporation was limited only under extreme mismatch of approximately 9 Å (Fig. S4*A*). L17, a peptide similar to LW21 that lacked double Trp (but retained double Lys) in the flanks, showed integration behavior very similar to that of LW21 (Fig. S3*C*). Taken together the data showed that cholesterol induced a selective limitation to the integration of negatively mismatched TM peptides at angstrom precision.

We next studied the impact of 3 mol% of LW21 (if integrated) on lipid packing. For this we used the fluorescent membrane probe C-laurdan, whose membrane hydration-dependent red shift in fluorescence emission can be translated into a relative index for lipid packing: the generalized polarization (GP) value (20, 21). We found a peptide-mediated increase in lipid packing (ΔGP) for all mismatch conditions in the absence of cholesterol (Fig. 2*B*). However, with cholesterol present, the lipid packing strongly decreased with increasing negative mismatch (Fig. 2*C*). In order to bridge between C18:1 and C20:1 PC we additionally used C18:1/C16:0 PC, which represents an intermediate lipid length (22). The shorter LW19 peptide showed the same trend (Fig. S4 *B* and *C*). This implied that the peptide generally rigidified the bilayer but that under negative mismatch in the presence of cholesterol the peptide induced a relative disordering of the bilayer.

Peptide Sorting. Next we tested the role of cholesterol on the distribution of TM peptides in mismatched vesicles. We prepared giant unilamellar vesicles (GUVs) for microscopy composed of PCs of different chain length, 3 mol% of a fluorescein-isothiocyanate (FITC)-labeled LW21 (FITC-LW21), and the lipid marker lissamine rhodamine-dioleoylphosphoethanolamine (Rh-DOPE) either by swelling LUVs or by swelling the dried lipid-peptide mixture. We always maintained 10 mol% of C18:1 PC to keep the bilayer fluid and more stable (see *SI Text*). Then we carefully infused 3.8 μM cholesterol as a methyl-β-cyclodextrin complex (MBCD-Chol) (23). This induced a substantial clustering of FITC-LW21 in the C24:1 PC membrane into line-shaped domains within minutes (Fig. 3 *A* and *B*). This segregation could be reversed by cholesterol extraction with 1 mM uncomplexed MBCD (Fig. 3*A*). The extent of segregation decreased with shorter PCs and was not observed under positive mismatch (Fig. 3*C*). These results suggested that cholesterol reversibly induced a segregating activity under negative mismatch. In the course of the cholesterol-loading reaction FITC fluorescence decreased to around 50% just before microscopic segregation and recovered after dissolution of the domains upon cholesterol extraction (Fig. S5 *B–D*). This implied that the FITC molecules concentrated and underwent a reversible self-quenching, which likely reflected peptide oligomerization during the transition to microscopic segregation. However, we also observed budding of

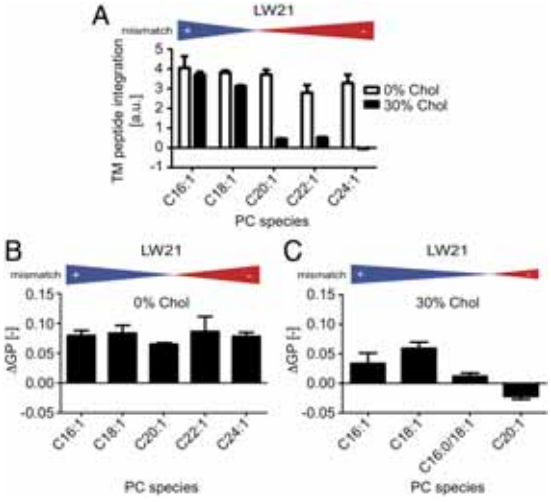

Fig. 2. Hydrophobic mismatch between transmembrane peptide and lipid affects protein integration and lipid packing. (*A*) Trp fluorescence emission indicates integration of LW21 peptide into PC LUVs in the absence and presence of 30 mol% cholesterol. (*B*) Differences in lipid packing (ΔGP) indicate the structural impact of 3 mol% LW21 peptide in the absence of cholesterol on unsaturated PC bilayers from C16:1 to C24:1 (error bars = SD, $n = 3$). (*C*) Differences in lipid packing (ΔGP) in the presence of 30 mol% cholesterol. All error bars are SD ($n = 3$).

domains from the cholesterol-loaded GUVs representing partial release of the TM peptides from the mother vesicles.

Next, we tested a positively mismatched peptide for cholesterol-dependent segregation. To this end we mixed 1.5 mol% of a long tetramethylrhodamine (TMR)-labeled LW peptide (TMR-LW29; Fig. S1*A*) into GUVs containing 1.5 mol% of FITC-LW21. It integrated best into C22:1 PC to C24:1 PC but not into C16:1 PC membranes (Fig. S6*A*). When we infused cholesterol at 8.1 μM into the C24:1 PC membrane, FITC-LW21 was selectively clustered into domains from which the longer TMR-LW29 was partially depleted (Fig. 3*D*). Results were independent of the preparation (swelling crude peptide/lipid mixture vs. LUVs; see *SI Text*). The behavior implied that the segregation force was acting selectively on FITC-LW21 and not on TMR-LW29. This correlated well with LUV experiments, where LW21 was excluded from the C24:1 PC-cholesterol bilayer, whereas TMR-LW29 was well integrated (Fig. S6*B*).

Lipid Sorting. The previous LUV experiments had shown that negative mismatch prevented peptide integration in the presence of cholesterol. Thus we tested whether TMD-matched lipids would "rescue" peptide integration. We reconstituted LW21 in the C24:1 PC bilayer and replaced 10, 20, and 25 mol% C24:1 PC with an equal amount of C18:1 PC. This led to an increase of Trp fluorescence, reflecting increased peptide integration through matching lipids (Fig. 4*A*). Next we added increasing amounts of LW21 to preparations containing 5, 10, 20, or 25 mol% of C18:1 PC in a C24:1 PC-cholesterol background. Here, peptide integration showed a saturation behavior (Fig. 4*B*). This indicated that the matching C18:1 PC became a limiting factor for the integration of LW21 into the mismatching C24:1 PC-cholesterol bilayer. It was suggestive of a lateral association between C18:1 PC and LW21.

Next, we tested whether short chain lipids would laterally associate with the clustered FITC-LW21 domain as implied by the previous result. We doped C24:1 PC GUVs containing FITC-LW21 and TMR-LW29 with the (neo)glycolipid di-C12:0-GM1

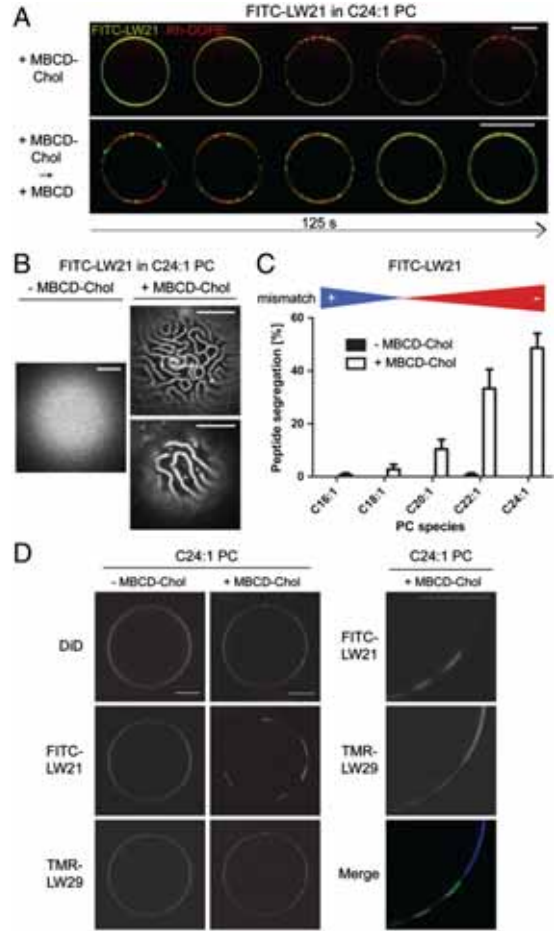

Fig. 3. Hydrophobic mismatch and cholesterol determine lateral transmembrane peptide distribution. (*A*) Fluorescence microscopy images of GUVs depicting the segregation of FITC-LW21 peptide (3 mol%) and lipid marker Rh-DOPE (0.05 mol%) C24:1 PC (87 mol%) with C18:1 PC (9.95 mol%) during of 3.8 μM MBCD-cholesterol loading (*Upper*) and subsequent cholesterol extraction with 1 mM MBCD (*Lower*) (125 s). (*B*) Fluorescence microscopy images of GUV apexes depicting the patterns of FITC-LW21 peptide before and after 3.8 μM MBCD-cholesterol loading. (*C*) Quantification of FITC-LW21 segregation in GUVs before and after 3.8 μM cholesterol loading in different PCs (bars = SEM, $n = 3$). (*D*) Fluorescence microscopy images of GUVs depicting the localization of FITC-LW21 peptide (1.5 mol%), TMR-LW29 peptide (1.5 mol%) and lipid marker DID (0.05 mol%) in C24:1 PC (87 mol%) with C18:1 PC (9.95 mol%) before and after 8.1 μM MBCD-cholesterol loading. All image bars = 10 μm.

(24) containing short acyl chains or the long chain C24:0/dC18:1-GM1 at 0.1 mol%. Addition of Alexa647-cholera toxin B (A647-CtxB) caused a homogeneous staining of GM1 in the membrane (Fig. 3*C*). After infusion of 8.1 μM MBCD-Chol di-C12:0-GM1 redistributed and colocalized with the FITC-LW21 domain (Fig. 3*C*). Redistribution was not seen in the absence of FITC-LW21. In contrast to di-C12:0-GM, C24:0/dC18:1-GM1 remained homogenously distributed in the presence of FITC-LW21 domains (Fig. 3*C*). These results showed that upon cholesterol loading the glycolipid with the short lipid chains became attracted to the FITC-LW21 domain, whereas the glycolipid with long chains did not. GM1s with intermediate chain length exhibited partial enrichment in the LW21 domain (Fig. S7).

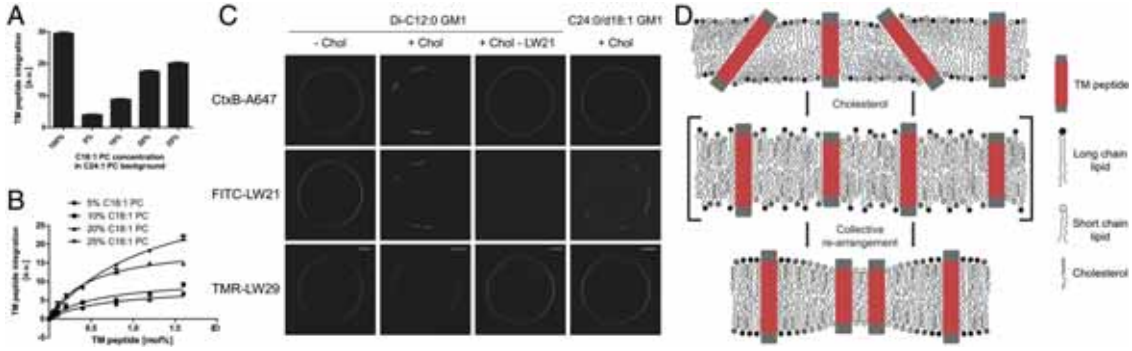

Fig. 4. Hydrophobic mismatch and cholesterol determine lateral lipid distribution. (*A*) Trp fluorescence emission indicates integration of LW21 peptide into LUVs with 100, 0, 10, 20, and 25 mol% C18:1 PC in a C24:1 PC background containing 30 mol% cholesterol (bars = SD, $n = 3$). (*B*) Trp fluorescence emission indicates integration of the titrated LW21 peptide into LUVs with 5, 10, 20, and 25 mol% C18:1 PC in a C24:1 PC background containing 30 mol% cholesterol (bars = SD, $n = 3$). (*C*) Fluorescence microscopy images of GUVs depicting the localization of FITC-LW21 (1.5 mol%), TMR-LW29 (1.5 mol%), and CtxB-A647-labeled Di-C12:0 GM1 (0.1 mol%) before and after MBCD-cholesterol loading and in the absence of FITC-LW21. Last column shows CtxB-A647-labeled C24:0/dC18:1 GM1 (0.1 mol%) after MBCD-cholesterol loading. bar = 10 μm. (*D*) Scheme of cholesterol's function to rearrange TM peptide and lipid distribution according to hydrophobic length. It extends the acyl chains of the lipids making them less adaptable to mismatching TM peptides.

Discussion

In this study we investigated (*i*) how hydrophobic mismatch between the lipid bilayer and a helical TM segment influences the structure of the interface, (*ii*) how cholesterol alters the lipid–peptide configuration, and (*iii*) whether structural alterations derandomize the long-range distribution of the molecules. We chose the common series of monounsaturated PCs from di-16:1 to di-C24:1 as well described model membranes in which thickness can be varied (13, 14, 19). These membranes are fluid at room temperature. We selected characterized poly-leucine-type hydrophobic peptides with Trps at the water-bilayer boundary and flanking lysines that readily form stable TM helices when reconstituted from organic solvent (6, 11, 15). We confirmed integral membrane association by protection from proteinase K digestion and helical structure by CD spectroscopy for LW19, LW21, and LW29 (Fig. S1 and Table S2). The peptides only differed in their amount of leucines in the TM segment (14 vs. 16 vs. 24).

First we performed atomistic MD simulations over 500 ns of LW21 in C16:1 PC and C24:1 PC in the absence and presence of 20 mol% cholesterol. These conditions covered similar positive and negative mismatch (Fig. 1*A* and Table S1). The data indicated local, peptide-induced acyl chain straightening and TM segment tilting as response to positive mismatch and acyl chain flexing as a result of negative mismatch (Fig. 1 *B*, *C* and *D*). This is in line with predictions of the mattress model and experimental results by others (14, 22). Related membrane protein induced changes in the structure and also the dynamics of lipids around the protein have been observed in recent atomistic simulations (25). The most striking effect was a considerable membrane thinning around the peptide under negative mismatch (Fig. 1*C*). Cholesterol counteracted this effect presumably by straightening lipid acyl chains. This concentrated the deformation in direct vicinity of the helix surface (Fig. 1 *B* and *C*) leading to a marked stretching of the α-helix into a 3_{10} conformation by more than 3 Å (Fig. 1*E*). We interpret this as a strain exerted by the stiffer lipid environment and a destabilization toward unfolding of the peptide (26, 27).

When we reconstituted LW21 in a series of PCs of different length, we indeed observed that efficiency of membrane integration decreased sharply under negative mismatch in the presence of 30 mol% cholesterol (Fig. 2*A*). Similar effects have also been reported by other groups (12–14, 28). This indicated that the activity of cholesterol made the peptide unstable in the membrane in agreement with our simulation data. A direct measurement of the increased 3_{10} helix content predicted by the simulation could not be realized due to the strong reduction of peptide content in the bilayer. A similar trend of reduced incorporation was observed for LW19 albeit shifted toward thinner bilayers as expected (Fig. S4*A*). Moreover, integration was also compromised under large negative mismatch (9 Å) in the absence of cholesterol, again suggesting that cholesterol increased the energy penalty for membrane deformation under negative mismatch. Importantly, L17 a peptide similar to LW21 but lacking the flanking Trps, recapitulated the reduced membrane integration under negative mismatch with cholesterol seen with LW21 (Fig. S3*C*). This suggested that a minimal TM architecture of the type "charge-hydrophobic stretch-charge" is sufficient for the behavior.

When we monitored lipid packing with C-laurdan we found that the peptide generally increased average membrane order except under growing negative mismatch with cholesterol (Fig. 2 *B* and *C*). Thus the rigid structure of the peptide reduces the conformational freedom of the lipids (29) whereas in thicker bilayers it caused a relative disordering. Here the peptide may obstruct the cholesterol-mediated straightening of the chains in agreement with the stretching of the helix observed in the simulations. Our results corroborate NMR data that indicate similar ordering effects (22). However, in our system we cannot fully rule out that the helix partially converts from a TM into a peripheral helix conformation as a result of the strain (12).

Our data clearly indicated that the lipid–peptide interface experienced a deformation strain under negative mismatch with cholesterol. We predicted that this strain represented a potential for lateral segregation because clustering of TM peptides into a domain should minimize the interface area (7, 9). Moreover, this reaction should be inducible by cholesterol and reversible. We reconstituted the fluorescent FITC-LW21 at 3 mol% into C24:1 PC GUVs and infused cholesterol by a recently developed MBCD-Chol exchange protocol. This allowed careful loading of membranes below saturation levels (23). Using confocal microscopy we observed the segregation of FITC-LW21 into micro-scaled, line-shaped domains within a fluid bilayer. Extraction of cholesterol reversed the reaction as predicted (Fig. 3*A*). Because this selective TM peptide segregation does not require or induce lipid phase immiscibility, it is fundamentally different from the packing-related exclusion of peptides and proteins from liquid ordered lipid phases (20, 30). Reversible self-quenching of the FITC-moieties along the reaction from dispersed to segregated TM peptides indicated peptide oligomerization as a transition state as expected (Fig. S5 *B–D*). We also noticed budding of domains, which represents an irreversible reaction beyond segregation.

Peptide segregation in GUVs was a function of negative mismatch (Fig. 3*C*) in line with the conclusions from our LUV experiments. Line-shaped domains (Fig. 3*B*) have also been observed for solid lipid domains in a cholesterol-PC phase (31). They require repelling forces that prevent coalescence. We speculate that the line shape observed here is a product of the rigid helices and the repulsion arising from the net positive charge due to the four lysines. Given the results from our LUV system, we predicted that a positively mismatched TM peptide should resist the segregating force. For this we reconstituted the very long TMR-LW29, which integrated only into the thick PC bilayer suggesting mismatch-limited TM integration as discussed above (Fig. S6*A*). When it was introduced at the same molar ratio as FITC-LW21 (1.5%) TMR-LW29 did not get sequestered upon cholesterol addition as did the shorter peptide. Instead it became depleted from the FITC-LW21 domains (the extent of which eluded further quantification due to the irregular shape of the domains) (Fig. 3*B*). We also validated the selective activity on the negatively mismatched peptide by the exclusion from LUVs. Here we observed a failure of integration for FITC-LW21, whereas TMR-LW29 was not affected (Fig. S6*B*). The data suggest that the failure of peptide incorporation at a fixed cholesterol level under negative mismatch translates into a propensity for TM length-based lateral segregation of peptides upon gradual cholesterol loading (13).

How then does the distribution of matching/mismatching lipids correlate? In our LUV system addition of LW21-matching C18:1 PC to a C24:1 PC bilayer increased the amount of incorporated peptide (Fig. 4*A*). Moreover, the peptide titration showed saturation trends implying the matching lipid to be a limiting factor for peptide incorporation (Fig. 4*B*). We interpret this behavior as a marked reduction of the mismatch-related strain by the matching lipid. Accordingly it should localize to the surface of the helix like an annular lipid. We tested this by labeling the short chain neoglycolipid di-C12:0-GM1 (0.1 mol %) with A647-CtxB. Upon segregation the lipid indeed colocalized with FITC-LW21 but remained homogeneous in the absence of the peptide, suggesting that the lipid sorting is dependent on the peptide domain. As a negative control we used the glycolipid C24:0/dC18:1-GM1 with long chains, which did not experience attraction by the peptide domain. Exclusion was not readily detectable due to the domain shape (Fig. 4*C*). A native and a neo-GM1 of intermediate chain length both exhibited partial enrichment in the peptide domain as expected. CtxB is pentavalent for GM1; therefore clustering may reinforce the sorting behavior of the individual lipid. The experiments showed that the model set up from the LUV system holds for the GUVs and that cholesterol induces the requirement and cosegregation of short chain lipids with the peptide.

In summary, we have demonstrated that cholesterol forces a membrane containing high amounts of TM peptide to undergo a collective rearrangement according to hydrophobic length (Fig. 4*D*). Differences of two amino acids (LW19 vs. LW21) or two methylene groups (C22:1 vs C24:1 PC) were significant. We propose that cholesterol sterically constrains acyl chain rearrangements required for mismatch adaptation. This could be an essential, physiological function of cholesterol at the molecular level.

In the eukaryotic secretory pathway, TM proteins of different lengths get integrated in the cholesterol-poor—therefore adaptable—membranes of the endoplasmic reticulum (1). Indeed, cholesterol loading blocks this integration (32). In the Golgi apparatus the concentration of cholesterol increases and promotes the sorting of short TM domain-containing Golgi proteins and short lipids for recycling out of the forward membrane flow (33) that carries significantly longer TMD proteins together with long phospholipids and cholesterol to the plasma membrane (10).

More work is required to clarify how hydrophobic matching relates to (*i*) sphingolipid-cholesterol(raft)-based lateral heterogeneity and (*ii*) chemically specific protein–lipid interactions (34). Another open issue is whether moderate length differences between lipids and proteins paired with 40 mol% cholesterol in the plasma membrane influence protein and lipid distribution as well as the conformation of receptor proteins and channels (35). Because the segregation potential also scales with the square of the radius of the TM segment there are interesting implications for multihelix proteins/complexes as well as for ligand-induced lipid and protein clustering (9).

Altogether, our data provide a structural perspective on TM protein–lipid interactions in sterol-rich membranes with interesting biological implications for the function of cholesterol and the organization of the secretory pathway.

Material and Methods

Reagents. LW21($K_2W_2L_8AL_8W_2K_2$),FITC-LW21(FITC-$(CH_2)_2$-$K_2W_2L_8AL_8W_2K_2$), LW19 peptide ($K_2W_2L_7AL_7W_2K_2$), L17 ($AK_2L_8AL_8K_2A$), and TMR-LW29 (TMR-$K_2W_2L_{12}AL_{12}W_2K_2$) peptides (>98% purity) were obtained from Genscript. Phosphatidylcholines (PC), cholesterol (Chol), and lissamine rhodamine B-dioleoylphosphatidylethanolamine (Rh-DOPE) were from Avanti polar lipids Inc. C24:0/dC18:1-GM1 was purchased from Sandro Sonnino, University of Milan, Italy. Di-C12:0-GM1 was synthesized in the lab of Ten Feizi, Imperial College London. Methyl-beta-cyclodextrin (MBCD), Proteinase K, D-(+)-Trehalose, SDS, and silica TLC plates, and organic solvents were from Sigma-Aldrich. Dioctadecyl-tetramethyl-indodicarbocyanine (DiD), and Alexa-647-cholera toxin B (A647-CtxB) was purchased from Invitrogen. 6-dodecanoyl-2-N-methyl-N-carboxymethyl-aminonaphthalene (C-laurdan) was a kind gift from Bong-Rae Cho, Korea University of Seoul. For more details see *SI Text*.

Molecular Dynamics Simulations. We performed 500-ns atomistic molecular dynamics simulations for four systems consisting of a lipid bilayer with a transmembrane peptide. Two systems were single-component bilayers comprised of either di-16:1 or di-24:1 PC lipids, and two other systems were mixtures of these PC systems with 20 mol% cholesterol. The transmembrane peptide used in the studies was LW21 ($K_2W_2L_8AL_8W_2K_2$). Simulations were performed with GROMACS (36) using the OPLS force field (37). The model for the membrane part is based on earlier work (38), which also describes the simulation protocol. Details of the model and its validation, data analysis, and additional results are described in *SI Text*.

Preparation and Analysis of Large Unilamellar Vesicles (LUVs). LUVs were prepared according to Kalvodova et al. (39) with 3.0 mol% of the respective peptide in ethanol being added to the lipid mixture before drying, hydration, and extrusion. Proteinase K protection, Trp fluorescence readings, peptide thin layer chromatography (TLC), and C-laurdan spectroscopy was performed as described in *SI Text*.

Preparation and Cholesterol-Loading of Giant Unilamellar Vesicles (GUVs). GUVs were prepared according to Bacia et al. (40) with peptides in ethanol being added to the lipid mixture before drying and swelling as described in *SI Text*. Alternatively GUVs were swelled from LUVs as described in Kahya et al. (41). For cholesterol loading, Chol was complexed to MBCD and afterwards mixed with uncomplexed MBCD in 300 mM sucrose according to Mahammad et al. (23) as specified in *SI Text*. Extraction was performed with 1 mM MBCD. Fluorescent CtxB was added to GUVs at 1 μg/mL after preparation.

Fluorescence Microscopy and Image Analysis. For confocal microscopy of GUVs, a Zeiss LSM 510 inverted setup with the appropriate filters and a 63× and 100× OI objective was used. Imaging was performed at room temperature. All images were recorded in 8 bit format, normalized, and background corrected and

contrast enhanced. Quantification of peptide segregation was performed as described in *SI Text*.

ACKNOWLEDGMENTS. We thank Sebastian Günther for preparation of the Pymol LW models, Erwin London for the initial donation of LW21 peptide, Bong-Rae Cho for the C-laurdan sample, and the Simons Lab for helpful discussions. Computational resources were provided by the Finnish IT Centre for Science (CSC). The Academy of Finland is thanked for funding. This work was also supported by Deutsche Forschungsgemeinschaft (DFG) "Schwerpunktprogramm1175" Grant SI459/2-1, DFG "Transregio 83" Grant TRR83 TP02, Bundesministerium für Bildung und Forschung "ForMaT" Grant 03FO1212, European Science Foundation "LIPIDPROD" Grant SI459/3-1, and the Klaus Tschira Foundation (to K.S.).

1. Hessa T, et al. (2007) Molecular code for transmembrane-helix recognition by the Sec61 translocon. *Nature* 450:1026–1030.
2. Tanford C (1978) The hydrophobic effect and the organization of living matter. *Science* 200:1012–1018.
3. Ejsing CS, et al. (2009) Global analysis of the yeast lipidome by quantitative shotgun mass spectrometry. *Proc Natl Acad Sci USA* 106:2136–2141.
4. Sharpe HJ, Stevens TJ, Munro S (2010) A comprehensive comparison of transmembrane domains reveals organelle-specific properties. *Cell* 142:158–169.
5. Mouritsen OG, Bloom M (1984) Mattress model of lipid-protein interactions in membranes. *Biophys J* 46:141–153.
6. Huschilt JC, Millman BM, Davis JH (1989) Orientation of alpha-helical peptides in a lipid bilayer. *Biochim Biophys Acta* 979:139–141.
7. Schmidt U, Weiss M (2010) Hydrophobic mismatch-induced clustering as a primer for protein sorting in the secretory pathway. *Biophys Chem* 151:34–38.
8. Sperotto MM, Ipsen JH, Mouritsen OG (1989) Theory of protein-induced lateral phase separation in lipid membranes. *Cell Biophys* 14:79–95.
9. Lundbaek JA, Andersen OS, Werge T, Nielsen C (2003) Cholesterol-induced protein sorting: an analysis of energetic feasibility. *Biophys J* 84:2080–2089.
10. Bretscher MS, Munro S (1993) Cholesterol and the Golgi apparatus. *Science* 261:1280–1281.
11. de Planque MR, et al. (1998) Influence of lipid/peptide hydrophobic mismatch on the thickness of diacylphosphatidylcholine bilayers. A 2H NMR and ESR study using designed transmembrane alpha-helical peptides and gramicidin A. *Biochemistry* 37:9333–9345.
12. Ren J, Lew S, Wang Z, London E (1997) Transmembrane orientation of hydrophobic alpha-helices is regulated both by the relationship of helix length to bilayer thickness and by the cholesterol concentration. *Biochemistry* 36:10213–10220.
13. Webb RJ, East JM, Sharma RP, Lee AG (1998) Hydrophobic mismatch and the incorporation of peptides into lipid bilayers: A possible mechanism for retention in the Golgi. *Biochemistry* 37:673–679.
14. de Planque MR, et al. (2001) Sensitivity of single membrane-spanning alpha-helical peptides to hydrophobic mismatch with a lipid bilayer: Effects on backbone structure, orientation, and extent of membrane incorporation. *Biochemistry* 40:5000–5010.
15. Fastenberg ME, Shogomori H, Xu X, Brown DA, London E (2003) Exclusion of a transmembrane-type peptide from ordered-lipid domains (rafts) detected by fluorescence quenching: Extension of quenching analysis to account for the effects of domain size and domain boundaries. *Biochemistry* 42:12376–12390.
16. Lewis BA, Engelman DM (1983) Bacteriorhodopsin remains dispersed in fluid phospholipid bilayers over a wide range of bilayer thicknesses. *J Mol Biol* 166:203–210.
17. Killian JA, Nyholm TK (2006) Peptides in lipid bilayers: The power of simple models. *Curr Opin Struct Biol* 16:473–479.
18. Marsh D, Horvath LI (1998) Structure, dynamics and composition of the lipid-protein interface. Perspectives from spin-labelling. *Biochim Biophys Acta* 1376:267–296.
19. Lewis BA, Engelman DM (1983) Lipid bilayer thickness varies linearly with acyl chain length in fluid phosphatidylcholine vesicles. *J Mol Biol* 166:211–217.
20. Kaiser HJ, et al. (2009) Order of lipid phases in model and plasma membranes. *Proc Natl Acad Sci USA* 106:16645–16650.
21. Kim HM, et al. (2007) A Two-Photon Fluorescent Probe for Lipid Raft Imaging: C-Laurdan. *Chembiochem* 8:553–559.
22. Nezil FA, Bloom M (1992) Combined influence of cholesterol and synthetic amphiphilic peptides upon bilayer thickness in model membranes. *Biophys J* 61:1176–1183.
23. Mahammad S, Dinic J, Adler J, Parmryd I (2010) Limited cholesterol depletion causes aggregation of plasma membrane lipid rafts inducing T cell activation. *Biochim Biophys Acta* 1801:625–634.
24. Chai W, Stoll MS, Galustian C, Lawson AM, Feizi T (2003) Neoglycolipid technology: Deciphering information content of glycome. *Methods Enzymol* 362:160–195.
25. Niemela PS, et al. (2010) Membrane proteins diffuse as dynamic complexes with lipids. *J Am Chem Soc* 132:7574–7575.
26. Millhauser GL (1995) Views of helical peptides: A proposal for the position of 3(10)-helix along the thermodynamic folding pathway. *Biochemistry* 34:3873–3877.
27. Popot JL, Engelman DM (1990) Membrane protein folding and oligomerization: The two-stage model. *Biochemistry* 29:4031–4037.
28. Ren J, Lew S, Wang J, London E (1999) Control of the transmembrane orientation and interhelical interactions within membranes by hydrophobic helix length. *Biochemistry* 38:5905–5912.
29. Jahnig F (1981) Critical effects from lipid-protein interaction in membranes. II. Interpretation of experimental results. *Biophys J* 36:347–357.
30. Schafer LV, et al. (2011) Lipid packing drives the segregation of transmembrane helices into disordered lipid domains in model membranes. *Proc Natl Acad Sci USA* 108:1343–1348.
31. Weis RM, McConnell HM (1985) Cholesterol stabilizes the crystal-liquid interface in phospholipid monolayers. *J Phys Chem* 89:4453–4459.
32. Nilsson I, Ohvo-Rekila H, Slotte JP, Johnson AE, von Heijne G (2001) Inhibition of protein translocation across the endoplasmic reticulum membrane by sterols. *J Biol Chem* 276:41748–41754.
33. Brugger B, et al. (2000) Evidence for segregation of sphingomyelin and cholesterol during formation of COPI-coated vesicles. *J Cell Biol* 151:507–518.
34. Lingwood D, Simons K (2010) Lipid rafts as a membrane-organizing principle. *Science* 327:46–50.
35. Jensen MO, Mouritsen OG (2004) Lipids do influence protein function-the hydrophobic matching hypothesis revisited. *Biochim Biophys Acta* 1666:205–226.
36. Van Der Spoel D, et al. (2005) GROMACS: Fast, flexible, and free. *J Comput Chem* 26:1701–1718.
37. Jorgensen WL, Maxwell DS, Tirado-Rives J (1996) Development and testing of the OPLS all-atom force field on conformational energetics and properties of organic liquids. *J Am Chem Soc* 118:11225–11236.
38. Bjorkbom A, et al. (2010) Effect of sphingomyelin headgroup size on molecular properties and interactions with cholesterol. *Biophys J* 99:3300–3308.
39. Kalvodova L, et al. (2009) The lipidomes of vesicular stomatitis virus, semliki forest virus, and the host plasma membrane analyzed by quantitative shotgun mass spectrometry. *J Virol* 83:7996–8003.
40. Bacia K, Schwille P, Kurzchalia T (2005) Sterol structure determines the separation of phases and the curvature of the liquid-ordered phase in model membranes. *Proc Natl Acad Sci USA* 102:3272–3277.
41. Kahya N, Brown DA, Schwille P (2005) Raft partitioning and dynamic behavior of human placental alkaline phosphatase in giant unilamellar vesicles. *Biochemistry* 44:7479–7489.

III

STRONG PREFERENCES OF DOPAMINE AND L-DOPA TOWARDS LIPID HEAD GROUP: IMPORTANCE OF LIPID COMPOSITION AND IMPLICATION FOR NEUROTRANSMITTER METABOLISM

by

Orłowski, A., Grzybek, M., Bunker, A., Pasenkiewicz-Gierula, M., Vattulainen, I., Männistö, P.T., & Róg, T. 2012.

Journal of Neurochemistry vol. 122, 681-690

Strong preferences of dopamine and L-dopa towards lipid head group: Importance of phosphatidylserine and its implication for neurotransmitters metabolism

Adam Orłowski[1,2], Michał Grzybek[3], Alex Bunker[4,5], Marta Pasenkiewicz-Gierula[2], Ilpo Vattulainen[1,6], Pekka T. Männistö[7], and Tomasz Róg[1]*

[1]Department of Physics, Tampere University of Technology, P.O. Box 692, FI-33101, Finland
[2]Department of Computational Biophysics and Bioinformatics, Jagiellonian University, Krakow, Poland
[3]Max Planck Institute for Molecular Cell Biology and Genetics, Pfotenhauerstr. 108, 01307 Dresden, Germany
[4]Centre for Drug Research, Faculty of Pharmacy, University of Helsinki, P.O. Box 56, FI-00014, Finland
[5]Department of Chemistry, Aalto University, P.O. Box 1600, FI-00076, Espoo, Finland
[6]MEMPHYS–Center for Biomembrane Physics, University of Southern Denmark, Odense, Denmark
[7]Division of Pharmacology and Toxicology, Faculty of Pharmacy, University of Helsinki, Finland

KEYWORDS: Dopamine, L-dopa, lipid membrane, phosphatidylserine, neurotransmitters, molecular dynamics simulation

Running Title: Neurotransmitters and Membranes

ABSTRACT
The interactions of the neurotransmitter dopamine, and its precursor L-dopa with membrane lipids were investigated using atomistic molecular dynamics simulations. The results obtained indicate that dopamine and L-dopa both strongly interact with the lipid head groups, e.g. via hydrogen bonds. These interactions anchor the molecules to the interfacial region of the membrane. The strength of this bonding is dependent on lipid composition – the presence of phosphatidylserine leads to increased bonding strength with a lifetime much longer than the timescale of our simulations. The high membrane association of dopamine and L-dopa both, extracellularly, favours the availability of these compounds for cell membrane uptake processes and, intracellularly, accentuates the importance of membrane-bound metabolizing enzymes over their soluble counterparts.

Introduction

The synapse is a functional junction between two neurons, or between a neuron and a specialized cell, through which connected cells can communicate. There are essentially two types of synapses: an electrical synapse and a chemical synapse (Binder et al. 2008). The action of a chemical synapse is initiated by the depolarization of the pre-synaptic neuronal membrane that gives rise to a signal cascade, the final function of which is to release neurotransmitters from the pre-synaptic vesicle to the synaptic cleft. Neurotransmitters then diffuse thorough the synapse and bind to the receptor at the post-synaptic membrane, initiating an appropriate signal cascade, and thus the desired action of the post-synaptic cell. This intuitively simple process is essential for brain functioning. While a number of studies have been performed concerning synaptic vesicle fusion with the pre-synaptic membrane, exocytosis and signal transduction, relatively little progress has been made towards understanding of the interactions between neurotransmitters and other macromolecules present in the synapse including, for example, membranes. At the same time there is a good number of reasons to expect that such interactions are taking place.

Neurotransmitters can be short peptides, amino acids (glutamate, aspartate, serine, γ-aminobutyric acid, and glycine), monoamines (dopamine, norepinephrine, epinephrine, serotonin, melatonin) or some other small molecules (acetylcholine, adenosine, anandamide, histamine). In this study, we consider only dopamine and its precursor L-dopa, used in the treatment of Parkinson's disease (chemical structures of the molecules are shown in Figure S1, Supplementary Materials). Both molecules have a hydrophobic aromatic ring and, at neutral pH, a positively charged amine group, NH_3^+; L-dopa also has a negatively charged carboxyl group, COO^- (Fig. S1). Thus, the structure of dopamine and L-dopa is similar to that of aromatic amino acids that, when interacting with membranes have been shown to preferentially locate at the membrane-water interface (MacCallum et al. 2008) and in membrane proteins often occupy those positions on the protein surface that are located within the membrane-water interface (Ulmschneider et al. 2005). It is thus likely that dopamine and L-dopa are also predisposed to preferentially locate to the membrane interface. In the current literature there is only one very recent experimental and computer simulation study that investigates interactions with the lipid bilayer of four neurotransmitters: glutamate, acetylcholine, γ-aminobutyric acid and glycine (Wang et al. 2011). That study showed that interactions between the neurotransmitters and the membrane lipids strongly depended on the lipid type, the chemical structure of the neurotransmitter, and particularly, on the charge carried by the neurotransmitter (Wang et al. 2011). Although in this study we did not consider peptidic neurotransmitters, it is worth mentioning that enkephaline, a representative of peptidic neurotransmitters, was shown to bind to the membrane surface (Kimura 2006, Chandrasekhar et al. 2006).

The chemical structure of the discussed neurotransmitters resembles that of a variety of compounds used as anaesthetics. Anaesthetics are known to adsorb to the membrane surface, which is believed to modify the bilayer structure (Frangopol and Mihailescu 2001). It has been previously hypothesized that neurotransmitters affect membranes in a similar fashion; they locate in the membrane interface and change the properties of the membrane; this in turn desensitizes the membrane receptors, thus, in effect, neurotransmitters might act as anaesthetics (Cantor 2003).

In this work, we used atomistic molecular dynamics simulations to elucidate the interactions of dopamine and L-dopa with bilayers of varying lipid composition. We found that dopamine and L-dopa strongly interact with lipid head groups via hydrogen bonds and electrostatic interactions, which anchor the molecules to the membrane interfacial region. The strength of this binding depends on the lipid type; in particular phosphatidylserine stably binds both dopamine and L-dopa. The high membrane association of dopamine and L-dopa both, extracellularly, favours the availability of these compounds for cell membrane uptake processes and, intracellularly, accentuates the importance of membrane-bound metabolising enzymes over their soluble counterparts.

Methods

We performed atomistic molecular dynamics (MD) simulations of nine lipid bilayer systems; three of them contained dopamine, three L-dopa, and three were reference systems without

neurotransmitters. The bilayers had different lipid compositions. Three of them were composed of 128 molecules of dilineoylphosphatidylcholine (DLPC, di-18:2-DLPC; PC bilayer); three were composed of 48 sphingomyelin (SM), 48 dioleoylphosphatidylcholine (DOPC), and 32 cholesterol molecules (SM-PC-CHOL bilayer); and the remaining three contained a mixture of 44 DLPC, 60 dilineoylphosphatidylethanolamine (DLPE, di-18:2-PE) and 24 dilineoylphosphatidylserine (DLPS, di-18:2-PS, negatively charged) molecules (PC-PE-PS bilayer). The chemical structure of all studied molecules is shown in Fig. S1 (Supplementary Material). The systems were hydrated with 11500 water molecules, and in six of them 20 dopamine or L-dopa molecules were randomly inserted into the water phase. The interbilayer distance of ~8 nm was three times larger than the thickness of a layer of water commonly observed in multilamellar liposomes (up to 30 water per lipids compared to 90 in our studies) and provided a ~4 nm thick slab of water not affected/ordered by the interface. The initial velocities of atoms were assigned randomly, preserving the Maxwell-Boltzmann distribution for the selected temperature. 160 or 210-ns long MD simulations of each bilayer were performed using the GROMACS software package (Hess et al. 2008), and the OPLS all-atom force field (Jorgensen and Tirado-Rives 1988) was used to parameterize all molecules. For water, we employed the TIP3P model that is compatible with OPLS parameterization (Jorgensen et al. 1983). The system setup used in this study was identical to that used in our previous simulations of lipid bilayers with OPLS-AA parameterization (Stepniewski et al. 2010, Rog et al. 2007). Periodic boundary conditions with the usual minimum image convention were used in all three directions. The LINCS algorithm (Hess et al. 1997) was used to preserve the length of each hydrogen atom covalent bond. The time step was set to 2 fs and the simulations were carried out at a constant pressure (1 bar) and temperature (310 K). The temperature and pressure were controlled by the Parrinello-Rahman and Nosé-Hoover methods, respectively (Parrinello and Rahman 1981, Nose 1984). The temperatures of the solute and solvent were controlled independently. For pressure, we used a semi-isotropic control. The Lennard-Jones interactions were cut off at 1.0 nm, and for the electrostatic interactions we employed the particle mesh Ewald method (Essman et al. 1995) with a real space cutoff of 1.0 nm, beta-spline interpolation (order of 6), and direct sum tolerance of 10^{-6}.

The three lipid bilayers employed in this study were composed of the most common lipid types present in the animal cell membrane. One should, however, note that the composition of extracellular and intracellular leaflets of the cell membrane that we modelled actually differ; the former is predominantly composed of PCs, sphingomyelins and cholesterol, the latter of PC, PE, and PS (Maxfield and Mondal 2006). Thus, the SM-PC-CHOL bilayer serves as a model of the extracellular leaflet, and the PC-PE-PS bilayer as a model for the intracellular leaflet, in addition to the pre-synaptic vesicles (Takamori et al. 2006), in which neurotransmitters are enclosed in the synaptic region to be eventually released to the synaptic cleft. From the perspective of neurotransmitter metabolism (more details can be found in the Discussion section) the reticulum and outer mitochondrial membrane can also be seen as highly important. The reticulum is composed of PC, PE, and PS (van Meer et al. 2008), and in the mitochondrial membrane PS is replaced by cardiolipin (CL) (Hoviusa et al. 1993). Due to the similarity of the anionic nature of CL and PS we can expect that our model well reproduces the behaviour also of the mitochondrial membrane in respect of the studied properties.

As a model of the extracellular leaflet, we constructed two systems, one composed of unsaturated DLPC and one composed of a mixture of SM, CHOL, and DOPC. The latter choice reflects the current view on lateral structure of extracellular leaflets of the cell membrane where sphingolipids, saturated PCs, and cholesterol segregate into domains often called rafts (Simons and Ikonen 1997) in bulk membranes composed of unsaturated phosphatidylcholines. DLPC and DOPC were chosen because linoleic (L) and oleoic (O) chains are some of the most common unsaturated chains in glycerol based cellular lipids (Uran et al. 2001). The presence of DLPC or DOPC in the bilayers ensures that the bilayers are in the liquid-disordered phase.

In the aforementioned bilayers, the 20 molecules of dopamine and L-dopa correspond to ~100 mM concentration. This concentration might be considered high but as pointed out by Cantor (Cantor 2003), it reflects the condition present in the pre-synaptic vesicle where 5000-10000 neurotransmitter molecules are encapsulated in a vesicle having a diameter of the order of 40-50 nm, which results in the concentration of neurotransmitter of the order of 250 mM (Cantor 2003).

Equilibration of the bilayer systems required 60 or 100 ns of MD simulation. This time was determined by observing dopamine and L-dopa adsorption to the membrane interface, reflected in the number of hydrogen bonds that these molecules established with the lipids. The averaged (equilibrium) results have therefore been established from the trajectories between 60 and 160 ns or 100-210 ns.

The experimental part of this study was performed in a trough surrounded by a water jacket connected to a temperature controlled water bath. All measurements were done at 23°C. Monolayers were formed by spreading over a subphase (25 mM HEPES, 150 mM NaCl, pH 7.25) a chloroform solution of DOPC or DOPC/DOPE/DOPS (44/60/24). After evaporation of chloroform and stabilisation of the initial surface pressure ($\prod = 25 \pm 1.5$ mN/m), dopamine or L-dopa were injected into the subphase (final concentration of dopamine 70 μM). The changes in $\prod$ were recorded over the next 600 s. Phospholipids were purchased from Avanti Polar Lipids and dopamine and L-DOPA from Sigma.

Results

Snapshots showing the studied systems at the beginning and at the end (160 ns) of their MD trajectories are presented in Fig. 1. They clearly demonstrate that while at the beginning of the simulations all dopamine and L-dopa molecules were placed in the water phase, after 160 ns of simulations they tended to associate with the membrane surface. The observed effect is much stronger for L-dopa than dopamine and is stronger for the mixed PC-PE-PS bilayer and SM-PC-CHOL membrane than for the PC bilayer.

To more accurately illustrate the distribution of the dopamine and L-dopa molecules in the simulation box, we calculated density profiles of selected atoms and groups of atoms along the bilayer normal (Figure 2). Each plot in Fig. 2 shows the density profile of the dopamine or L-dopa atoms together with those of the lipid phosphate and nitrogen atoms, the latter to mark the borders of the bilayer/water interface. In all systems, the density profiles of dopamine and L-dopa atoms have clear peaks in the interfacial region, and those for L-dopa are higher than those for dopamine. In the PC bilayer, some fraction of dopamine and L-dopa molecules remained in the water phase while in the PC-PE-PS bilayer, where negatively charged PS was present, the number of the molecules in the water phase was negligible, indicating their stronger binding by the bilayer lipids. Similarly strong binding was observed in the raft forming mixture, where SM was present. We did not observe penetration of dopamine or L-dopa into the hydrocarbon core of the bilayer; however the dopamine was located deeper in the bilayer than L-dopa. A general conclusion that one can draw from the atomic density profiles shown in Fig. 2 is that dopamine and L-dopa associate with the lipid bilayer and the association is stronger with the bilayer containing the mixture of lipids, among them negatively charged PS (Fig. 1). Uneven distribution of dopamine and L-dopa between the two leaflets observed in PC-PE-PS system results from random features of the initial structure. As binding time was longer than simulation time, we did not observe an equilibrium distribution of binding between the two leaflets.

The dynamics of the association of dopamine and L-dopa with the bilayer is illustrated in Fig. 3, where we see the time profiles of the Z-coordinate (normal to the bilayer surface) of the centre-of-mass of selected molecules. In the PC bilayer, most of dopamine and L-dopa remained associated with the bilayer for a relatively short time, of the order of tens of nanoseconds. We were not able to obtain sufficient sampling of these events to quantitatively estimate the binding time. In the PC-PE-PS bilayer, once the system equilibrated, dopamine and L-dopa mostly remained associated with the bilayer interface. During the simulation time, there were only two cases when dopamine dissociated from the interface for a period shorter than 1 ns and there was no such a case for L-dopa. Once again, we were not able to obtain a quantitative estimate of the binding time. For the SM-PC-CHOL bilayer, we observed that the molecules attached to the bilayer surface. However, the time needed for their total attachment was longer than in case of the PC-PE-PS bilayer.

To measure the orientation of dopamine and L-dopa relative to the bilayer, we calculated the angle between the vector connecting atoms CB and CZ (see Fig. S1) and the bilayer normal. Average values of this angle as a function of the molecules' distance from the bilayer surface are shown in Fig. S4. When molecules are distant from the bilayer surface and their orientations are random, the

average value of the angle is 90°. When they approach the bilayer surface, they orient their NH_3 groups towards lipid headgroups. However, when they get deeper into the bilayer interface, they change their orientation, the aromatic rings pointing towards the hydrocarbon core, and the NH_3 groups towards the bulk water phase.

Figures 1 and S4 (Suppl. Material) indicate that dopamine and L-dopa interact with the bilayer differently. To identify the atomic level mechanisms responsible for this difference, we performed an analysis of the hydrogen (H) bonding network and other possible short-distance interactions between dopamine and L-dopa, and the lipids. Dopamine and L-dopa possess two hydroxyl groups, which can act both as H-bond donors and acceptors, and an amine group that, in the protonated state, can only act as a hydrogen donor. L-dopa additionally has a carboxyl group, which in the deprotonated state is an H-bond acceptor. The phosphate, carbonyl and ether groups of PC, PE, SM and PS are only H-bond acceptors. The amine group of PE and PS as well as the amide group of SM are H-bond donors, the carboxyl group of PS is additionally an H-bond acceptor, and the hydroxyl group of SM is both an H-bond donor and acceptor (see Fig. S1). PC and SM molecules can also participate in intermolecular charge pairing - electrostatic interactions between negatively charged oxygen atoms of a neurotransmitter molecule and positively charged methyl groups of the PC and SM choline moieties (Murzyn et al. 2001). Mutual interactions among these polar and charged groups are numerous, thus in the analysis below, only the total numbers of H-bonds between dopamine and L-dopa, and each lipid species are provided. More detailed data are given in Supplementary Materials.

The time developments of the number of hydrogen bonds between lipids, and dopamine and L-dopa are shown in Figure 4. As can be seen, the number of H-bonds stabilized after about 60 ns of MD simulation except of the SM-PC-CHOL bilayer where the number of H-bonds stabilizes after 100 ns. Average numbers of H-bonds obtained for trajectories between 60 and 160 ns or 100 and 210 ns are given in Figure 4. For the PC bilayer, the number of H-bonds between lipids and dopamine is 0.70±0.01 per dopamine and 0.91±0.01 per L-dopa. L-dopa also participates in 0.30±0.01 charge pairs with PC. These numbers largely explain the stronger and more stable binding of L-dopa with the PC bilayer. This result is in good agreement with existing experimental data, showing that the affinity of amino acid neurotransmitters to the lipids is higher than that for monoamine neurotransmitters (Wang et al. 2011).

In the PC-PE-PS bilayer, the number of hydrogen bonds between lipids and neurotransmitters is 3.3 per dopamine and 3.4 per L-dopa, i.e., much larger than in the PC bilayer. This explains a higher stability of the association of both molecules with the interface of this mixed-lipid bilayer. The number of hydrogen bonds between dopamine and each lipid species is ~1 per dopamine (Fig. S3), whereas L-dopa preferentially makes H-bonds with PE (Fig. S3). However, in these comparisons, one should remember that the number of lipid molecules of each type in the PC-PE-PS bilayer is different. The number of PS molecules is half the number of PC and 2/5 that of PE. This indicates that the affinities of both dopamine and L-dopa for PS are higher than those for PC and PE. Examples of dopamine and L-dopa H-bonded to different lipid head groups are shown in Fig. S2 (SM).

In the SM-PC-CHOL bilayer, the number of hydrogen bonds between lipids and neurotransmitters was found to be 3.0 per dopamine and 3.2 per L-dopa, i.e., much larger than in the PC bilayer and slightly lower than in the PC-PE-PS bilayer (Fig. 4). The number of hydrogen bonds of L-dopa with PC and SM was similar, whereas dopamine interacted with PC more favourably (Fig. S3). Interestingly, the number of direct interactions between neurotransmitter and cholesterol was negligible as a result of the relatively deep location of the cholesterol hydroxyl group and its strong interaction with phospholipids (Róg et al. 2009).

To investigate the effect of dopamine and L-dopa on the bilayer properties we calculated standard parameters such as the surface area per lipid molecule, the bilayer thickness (using the so-called P-P distance as a measure for the thickness), and the deuterium order parameter S_{cd} of the *sn*-1 acyl chain. All data are presented in Supplementary Material (Tables S3 and S4, Fig. S5). First, our results indicate the lack of any neurotransmitter-induced changes in in the SM-PC-CHOL bilayer. This should not come as a surprise since this bilayer is the most rigid due to the presence of cholesterol (Róg et al. 2009). Secondly, dopamine, while bonded to the PC or PC-PE-PS bilayers

increases the area per lipid. This change is also manifested in a drop of the bilayer thickness clearly observed in the PC bilayer (in the PC-PE-PS bilayer, a drop of the thickness is in the error range) as well as in a drop of the order parameter observed in the PC-PE-PS bilayer (Fig. S5). Thirdly, L-dopa practically does not change the area per lipid, though the thickness of the PC-PE-PS bilayer is higher. Changes in the order parameter for the segments located closest to the interface can be seen for the case of the PC-PE-PS bilayer. As the observed changes are relatively small, we additionally calculated the profile of the lateral pressure throughout the bilayer (Fig. S6). The changes in the profiles are evident only in the PC-PE-PS bilayer, in particular when dopamine is present, but they are not large.

Summarizing our observations of the effect of dopamine and L-dopa on the bilayer properties, we can say that changes of the properties are not large but they are consistent and depend on the lipid composition of the bilayer. Cholesterol seems to play a significant role in preserving the bilayer properties. Importantly, even though dopamine interacts with the lipids less strongly than is the case of L-dopa, it can still exert a greater effect. This results from the fact that it can be located deeper in the bilayer (Fig. 2), and in addition it is positively charged while L-dopa is neutral. Thus, the binding of dopamine leads to an accumulation of positive charge at the interface, which causes expansion of the bilayer surface. This effect is also present in the PC-PE-PS bilayer even though PS bears a negative charge; this charge is however neutralized by counter ions adsorbed at the bilayer interface (Zhao et al. 2007).

To confirm our predictions, a simple biochemical experiment was performed that involved measurements of the interactions of dopamine and L-dopa with lipids forming a monolayer. This technique allows for the monitoring of changes in surface pressure ($\prod$) that indicate whether or not the studied compounds have any affinity for the lipids. For both dopamine and L-dopa no changes in $\prod$ were observed when the monolayer was formed only of DOPC. This suggests that the compounds did not interact with the lipids. Consistent changes in the value of $\prod$ were, however, observed when either dopamine or L-dopa were added to the monolayers formed of DOPC/DOPE/DOPS, with the effect being slightly stronger for L-dopa ($\Delta\prod = 0.31$) than for dopamine ($\Delta\prod = 0.25$) (see Fig. 5). This could result from the difference of the extent to which they penetrate the monolayer, as described above. Our experimental results thus fully support the results obtained in MD simulations that dopamine and L-dopa affect the properties of the PC-PE-PS bilayer but not those of the PC bilayer.

Discussion

In this study, we have shown, through a combination of computational and experimental investigation that the neurotransmitter dopamine and its precursor L-dopa readily associate with the investigated lipid bilayers. This association strongly depends on the lipid composition of the bilayer. In the mixed-lipid bilayer, which includes anionic phosphatidylserine, we observed a complete adsorption of dopamine and L-dopa at the bilayer surface. However, adsorption at the surface of the mono-lipid PC bilayer was incomplete. Similar observations have been recently made experimentally for other neurotransmitters including glutamate, *γ*-aminobutyric acid, and glycine (Wang et al. 2011). Meanwhile, association of small molecules of similar structure with a bilayer is a well-known phenomenon (Lee et al. 2005). Our study additionally revealed that both dopamine and L-dopa interact via weak short-range interactions (H-bonds and charge pairs) with polar and charged groups of the bilayer lipids. Hydrogen bonds were formed mainly with lipid phosphate oxygen atoms and less frequently with lipid carbonyl groups. Binding with carbonyl groups, which are located deeper in the bilayer than phosphate groups, is more frequent for dopamine, which locates a bit deeper in the bilayer than L-dopa. Both hydroxyl and amine groups of dopamine and L-dopa participate in H-bonding, though the pattern of these bonds is specific for each bilayer and the lipid type. For the mixed PC-PE-PS membranes**,** we observed a clear preference for interactions with PS. Binding of dopamine and L-dopa to the SM-PC-CHOL bilayer is also relatively strong (Fig. 4). This strong binding may be associated with a larger separation of lipid headgroups due to the cholesterol spacing effects (Róg et al. 2009) as interactions of neurotransmitters with SM and PC are comparable. Similar non-specific effects of cholesterol on carbohydrate headgroups binding with the membrane surface were observed for the case of ganglioside GM3 headgroups (Lingwood et al.

2011).

Alterations of lipid composition and lipid metabolism have been observed in several neurodegenerative diseases (Adibhatla and Hatcher 2007, Adibhatla et al. 2006, Fenton et al. 2000). In a post-mortem study of the brain lipids, it was shown that in schizophrenic patients the level of PC, sphingomyelin, and galactocerebrosides are decreased while phosphatidylserine level is increased (Schmitt et al. 2004, Harrison and Weinberger 2005). This observation can be linked with our observations concerning dopamine and L-dopa adsorption to the membrane surface when phosphatidylserine is present in the membrane. We can thus hypothesize that excessive association of dopamine and its precursor L-dopa with membranes of increased phosphatidylserine content may eventually limit the free use of dopamine as a synaptic transmitter. And further, we can speculate that this could possibly be a molecular level mechanism responsible for some of neurodegenerative disorders.

A majority of antidepressants are designed to increase the level of neurotransmitters in the brain by inhibiting reuptake of neurotransmitters or inhibiting their catabolism (Binder et al. 2008). Association of catecholamines with the neural cell membrane and pre-synaptic vesicles might, in the first place, be a possible mechanism for depressive disorders, and also impede the effectiveness of L-dopa as an antiparkinsonian drug.

Links between cholesterol and depressive disorders have also been found to exist. For example, a low level of cholesterol in the blood has been correlated with certain depressive behaviours and suicidal ideation, and cholesterol has been clearly documented as one of the necessary membrane lipids in the synapses (Barres and Smith 2001, Koudinov and Koudinova 2001). The effect of membrane cholesterol on the association of dopamine and L-dopa with lipid bilayers is a subject of our on-going study. Though, we would like to add that the relationship between cholesterol level in the plasma blood and the brain tissue composition and thus the aforementioned mental disorders, is known to be complex (Ponizovsky et al. 2003), and this remains an open question.

This computer simulation study originated from our interest in catechol-O-methyltransferase (COMT) that is responsible for the inactivation of catechols, including L-dopa and the neurotransmitters dopamine, noradrenaline, and adrenaline (Mannisto and Kaakkola 1999). COMT has, in addition to the free soluble isoform (S-COMT), a membrane bound form (MB-COMT) (Mannisto and Kaakkola 1999). The catalytic domain of both forms is identical, and the structural difference is limited to the single trans-membrane helical fragment and the linker that connects the catalytic domain (the entire S-COMT structure) to the trans-membrane helix. This fact leads, however, to a significant difference in the enzyme kinetics of the two isoforms.

To discuss the importance of the membrane affinities of L-dopa and dopamine, it is necessary to consider how these compounds are synthesized and metabolized, and what role the interaction with the membrane plays in these processes (Siegel et al. 2005, Iversen et al. 2009, Männistö et al. 1992). Synthesis and metabolism of L-dopa and catecholamines occur only intracellularly. Dopamine is synthesized in the cytoplasm of catecholaminergic neurons from where it is rapidly and effectively stored inside the storage vesicle where can be further metabolized to noradrenaline. Enzymes metabolising dopamine include: MB-COMT and UDP-glucurosyltransferase (UTG), both located in the rough endothelial reticulum (RER), the former facing into the vesicles (Ulmanen et al. 1997) and the latter into the cytoplasm (Finel and Kurkela 2008), monoamine oxidases (MAO-A and MAO-B), located at the outer membrane of mitochondria facing towards the cytoplasm (Binda et al. 2004) and S-COMT and sulphotransferase (SULT) located in the cytoplasm; S-COMT also exists in cell nucleus (Ulmanen et al. 1997, Itäaho et. al. 2009).

Chronologically, the metabolism proceeds as follows (for reviews see: Iversen et al. 2009, Männistö et al. 1992, Kopin 1985): if dopamine and noradrenaline fail to enter the storage vesicles after their cytoplasmic synthesis, both will be metabolized by MAO-A, or, to a lesser extent, by SULT. In contrast, COMT is not present in presynaptic nerves (Rivett et al. 1983, Kaakkola et al. 1987). After being released by an action potential from the vesicles, diffused to and dissociated from their postsynaptic receptors, most of the amines are rapidly and effectively taken up to their own presynaptic nerve endings via specialized transporters where the same metabolic enzymes are waiting. Alternatively, dopamine may enter neighboring glial cells or postsynaptic neurons. Inside

either cell type, MAO-B (or MAO-A), MB-COMT, S-COMT, SULT or UTG, are all able to metabolize the amine. Which enzyme is acting first, depends on several factors but at physiological conditions the ranking order in the human brain is as follows: MB-COMT, MAO-A, MAO-B, PST = S-COMT for noradrenaline, and MAO-A, MAO-B = MB-COMT, PST = S-COMT for dopamine (Roth 1992).

Although the results of our simulations of plasma and intracellular membrane models are clear, their biological implications remain hypothetical. Considering the different intracellular membrane associations of catecholamine synthesizing and metabolizing enzymes, some conclusions are however possible. Since MAO-A and MAO-B are facing the cytosolic side (Binda et al. 2004, Edmondson et al. 2004), it is natural that MAO is favoured as a first-line metabolizer of dopamine if this neurotransmitter has a high affinity for mitochondrial type membranes. Since MB-COMT faces the interior of the RER vesicles (Ulmanen et al. 1997), it is inferior to MAO. A favourable location of UTG in the RER, facing outside (Finel and Kurkela 2008), is hampered by its low affinity for dopamine at a low millimolar range; (Itäaho et al. 2007), and therefore its role comes only after MAO and COMT.

Since all catechol-metabolizing enzymes are intracellular, the membrane affinity of the substrates is important. In all cases, the transport of dopamine and L-dopa is supported by their avidity to membrane lipids of the plasma membranes that causes an abundant presence of dopamine and L-dopa in the vicinity of the transporter proteins. As a general biochemical conclusion it can be said that the high membrane association of dopamine and L-dopa clearly favours both, extracellularly, the availability of these compounds for cell membrane uptake processes and, intracellularly, accentuates the importance of membrane-bound metabolising enzymes over soluble enzymes.

The results of the present study together with previous theoretical and experimental investigations of anaesthetics (Jerabek et al. 2010) can suggest an additional function of MB-COMT and other membrane bond enzymes: protecting the membrane from the physical changes that can be induced by small amphipathic molecules strongly adsorbed at the water-membrane interface. Evidence that anaesthetics, alcohols and other similar small molecules affect membrane properties exist in the literature (Terämä et al. 2008, Patra et al. 2006). Here of special interest is the profile of the lateral pressure through the membrane (Ollila et al. 2007, Niemelä et al. 2007, Xing et al. 2009). It has been demonstrated that changes in the lateral pressure can facilitate changes of the state of an ion channel from open to closed (Ollila et al. 2011). Since all cellular membranes are hosts to numerous proteins and their properties are strictly regulated (van Meer et al. 2008), the presence of enzymes protecting the membranes of specialized cells from effects of e.g. neurotransmitters can reasonably be expected. Our results for the effects of dopamine on the PC-PE-PS bilayer properties (ordering, thickness, surface area, and lateral pressure profile) are in full agreement with this picture.

ACKNOWLEDGMENT: We thank the Academy of Finland (TR, IV) and the Erasmus program for their financial support. We also wish to thank the Finnish IT Centre for Scientific Computing for computer resources.

SUPPLEMENTARY MATERIAL: Additional material includes pictures of molecular structures, snapshots of dopamine and L-dopa interacting with lipids, and a table summarizing the number of hydrogen bonds between the different molecules in a system.

REFERENCES

Adibhatla R. M. and Hatcher J. F. (2007) Role of lipids in brain injury and diseases. Fut. Lipidol. 2, 403-422.

Adibhatla R. M., Hatcher J. F. and Dempsey R. J. (2006) Lipids and lipidomics in brain injury and diseases. AAPS J. 8, 314-321.

Barres B. A. and Smith S. J. (2001) Cholesterol making or breaking synapse? Science 294, 1296-1297.

Binda C., Hubálek F., Li M., Edmondson D. E. and Mattevi A. (2004) Crystal structure of human monoamine oxidase B, a drug target enzyme monotopically inserted into the mitochondrial outer membrane. FEBS Lett. 564, 225-228.

Binder M. D., Hirokawa N. and Windhorst U. (2008) Encyclopedia of Neuroscience. 1st ed. Springer, Berlin, Heidelberg.

Cantor R. S. (2003) Receptor desensitization by neurotransmitters in membranes: are neurotransmitters the endogenous anesthetics? Biochemistry 42, 11891-11897.

Chandrasekhar I., van Gunsteren W. F., Zandomeneghi G., Williamson P. T. F. and Meier B. H. (2006) Orientation and Conformational Preference of Leucine-Enkephalin at the Surface of a Hydrated Dimyristoylphosphatidylcholine Bilayer: NMR and MD Simulation. J. Am. Chem. Soc. 128, 159–170.

Edmondson D. E., Mattevi A., Binda C., Li M. and Hubálek F. (2004) Structure and mechanism of monoamine oxidase. Curr. Med. Chem. 11, 1983-1993.

Essman U., Perera L., Berkowitz M. L., Darden H. L. T. and Pedersen L. G. (1995) A smooth particle mesh Ewald method. J. Chem. Phys. 103, 8577-8592.

Fenton W. S., Hibbeln J. and Knable M. (2000) Essential fatty acids, lipid membrane abnormalities, and the diagnosis and treatment of schizophrenia. Biol. Psych. 47, 8-21.

Finel M. and Kurkela M. (2008) The UDP-glucuronosyltransferases as oligomeric enzymes. Curr Drug Metab. 9, 70-6.

Frangopol P. T. and Mihailescu D. (2001) Interactions of some local anesthetics and alcohols with membranes. Coll. Surf. B. 22, 3-22.

Harrison P. J. and Weinberger D. R. (2005) Schizophrenia genes, gene expression, and neurophatology: on the matter of their convergence. Mol. Psych. 10, 40-68.

Hess B., Bekker H., Berendsen H. J. C. and Fraaije J. G. E. M.. (1997) LINCS: A linear constraint solver for molecular simulations. J. Comput. Chem. 18, 1463-1472.

Hess B., Kutzner C., van der Spoel D. and Lindahl E. (2008) GROMACS 4: Algorithms for highly efficient, load-balanced, and scalable molecular simulation. J. Chem. Theory. Comput. 4, 435-447.

Hoviusa R., Thijssen J. C., van der Linden P. and de Kruijff K. N. B. (1993) Phospholipid asymmetry of the outer membrane of rat liver mitochondria. Evidence for the presence of cardiolipin on the outside of the outer membrane. FEBS Letter 330, 71-76.

Humphrey W., Dalke A. and Schulten K. (1996) VMD - Visual Molecular Dynamics. J. Molec. Graphics 14, 33-38.

Itäaho K., Alakurtti S., Yli-Kauhaluoma J., Taskinen J., Coughtrie M. W. and Kostiainen R. (2007) Regioselective sulfonation of dopamine by SULT1A3 in vitro provides a molecular explanation for the preponderance of dopamine-3-O-sulfate in human blood circulation. Biochem. Pharmacol. 74, 504-510.

Itäaho K., Court M. H., Uutela P., Kostiainen R., Radominska-Pandya A. and Finel M. (2009) Dopamine is a low-affinity and high-specificity substrate for the human UDP-glucuronosyltransferase 1A10. Drug Metab. Dispos. 37, 768-775.

Jerabek H., Pabst G., Rappolt M. and Stockner T. (2010) Membrane-mediated effect on ion channels induced by the anesthetic drug ketamine. J. Am. Chem. Soc. 132, 7990-7997.

Iversen L., Iversen S., Bloom F. E. and Roth R. H. (2009) Introduction to Neuro psychopharmacology, Oxford University Press, New York, USA.

Jorgensen W. L., Chandrasekhar J., Madura J. D., Impey R. and Klein M. L. (1983) Comparison of simple potential functions for simulating liquid water. J. Chem. Phys. 79, 926-935.

Jorgensen W. L. and Tirado-Rives J. (1988) The OPLS potential functions for proteins: energy minimization for crystals of cyclic peptides and crambin. J. Am. Chem. Soc. 110, 1657-1666.

Kaakkola S., Männistö P. T. and Nissinen E. (1987) Striatal membrane-bound and soluble catechol-O-methyltransferase after selective neural lesions in the rat. J. Neural. Transm. 69, 221-228.

Kimura T. (2006) Human opioid peptide Met-enkephalin binds to anionic phosphatidylserine in high preference to zwitterionic phosphatidylcholine: Natural-abundance 13C NMR study on the binding state in large unilamellar vesicles. Biochemistry. 45, 15601-15609.

Kopin I. J. (1985) Catecholamine metabolism: basic aspects and clinical significance. Pharmacol. Rev. 37, 333-364.

Koudinov A. R. and Koudinova N. V. (2001) Essential role for cholesterol in synaptic plasticity and degeneration. Faseb. J. 15, 1858.

Lee B. W., Faller R., Sum A. K., Vattulainen I., Patra M. and Karttunen M. (2005) Structural effects of small molecules on phospholipid bilayers investigated by molecular simulations. Fluid Phase Equilib. 228, 135-140.

Lingwood D., Binnington B., Róg T., Vattulainen I., Grzybek M., Coskun Ü., Lingwood C. A. and Simons K. (2011) Cholesterol modulates glycolipid conformation and receptor activity. Nature Chem. Biol. 7, 260-262.

MacCallum J. L., Bennett W. F. D. and Tieleman D. P. (2008) Distribution of amino acids in a lipid bilayer from computer simulations. Biophys. J. 94, 3393-3404.

Mannisto P. T. and Kaakkola S. (1999) Catechol-O-methyltransferase (COMT): biochemistry, molecular biology, pharmacology, and clinical efficacy of the new selective COMT inhibitors. Pharm. Rev. 51, 593-628.

Männistö P. T., Ulmanen I., Lundström K., Taskinen J., Tenhunen J., Tilgmann C. and Kaakkola S.

(1992) Characteristics of catechol O-methyltransferase (COMT) and properties of selective COMT inhibitors. Prog. Drug. Res. 39, 291-350.

Maxfield F. R. and Mondal M. (2006) Sterol and lipid trafficking in mammalian cells. Biochem. Soc. Trans. 34, 335-339.

van Meer G., Voelker D. R. and Feigenson G. W. (2008) Membrane lipids: where they are and how they behave. Nature Rev. Mol. Cell Biol. 9, 112-124.

Murzyn K., Róg T., Jezierski G., Kitamura K. and Pasenkiewicz-Gierula M. (2001) Effects of phospholipid unsaturation on the membrane/water interface: a molecular simulation study. Biophys. J. 81, 170-183.

Niemelä P. S., Ollila S., Hyvönen M. T., Karttunen M. and Vattulainen I. (2007) Assessing the nature of lipid membranes. PLoS Comput. Biol. 3, 304-312.

Nose S. (1984) A unified formulation of the constant temperature molecular dynamics methods. J. Chem. Phys. 81, 511-519.

Ollila O. H. S., Louhivuori M., Marrink S. J. and Vattulainen I. (2011) Protein shape change has a major effect on the gating energy of a mechanosensitive channel. Biophys. J. 100, 1651-1659.

Ollila O. H. S., Róg T., Karttunen M. and Vattulainen I. (2007) Role of sterol type on lateral pressure profiles of lipid membranes affecting membrane protein functionality: Comparison between cholesterol, desmosterol, 7-dehydrocholesterol and ketosterol. J. Struc. Biol. 159, 311-323.

Parrinello M. and Rahman A. (1981) Polymorphic transitions in single crystals: A new molecular dynamics method. J. Appl. Phys. 52, 7182-7190.

Patra M., Salonen E., Terämä E., Vattulainen I., Faller R., Lee B. W., Holopainen J. and Karttunen M. (2006) Under the influence of alcohol: The effect of ethanol and methanol on lipid bilayers. Biophys. J. 90, 1121-1135.

Ponizovsky A. M., Barshtein G. and Bergelson L. D. (2003) Biochemical alterations of erythrocytes as an indicator of mental disorders: An overview. Harvard Rev. Psych. 11, 317-332.

Róg T., Bunker A., Vattulainen I. and Karttunen M. (2007) Effect of glucose and galactose headgroup on lipid bilayer properties. J. Phys. Chem. B 111, 10146-10154.

Róg T., Pasenkiewicz-Gierula M., Vattulainen I. and Karttunen M. (2009) Ordering effects of cholesterol and its analogues. Biochim. Biophys. Acta. 1788, 97-121.

Rivett A. J., Francis A. and Roth J. A. (1983) Distinct cellular localization of membrane-bound and soluble forms of catechol-O-methyltransferase in brain. J. Neurochem. 40, 215-219.

Roth J. A. (1992) Membrane-bound catechol-O-methyltransferase: a reevaluation of its role in the O-methylation of the catecholamine neurotransmitters. Rev. Physiol. Biochem. Pharmacol. 120, 1-29.

Schmitt A., Wilczek K., Blennow K., Maras A., Jatzko A., Petroianu G., Braus D. F. and Gattaz W. F. (2004) Altered thalamic membrane phospholipids in schizophrenia: a postmortem study. Biol. Psych. 56, 41-45.

Siegel G. M. D., Albers R. W., Brady S. and Price D. (2005) Basic Neurochemistry, 7th Edition:

Molecular, Cellular and Medical Aspects, Elsevier Academic Press, London, UK.

Simons K. and Ikonen E. Functional rafts in cell membranes. (1997) Nature 387, 569-572.

Stepniewski M., Bunker A., Pasenkiewicz-Gierula M., and Karttunen M. and Róg T. (2010) Effects of the lipid bilayer phase state on the water membrane interface. J. Chem. Phys. B 114, 11784-11792.

Takamori S., Holt M., Stenius K., Lemke E. A., Grønborg M., Riedel D., Urlaub H., Schenck S., Brügger B., Ringler P., Müller S. A., Rammner B., Gräter F., Hub J. S., De Groot B. L., Mieskes G., Moriyama Y., Klingauf J., Grubmüller H., Heuser J., Wieland F. and Jahn R. (2006) Molecular Anatomy of a Trafficking Organelle. Cell 127, 671-673.

Terämä E., Ollila O. H. S., Salonen E., Rowat A. C., Trandum C., Westh P., Patra M., Karttunen M. and Vattulainen I. (2008) Influence of ethanol on lipid membranes: From lateral pressure profiles to dynamics and partitioning. J. Phys. Chem. B 112, 4131-4139.

Ulmanen I., Peränen J., Tenhunen J., Tilgmann C., Karhunen T., Panula P., Bernasconi L., Aubry J. P. and Lundström K. (1997) Expression and intracellular localization of catechol O-methyltransferase in transfected mammalian cells. Eur. J. Biochem. 243, 452-459.

Ulmschneider M. B., Sansom M. S. P. and Di Nola A. (2005) Properties of integral membrane protein structures: derivation of an implicit membrane potential. Proteins 59, 252-265.

Uran S., Larsen A., Jacobsen P. B. and Skotland T. (2001) Analysis of phospholipid species in human blood using normal-phase liquid chromatography coupled with electrospray ionization ion-trap tandem mass spectrometry. J. Chromatogr. B Biomed. Sci. Appl. 758, 265–275.

Wang C., Ye F., Valardez G. F., Peters G. H. and Westh P. (2011) Affinity of four polar neurotransmitters for lipid bilayer membranes. J. Phys. Chem. B 115, 196-203.

Xing C. Y., Ollila O. H. S., Vattulainen I. and Faller R. (2009) Asymmetric nature of lateral pressure profiles in supported lipid membranes and its implications for membrane protein functions. Soft Matter 5, 3258-3261.

Zhao W., Róg T., Gurtovenko A. A., Vattulainen I. and Karttunen M. (2007) Structure and electrostatics of POPG lipid bilayers with Na^+ counterions: Molecular dynamics simulation. Biophys. J. 92, 1114-1124.

Figure legends

Figure 1. Snapshots showing simulated systems (a, c, e, g) at the beginning, and (b, d, f, h) at the end of simulations. (a, b, c, d) Dopamine molecules are shown in blue, and (e, f, g, h) L-dopa molecules in red. Lipid molecules depicted here are (c, d, g, h) DLPC and (a, b, e, f) DLPC-DLPE-DLPS. Water is not shown for clarity. Snapshots were prepared using the VMD package (51).

Figure 2. Density profiles of (a, b) L-dopa and (c, d) dopamine (black line), lipids' nitrogen (blue line), lipids' phosphate (pink line), and all lipid atoms (red line). Data corresponds to (a, c) DLPC and (b, d) DLPC-DLPE-DLPS bilayers. Position of the lipid bilayer is shown schematically.

Figure 3. Trajectories of centre of mass of (a, c) dopamine and (b, d) L-dopa in (a, b) PC and (c, d) PC-PE-PS bilayers of selected molecules. Each molecule is represented by different color.

Figure 4. (a) Time development of the number of hydrogen bonds between lipids and dopamine in PC bilayer (black line) and in PC-PE-PS bilayer (green line), and between lipids and L-dopa in PC bilayer (red line) and in PC-PE-PS bilayer (blue line). (b) Similar data between dopamine and PC (black line), PE (green line), PS (red line) in a mixed bilayer, and (c) between L-dopa and PC (black line), PE (green line), PS (red line) in a mixed bilayer. Horizontal dashed lines indicate equilibrium averages. Numbers are given per dopamine or L-dopa molecules.

Figure 5. (a) Examples of changes in surface pressure induced by dopamine or L-dopa on monolayers composed of DOPC or DOPC/DOPE/DOPS. (b) Average changes in Π observed after 600 s of addition of either dopamine or L-dopa to the monolayers (n=3).

Figure 1.

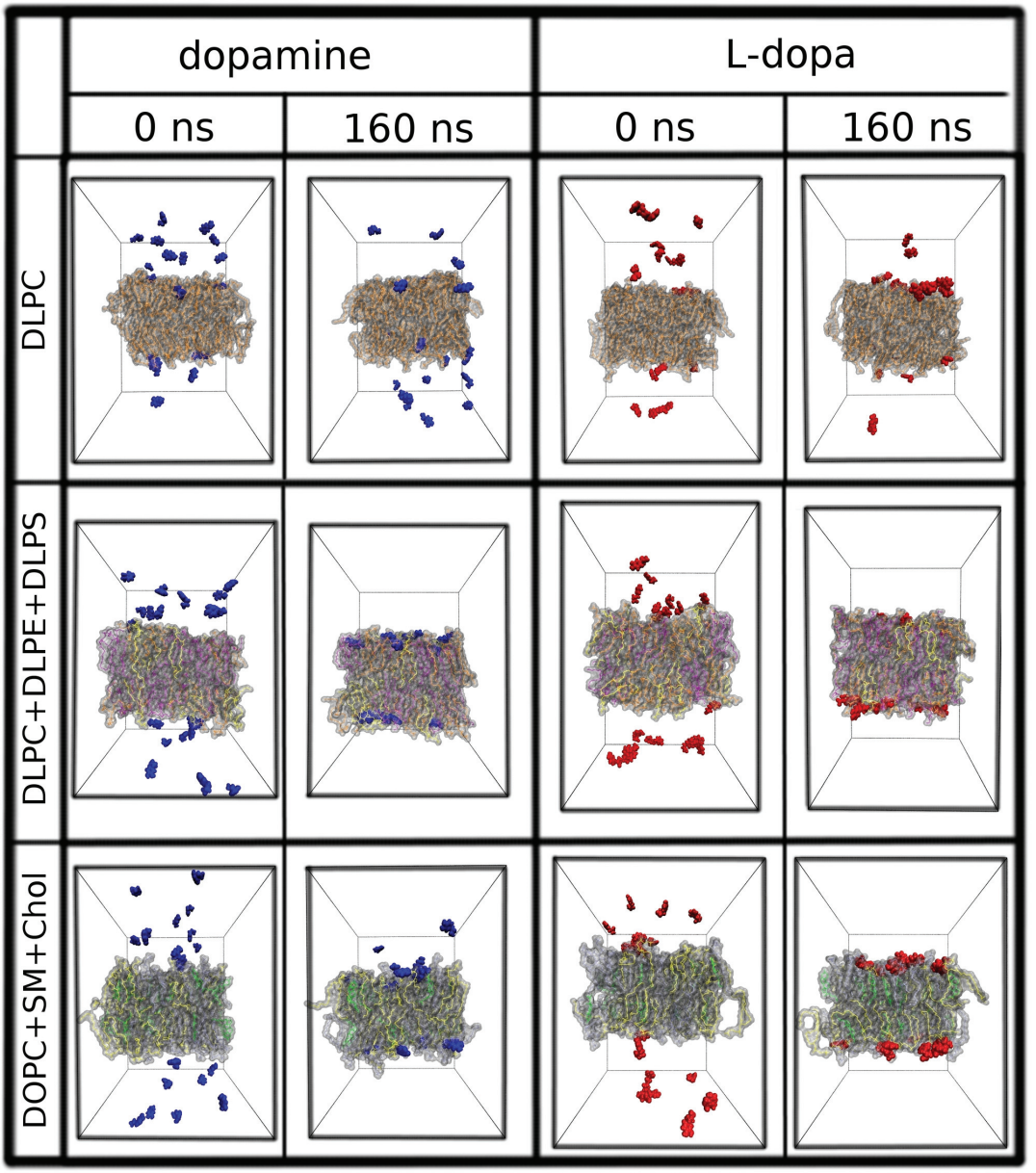
dopamine
L-dopa
0 ns
160 ns
0 ns
160 ns
DLPC
DLPC+DLPE+DLPS
DOPC+SM+Chol

Figure 2.

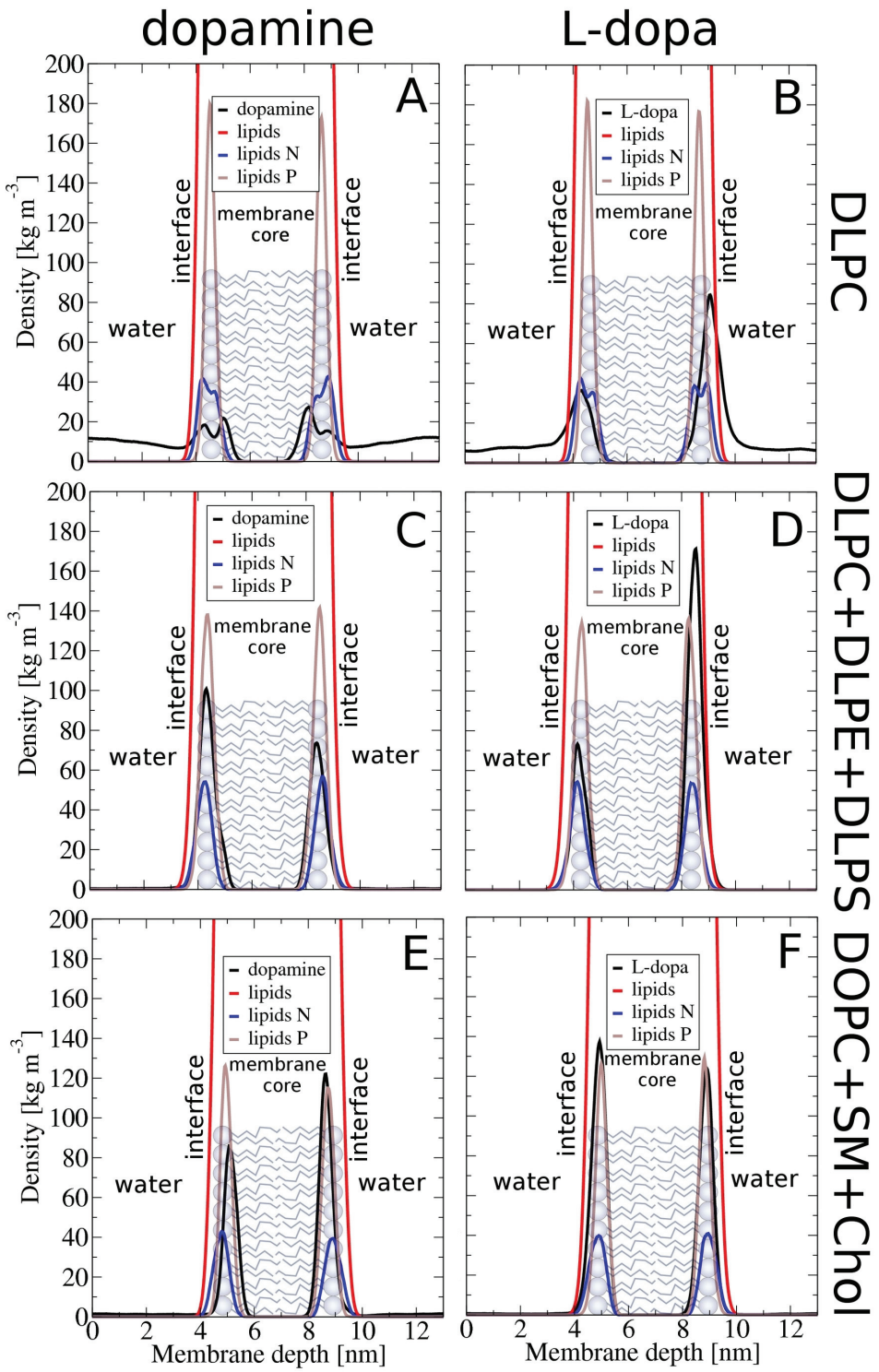
dopamine
L-dopa
DLPC
DLPC+DLPE+DLPS DOPC+SM+Chol
A
B
C
D
E
F
dopamine
L-dopa
lipids
lipids N
lipids P
membrane core
interface
water
Density [kg m^{-3}]
Membrane depth [nm]

Figure 3.

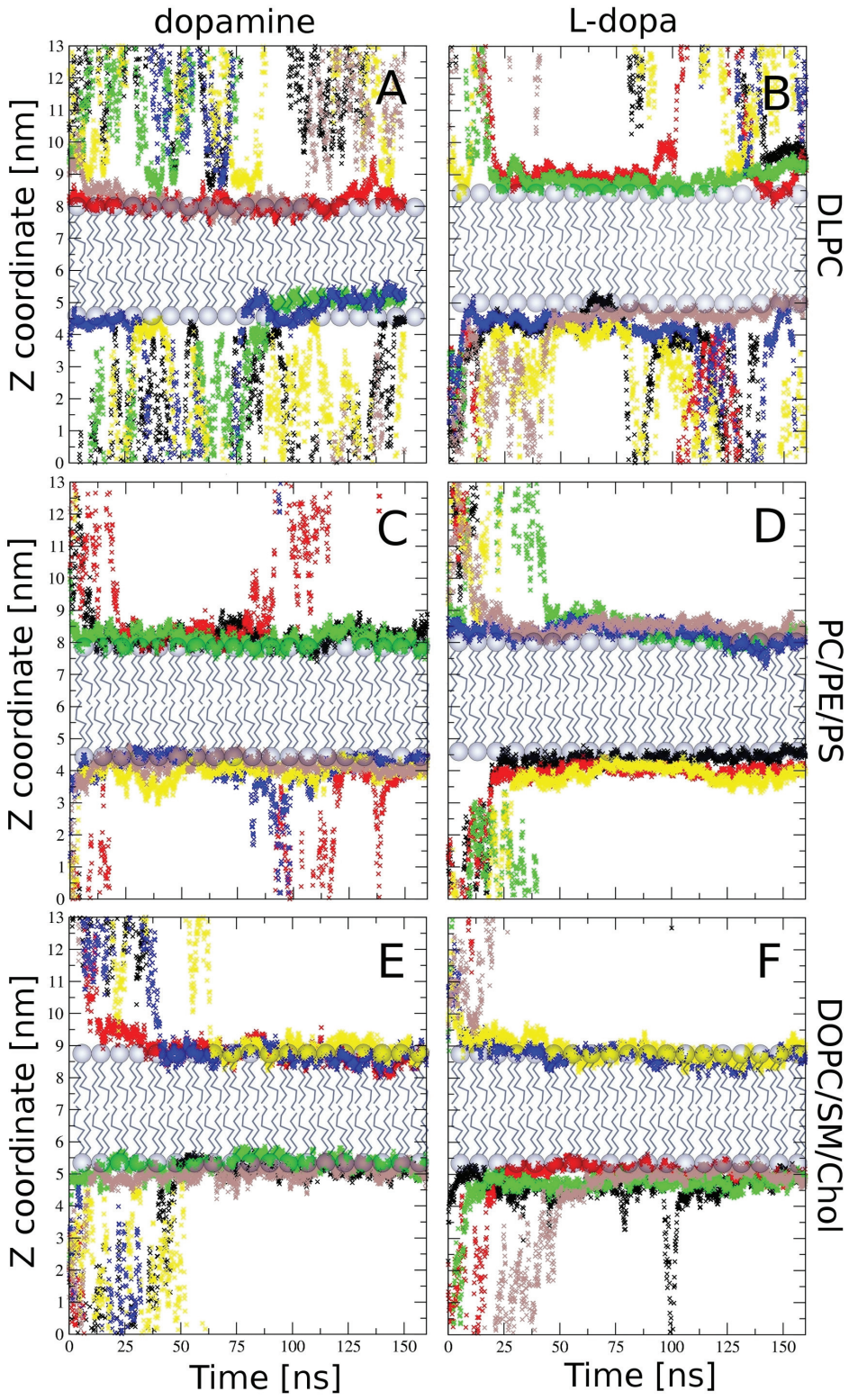

Figure 4.

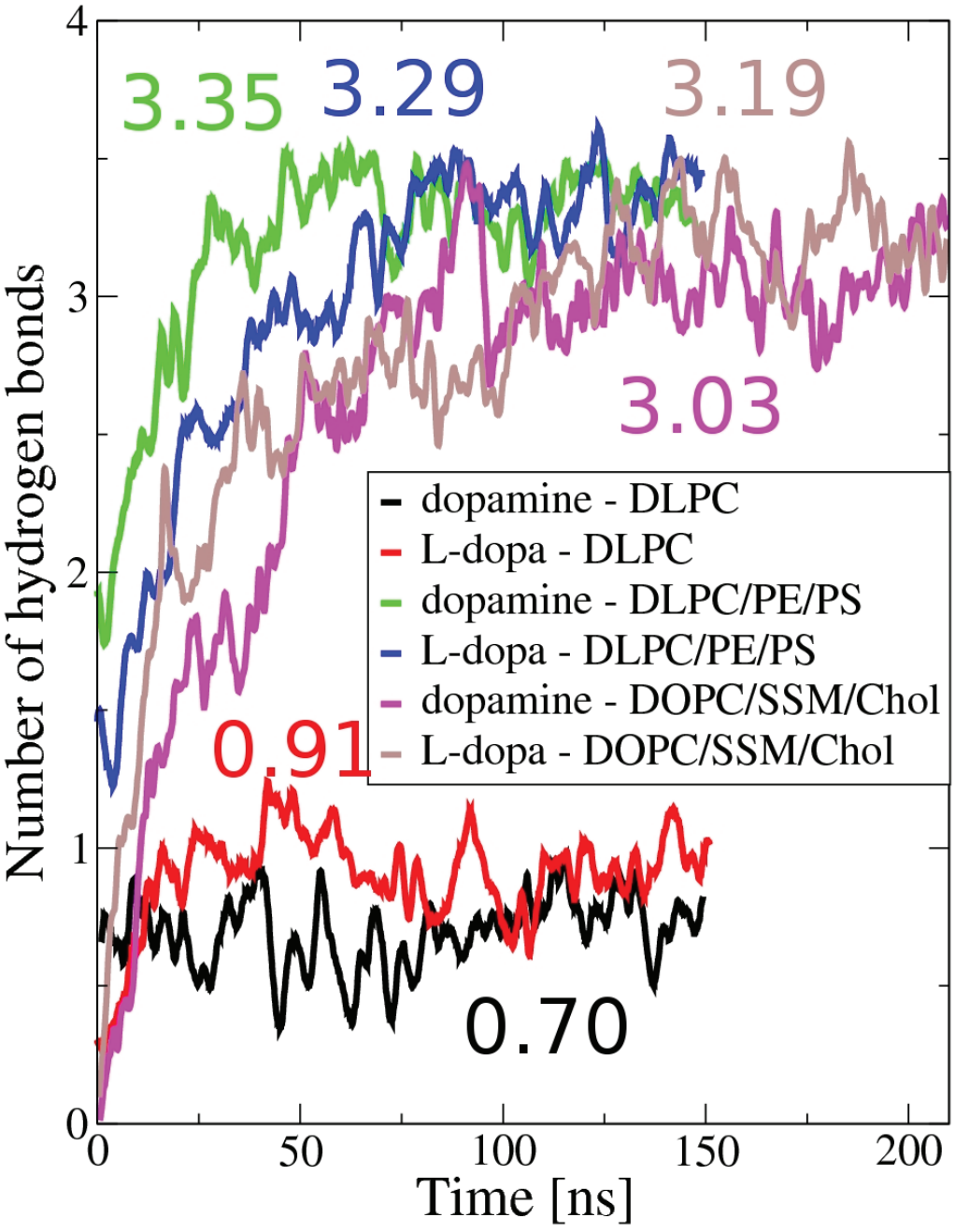
3.35
3.29
3.19
3.03
0.91
0.70
dopamine - DLPC
L-dopa - DLPC
dopamine - DLPC/PE/PS
L-dopa - DLPC/PE/PS
dopamine - DOPC/SSM/Chol
L-dopa - DOPC/SSM/Chol
Number of hydrogen bonds
Time [ns]
0
1
2
3
4
0
50
100
150
200

Figure 5.

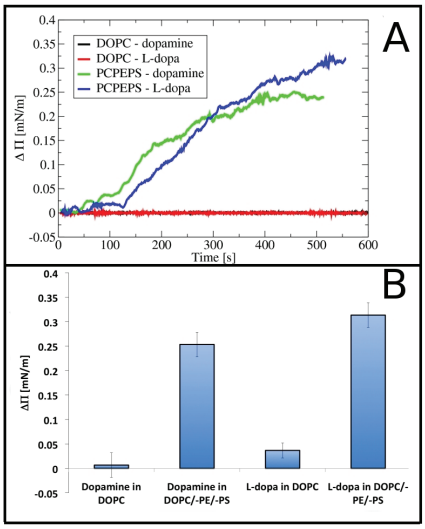
A
DOPC - dopamine
DOPC - L-dopa
PCPEPS - dopamine
PCPEPS - L-dopa
Δ Π [mN/m]
Time [s]
B
ΔΠ [mN/m]
Dopamine in DOPC
Dopamine in DOPC/-PE/-PS
L-dopa in DOPC
L-dopa in DOPC/-PE/-PS

Tampereen teknillinen yliopisto
PL 527
33101 Tampere

Tampere University of Technology
P.O.B. 527
FI-33101 Tampere, Finland

ISBN 978-952-15-3362-4
ISSN 1459-2045